MASTER

Towards a three-dimensional Finite Element Model for the post-filling stage of Injection Moulding

Selen, J.H.A.

Award date:
1995

Towards a three-dimensional Finite Element Model for the post-filling stage of Injection Moulding

WFW-report 92.124

J.H.A. Selen

Oktober 1992

Towards a three-dimensional Finite Element Model for the post-filling stage of Injection Moulding

J.H.A. Selen

Oktober 1992

Coach: Prof. dr. ir. F.P.T. Baaijens.

WFW-report 92.124

Smile ... tomorrow will be worse. (The Murphy Philosophy)

Abstract

In this report, the development of a three dimensional finite element model for the post-filling stage of the injection moulding process, is presented. This model is meant for the injection moulding process of products with high demands on accurate geometrical shape, like lenses for CD-players. An important aspect concerning geometrical shape is the generation of residual stresses. The development is divided in two parts.

The first part is the development of a finite element model describing the thermal and visco-elastic behaviour based on a the Lagrange approach. The second part is the development of a Updated ALE algorithm. This algorithm is needed because large mesh distortions are expected when extra material is pushed in the mould to compensate the shrinkage. This report deals only with the first part.

For modelling the process the balance laws are given and the constitutive equations for cauchy stress tensor, the internal energy and the heat flux vector are presented. The Cauchy stress tensor is described using the generalized Newtonian Fluid model and the generalized Multimode Maxwell model dependent on the temperature. These two models are worked out for both infinitesimal strain theory and nonlinear theory. The nonlinear model may be needed for the packing and holding stage.

The thermal - and visco-elastic problem are solved decoupled, using temperature, displacement and pressure as unknowns. On the nonlinear visco-elastic problem the Newton Raphson solution method is applied. For both problems the enriched trilinear element is used.

The performed simulations of the cooling stage under atmospheric pressure show good comparison with results obtained from the literature. Simulations with the nonlinear model gives nearly the same results as obtained from the linear model. Also investigations on mesh size and time step size are presented.

Preface

This report treats the work I have done for my master's degree of science, from the University of Technology in Eindhoven. The research was performed in the Continuum mechanics, System & Control and Tribology group at the Philips Research Laboratories in Eindhoven, The Netherlands.

I would like to thank my coach Frank Baaijens for his support and guidance. Further, I would like to thank everyone who in some way has been involved in the progress of this project.

Sjaak Selen.

Contents

Notation

Quantities

A, a	scalar
$\vec{a}$	vector
$\boldsymbol{A}$	second order tensor
$\underline{A}$	matrix
$\underset{\sim}{a}$	column
$\boldsymbol{I}$	second order unit tensor

Operations and functions

$\boldsymbol{A}^c$	conjugation
$\vec{a} \cdot \vec{b}$, $\boldsymbol{A} \cdot \vec{b}$, $\vec{a} \cdot \boldsymbol{B}$, $\boldsymbol{A} \cdot \boldsymbol{B}$	inner product
$\boldsymbol{A} : \boldsymbol{B}$	double inner product
$\boldsymbol{A}^{-1}$, $\underline{A}^{-1}$	inversion
$\|\vec{a}\|$, $\|\boldsymbol{A}\|$	norm
$tr(\boldsymbol{A})$	trace of a second order tensor
$det(\boldsymbol{A})$	determinant of a second order tensor
$\boldsymbol{A}^d = \boldsymbol{A} - \frac{1}{3}tr(\boldsymbol{A})\boldsymbol{I}$	deviatoric part of a second order tensor
$\underset{\sim}{a}^T$, $\underline{A}^T$	transposition
$\vec{\nabla}$	gradient operator
$\dot{a}$	material time dervative
$\frac{\partial a}{\partial t}$	spatial time dervative

Chapter 1

Introduction

On a continuously increasing scale, polymer materials are applied in industrial products in diverse fields as e.g.: the automotive and aviation industry, consumer electronics, bio-prosthesis etc. Polymers intrinsically exhibit a range of advantageous properties, compared to more traditional materials. Their primary asset is their low density, resulting in a relatively high specific strength and stiffness. Other properties that are useful in a variety of applications are: impact resistance, electrical properties, temperature resistance, water resistance, surface finish and chemical inertness. Most important, however, is that polymers are easy to process; complex shaped and integrated parts can be manufactured in automatic mass production equipment.
(Douven [14])

1.1 Injection moulding

Although a large number of industrial processes for the manufacturing of plastics products exists, about 30 per cent of all polymers is processed by *injection moulding.*

Description of equipment and operations

In figure 1.1 a schematic representation of a reciprocating screw injection moulding machine is given. Two main parts can be recognized:

- The injection unit,
- The clamping unit containing the mould.

The screw plasticizes the granulated polymer, fed by a hopper, by heat conduction from the heat bands and by viscous heating generated by the screw

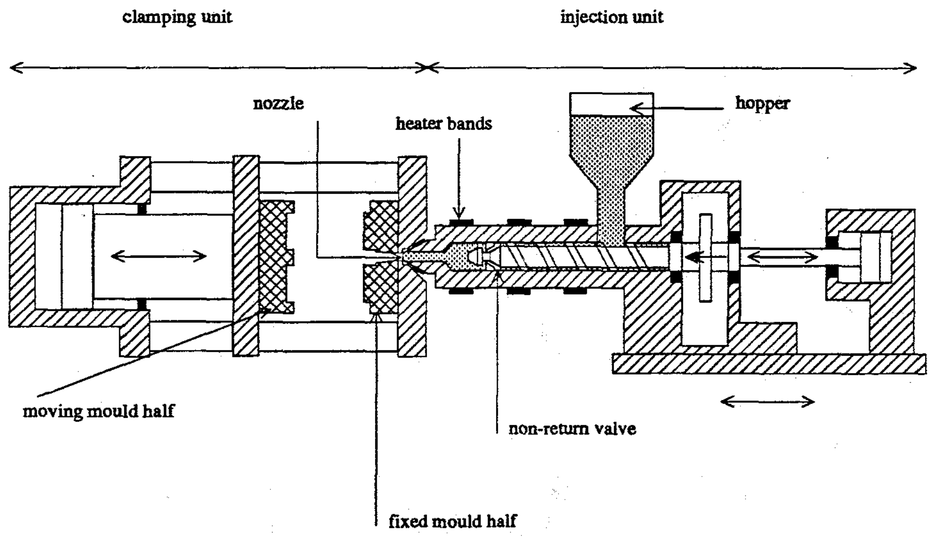

Figure 1.1: The reciprocating screw injection moulding machine.

rotation. The polymer is pressurized and further homogenized in the metering zone of the screw. Because the small diameter nozzle is sealed by solidified polymer, the melt pushes the screw backwards against a controllable pressure. If sufficient material is metered, the screw rotation stops.

After closing the mould, the screw is pushed forward. A non-return valve at the tip of the screw prevents the melt from leaking backwards. The polymer is injected at high speed through the nozzle, via the sprue that leads to the runner(s), into the cavity. At the entry of the cavity restrictions are present, so-called gates, that control the flow into the mould and promote the removal of the sprue and runner(s). The mould halves are fixed to the clamp unit, that is designed to withstand the high pressure exerted on the mould and prevent it from opening. This stage of the process is called the *injection* or *filling stage.*

The mould is thermostated by recirculating water or oil through cooling or heating channels. The polymer starts to solidify immediately at the mould walls. When the mould is completely filled, additional material is forced in the mould to compensate the shrinkage. These stages are called the *packing* and *holding stage* of the injection moulding process. The material continues to enter the mould cavity until the gate freezes off, thus defining the start of the *cooling stage.* When the product is sufficiently cooled, the mould is opened and the product is ejected. (Douven [14])

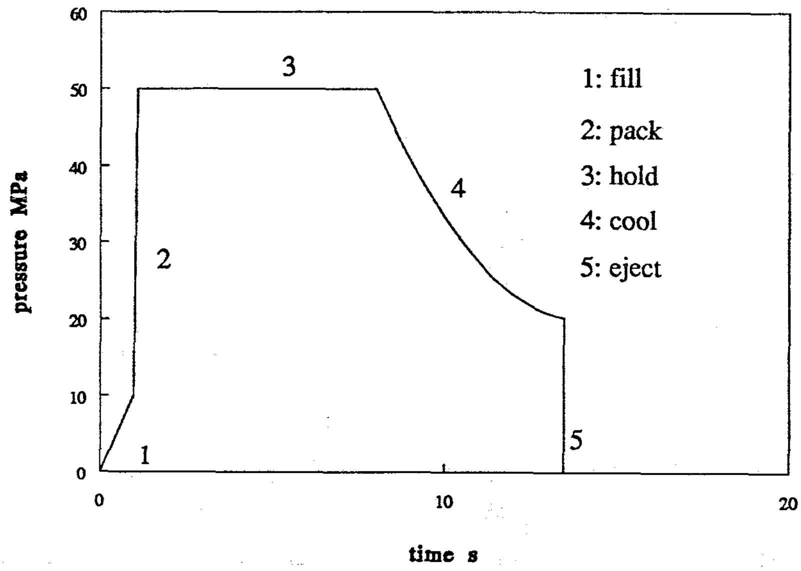

Figure 1.2: Pressure versus time at the gate.

Problem under consideration

This report focuses upon the injection moulding process of products with high demands on accurate geometrical shape, like lenses for CD-players. An important aspect concerning geometrical shape is the generation of residual stresses. One distinguishes residual flow stresses which develop during the filling of the mould and the packing stage, and the residual stresses generated during the cooling. The latter one, also denoted as thermally induced stresses, is caused by differential shrinkage and gives rise to the highest contribution to the residual stresses. A three-dimensional approach is needed to calculating residual stresses.

Literature

The present state of research concerning the modelling of the injection moulding process is marked by recently works like Chiang [11], [12] and Douven [14]. They focused on a $2\frac{1}{2}$D analysis of the whole injection moulding cycle.

Concerning residual stresses, Baaijens [3] gave a $2\frac{1}{2}$D model to calculate both flow- and thermally induced stresses. A 3D approach to this subject but only describing thermally induced stresses is given by Kabanemi [19]. Experimental work on thermally induced stresses was done by Lee [20], Saffell [23] and Wust [29].

1.2 Objective of the research

The objective of the research presented in this report is the development of a three-dimensional finite element model for the post-filling stage of the injection moulding process. The work will be divided in two parts from which the only the first one has been accomplished.

The first part is the development of a finite element model based on the Lagrange approach describing the thermal and visco-elastic behaviour of the process. With use of this model the cooling stage can be simulated. Experimental data from the literature is available to check the model.

The second part is the implementation of an Updated-ALE algorithm. This algorithm is needed to simulate the pack and hold stage.

Also part of the research is a geometrical nonlinear constitutive model for the visco-elastic behaviour and the implementation of the enriched trilinear element. The nonlinear model may be needed in the pack and hold stage.

1.3 Layout of the report

In the first chapter an introduction on injection moulding is given and the objective of the research is presented.

In chapter 2 a brief introduction is given to continuum mechanics and thermodynamics is given. The aim is to determine fields of density, motion and temperature of a body. These fields must obey balance laws. Some extra relations, so-called constitutive equations, have to be defined to create a solvable set of equations.

In chapter 3 the constitutive equations for the Cauchy stress tensor, the internal energy and the heat flux vector are presented.

In chapter 4 the equations of the previous two chapters are used to model the injection moulding process. Definitions of the temperature and visco-elastic problem are presented. The visco-elastic problem is worked out for both geometrical linear and nonlinear theory.

In chapter 5 the FEM discretization of the temperature and visco-elastic problems are worked out. On the nonlinear visco-elastic problem the Newton-Raphson solution method is applied. Further the enriched trilinear element is formulated.

In chapter 6 the results of some simulations of the cooling stage are given. They are compared to results from the literature. Also investigations on the influences of mesh sizes and time step size are presented. Further the linear and nonlinear visco-elastic models are compared.

In chapter 7 some conclusions and recommendations for further research are given.

Chapter 2

Theoretical background

Continuum mechanics is concerned with the thermo-mechanical behaviour of continuous media on a macroscopic scale. The main goal of continuum mechanics is to determine the fields of density, temperature and motion for all material points considered, as a function of time (Müller [21]).
In this chapter the basic concepts of continuum mechanics are summerized. (Douven [14], Oomens [22] and Schreurs [24])

2.1 Kinematics

The kinematics of a problem contain the field of motion and its derivatives with respect to time and position.

A continuum is considered to exist of a set of material points. These material points can be identified by their material coordinates, denoted by a column $\underset{\sim}{\xi}$. The position vector of a material point, denoted by $\vec{x}$, is a function of the material coordinates $\underset{\sim}{\xi}$ and of the time t.
The material points of a continuum at time t can be identified by their position vectors $\vec{x}_0$ in a reference state. Using the Lagrangian description the underformed initial state is chosen as the reference state. Thus an arbitrary scalar field α can be written in the following form

$$\alpha = \hat{\alpha}(\vec{x}_0, t) \tag{2.1}$$

The motion of a continuum is denoted as the vector field $\vec{\varphi}$. The position of a material particle at time t, identified by the position $\vec{x}_0$ in the reference state, is given by $\vec{x} = \vec{\varphi}(\vec{x}_0, t)$.
The gradient operator is defined

$$\vec{dx} \cdot \vec{\nabla}\alpha = \alpha(\vec{x} + \vec{dx}) - \alpha(\vec{x}) \tag{2.2}$$

where $\vec{dx}$ is an arbitrary vector of infinitesimal length.

The material time derivative $\dot{\alpha}$ is defined as the rate of change from α at a fixed material point. The spatial time derivative $\partial\alpha/\partial t$ is defined as the rate of change of α at a fixed position in the space. The relation between these derivatives

$$\dot{\alpha} = \frac{\partial \alpha}{\partial t} + \vec{v} \cdot \vec{\nabla}\alpha \tag{2.3}$$

In equation (2.3) the velocity of a material point is defined as

$$\vec{v} = \dot{\vec{\varphi}} = \frac{\partial \vec{\varphi}}{\partial t} \tag{2.4}$$

The deformation tensor is defined as

$$\boldsymbol{F} = (\vec{\nabla}_0 \vec{\varphi})^c \tag{2.5}$$

where $\vec{\nabla}_0$ is the gradient operator with respect to the reference state.
A unique decomposition of the deformation tensor is given by

$$\boldsymbol{F} = \boldsymbol{R} \cdot \boldsymbol{U} \tag{2.6}$$

where $\boldsymbol{U}$ is a stretch tensor and $\boldsymbol{R}$ is a rotation tensor, i.e. $\boldsymbol{R}^c \cdot \boldsymbol{R} = \boldsymbol{I}$ and $det(\boldsymbol{R}) = 1$. The right Cauchy-Green tensor is defined as

$$\boldsymbol{C} = \boldsymbol{F}^c \cdot \boldsymbol{F} \tag{2.7}$$

The velocity gradient tensor is defined as

$$\boldsymbol{L} = (\vec{\nabla}\vec{v})^c = \dot{\boldsymbol{F}} \cdot \boldsymbol{F}^{-1} \tag{2.8}$$

This tensor can be split into a symmetric part $\boldsymbol{D}$, the deformation rate tensor, and a skew-symmetric part $\boldsymbol{\Omega}$, the spin tensor.

$$\boldsymbol{D} = \frac{1}{2}\left((\vec{\nabla}\vec{v})^c + (\vec{\nabla}\vec{v})\right) \tag{2.9}$$

$$\boldsymbol{\Omega} = \frac{1}{2}\left((\vec{\nabla}\vec{v})^c - (\vec{\nabla}\vec{v})\right) \tag{2.10}$$

The displacement field is defined $\vec{u} = \vec{x} - \vec{x}_0$. In case of linear deformations the spatial gradients of $\vec{u}$ are assumed to be small;

$$||\vec{\nabla}_0 \vec{u}|| \ll 1 \tag{2.11}$$

where $||\cdot||$ is a norm for second order tensor. It can be shown that in this case $\vec{\nabla}_0 = \vec{\nabla}$. At last, the linear strain tensor is given by

$$\boldsymbol{\varepsilon} = \frac{1}{2}\left((\vec{\nabla}_0\vec{u})^c + (\vec{\nabla}_0\vec{u})\right) \tag{2.12}$$

2.2 Balance laws

The basic equations of continuums mechanics are the equations of balance. In their local form they can be written as

Balance of mass (continuity equation)

$$\dot{\rho} + \rho\vec{\nabla} \cdot \vec{v} = \dot{\rho} + \rho\, tr(\boldsymbol{D}) = 0 \tag{2.13}$$

Balance of momentum

$$\vec{\nabla} \cdot \boldsymbol{\sigma}^c + \rho\vec{f} = \rho\dot{\vec{v}} \tag{2.14}$$

Balance of angular momentum

$$\boldsymbol{\sigma} = \boldsymbol{\sigma}^c \tag{2.15}$$

Balance of energy

$$\rho\dot{e} = \boldsymbol{\sigma} : \boldsymbol{D} - \vec{\nabla} \cdot \vec{h} + \rho r \tag{2.16}$$

where: ρ is the density
$\vec{\nabla}$ is the gradient operator with respect to the current configuration
$\vec{v}$ is the velocity vector
$\boldsymbol{D}$ is the strain rate tensor
$\boldsymbol{\sigma}$ is the Cauchy stress tensor
$\vec{f}$ is the specific body force
e is the specific internal energy
$\vec{h}$ is the heat flux vector
r is the specific heat source

To create a solvable set of equations, beside the balance laws, some extra equations have to be formulated. These equations, so-called constitutive equations, must be established for the Cauchy stress tensor, the heat flux vector and the specific internal energy as functions of density, temperature and motion. This is the subject of the next chapter.

Chapter 3

Material behaviour

In this chapter the constitutive equations for the Cauchy stress tensor, density and the specific internal energy will be given that represent the behaviour of amorphous polymers. These properties can be divided in thermo-mechanical and thermal behaviour.

3.1 Thermo-mechanical behaviour

It is common practice to split the Cauchy stress tensor into $\boldsymbol{\sigma} = -p\boldsymbol{I} + \boldsymbol{\tau}$, where $\boldsymbol{\tau}$ is the extra stress tensor and p is a pressure term. In case of multimode application:

$$\boldsymbol{\sigma} = -p\boldsymbol{I} + \sum_{i=1}^{m} \boldsymbol{\tau}_i \tag{3.1}$$

Where m is the number of modes.
If the extra stress tensor is deviatoric, p is the hydrostatic pressure.

Idealized, during the injection moulding process, the material appears in two different physical states. The first one is the molten, liquid alike, state. For simplicity the elastic behaviour of the polymer in this state will be ignored. Only viscous effects are taken into account. Under these assumptions the molten material can be well described with the generalized Newtonian Fluid model.

Below the glass transition temperature the polymer is solidified, the so-called glassy state. In this state, visco-elastic phenomena play an important role. The material in the glassy state will be described with the generalized Multimode Maxwell model.

3.1.1 Generalized Multimode Maxwell model

The Multimode Maxwell model is based upon the linear visco-elastic theory. The multimode application of the model is used because the single-mode model gives poor results. The Maxwell model in rate-form:

$$\overset{\diamond}{\boldsymbol{\tau}} + \frac{1}{\theta}\boldsymbol{\tau} = \frac{2\eta}{\theta}\boldsymbol{D}^d \tag{3.2}$$

Where $\overset{\diamond}{(\cdot)}$ denotes some objective rate of $(\cdot)$, θ is the relaxation time and η is the viscosity. Using the fundamental theorem:

> *To each objective tensor $\boldsymbol{\sigma}$ an invariant tensor $\overline{\boldsymbol{\sigma}}$ can be associated such that*
>
> $$\overline{\boldsymbol{\sigma}} = \boldsymbol{A} \cdot \boldsymbol{\sigma} \cdot \boldsymbol{A}^c \tag{3.3}$$
>
> $$\dot{\boldsymbol{A}} = -\boldsymbol{A} \cdot (\boldsymbol{\Omega} + \mathrm{H}), \qquad \boldsymbol{A}(t = \tau) = \boldsymbol{I} \tag{3.4}$$
>
> *where τ is some reference time. The material time derivative of $\overline{\boldsymbol{\sigma}}$ can be associated to a so-called objective rate through the relations*
>
> $$\dot{\overline{\boldsymbol{\sigma}}} = \boldsymbol{A} \cdot \overset{\diamond}{\boldsymbol{\sigma}} \cdot \boldsymbol{A}^c \tag{3.5}$$
>
> $$\overset{\diamond}{\boldsymbol{\sigma}} = \dot{\boldsymbol{\sigma}} - (\boldsymbol{\Omega} + \mathrm{H}) \cdot \boldsymbol{\sigma} - \boldsymbol{\sigma} \cdot (\boldsymbol{\Omega} + \mathrm{H})^c \tag{3.6}$$
>
> *where* **H** *is some objective tensor.*

The equation (3.2) can be rewritten

$$\dot{\overline{\boldsymbol{\tau}}} + \frac{1}{\theta}\overline{\boldsymbol{\tau}} = \frac{2\eta}{\theta}\overline{\boldsymbol{D}}^d \tag{3.7}$$

Integrating this equation leads to the integral-form of the Maxwell model:

$$\overline{\boldsymbol{\tau}} = \int_{-\infty}^{t} \frac{2\eta}{\theta} e^{-\frac{(t-s)}{\theta}} \overline{\boldsymbol{D}}^d \, ds \tag{3.8}$$

The integral-form will be used because of numerical advantages. The rate-form implies, after time discretization, time steps factor ten smaller than the relaxation time to get reasonable result. With use of the integral-form this is not necessary, if $\boldsymbol{D}$ is known sufficiently well during the time interval of interest.

The temperature dependency of the material constants is treated by assuming thermorheological simple material. Defining:

$$\theta(T) = a_T \theta_0 \tag{3.9}$$

$$\eta(T) = a_T \eta_0 \tag{3.10}$$

Where $(.)_0$ denotes $(.)$ at the reference temperature and a_T is the shift factor. The time-temperature shift function a_T is governed by

$$a_T = e^{-c_3(T-T_0)} \tag{3.11}$$

Where c_3 and T_0 are constants.
The pressure dependence of the shift factor:

$$T_0(p) = T_0(0) + sp \tag{3.12}$$

Where s is a constant.
Finally applying the temperature dependence of relaxation times and viscosities to the integral-form of the Maxwell model leads to the introduction of reduced time (see appendix A).
Full expression of the generalized Multimode Maxwell model:

$$\boldsymbol{\sigma} = -p\boldsymbol{I} + \sum_{i=1}^{m} \boldsymbol{\tau}_i \tag{3.13}$$

With expression for extra stress tensor:

$$\overline{\boldsymbol{\tau}}_i = \int_0^t \frac{2\eta_{i0}}{\theta_{i0}} e^{-(\xi(t)-\xi(s))/\theta_{i0}} \overline{\boldsymbol{D}}^d ds \tag{3.14}$$

And the definition of reduced time:

$$\xi(\tau) = \int_0^\tau \frac{1}{a_T} ds \tag{3.15}$$

Assuming the material is unloaded in time interval $\langle -\infty, 0]$.

3.1.2 Generalized Newtonian Fluid model

In the molten state the material is described by the Newtonian fluid model. Using this model the elastic behaviour of the material will be ignored. The model is defined in the following way:

$$\boldsymbol{\sigma} = -p\boldsymbol{I} + \boldsymbol{\tau} \tag{3.16}$$

The extra stress tensor is defined:

$$\boldsymbol{\tau} = 2\bar{\eta}\boldsymbol{D}^d \tag{3.17}$$

Where $\bar{\eta}$ is the steady state shear viscosity.
Assuming the Leonov model to hold (Douven [14]), the steady state shear viscosity may be expressed as:

$$\bar{\eta} = \eta_r + \sum_{i=1}^{m} \frac{2\eta_i}{1 + X_i}, \qquad X_i = \sqrt{1 + (2\theta_i \dot{\gamma})^2} \tag{3.18}$$

Where the shear rate is defined:

$$\dot{\gamma} = \sqrt{2\boldsymbol{D} : \boldsymbol{D}} \tag{3.19}$$

The temperature dependence of the relaxation times and viscosities is treated in the same way as in the glassy state. In this case the WLF equation is used to calculate the shift factor. Recalling

$$\theta(T) = a_T \theta_0 \tag{3.20}$$

$$\eta(T) = a_T \eta_0 \tag{3.21}$$

The WLF-equation:

$$\log a_T = -\frac{c_1(T - T_0)}{c_2 + T - T_0} \tag{3.22}$$

Pressure dependence:

$$T_0(p) = T_0(0) + sp \tag{3.23}$$

$$c_2(p) = c_2(0) + sp \tag{3.24}$$

Where c_1, c_2 and T_0 are constants.

3.2 Density

The Newtonian and Maxwell model only describe the extra stress tensor. The pressure part p is physically related to volume changes. These are mainly caused by changes in pressure and temperature. These effects are incorporated through the continuity equation:

$$\frac{\dot{\rho}}{\rho} + tr(\boldsymbol{D}) = 0 \tag{3.25}$$

Where $\rho = \rho(T, p)$ is the density.
This yields:

$$\alpha \dot{T} + \kappa \dot{p} + tr(\boldsymbol{D}) = 0 \tag{3.26}$$

$$\alpha = \frac{1}{\rho}\frac{\partial \rho}{\partial T}, \qquad \kappa = \frac{1}{\rho}\frac{\partial \rho}{\partial p} \tag{3.27}$$

The constants α and κ are calculated with use of an empirical pνT-relation, the so-called Tait equation for amorphous polymers (Zoller [30]):

$$\nu(\mathrm{p},\mathrm{T}) = \begin{cases} (a_{0m} + a_{1m}(T - T_g))(1 - 0.0894\ln(1 + \frac{p}{B_m})) & if\, T \geq T_g \\ (a_{0s} + a_{1s}(T - T_g))(1 - 0.0894\ln(1 + \frac{p}{B_s})) & if\, T \leq T_g \end{cases} \tag{3.28}$$

With:

$$B_m(T) = B_{0m}e^{-(B_{1m}T)}, \qquad B_s(T) = B_{0s}e^{-(B_{1s}T)} \tag{3.29}$$

$$T_g(p) = T_g(0) + sp \tag{3.30}$$

Where ν is specific volume, T_g is pressure dependent glass transition temperature and a_{0m}, a_{1m}, B_{0m}, B_{1m}, a_{0s}, a_{1s}, B_{0s}, B_{1s} and s are constants.

3.3 Thermal behaviour

In this section the constitutive equations concerning the thermal behaviour are presented. The heat flux vector $\vec{h}$ is assumed to be proportional to the temperature gradient:

$$\vec{h} = -\lambda\vec{\nabla}T \tag{3.31}$$

Where λ is the thermal conductivity coefficient.
This equation is known as Fourier's law. Ignoring elastic effects, the specific internal energy e can be written as (Sitters [26]):

$$\dot{e} = c_p(\dot{T}) - \frac{p}{\rho}tr(\boldsymbol{D}) + \frac{T}{\rho^2}\frac{\partial \rho}{\partial T}\dot{p} \tag{3.32}$$

Chiang [11] proposed for the thermal capacity at constant pressure:

$$c_p(T) = c_{p1} + c_{p2}(T - c_{p5}) + c_{p3}\tanh(c_{p4}(T - c_{p5})) \tag{3.33}$$

Where c_{p1}, c_{p2}, c_{p3}, c_{p4} and c_{p5} are constants.

Chapter 4

Modelling the injection moulding process

In this chapter the balance laws and constitutive equations will be utilized to model the injection moulding process.

Since it is our aim to develop a three-dimensional model no simplifications due to mould geometry can be made. Modelling the filling stage is rather difficult in a 3D enviroment. Also it is assumed that the impact of this stage on the next stages is small. The simulation will therefore start with an already filled mould. The process will be modelled using a Lagrangian description with displacements as the unknowns, rather than a Eulerian description with velocities as unknowns. During the packing stage, difficulties may occur due to large mesh distortions. This problem may be overcome by employing an Updated ALE algorithm, Baaijens [2].

In the next sections the definition of the thermal - and visco-elastic problem will be given.

4.1 Temperature problem

The temperature problem will be derived from the energy equation, using Fourier's law and the relation for specific energy. An internal heat source is assumed not to be present.

Applying time discretization, the time domain $\mathcal{S} = [0, T_e]$ is divided in n_t intervals according to:

$$\mathcal{S} = \bigcup_{n=0}^{n_t} \mathcal{S}_n, \qquad \mathcal{S}_n = [t_n, t_{n+1}], \qquad \Delta t = t_{n+1} - t_n \tag{4.1}$$

Employing the backward difference scheme to discretize time derivatives:

$$\dot{T} \approx \frac{T_{n+1} - T_n}{\Delta t} \tag{4.2}$$

$$\dot{p} \approx \frac{p_{n+1} - p_n}{\Delta t} \tag{4.3}$$

Where $(\cdot)_{n+1}$ denotes $(\cdot)$ at $t = t_{n+1}$ and $(\cdot)_n$ denotes $(\cdot)$ at $t = t_n$.
Defining the domain Ω with boundary $\Gamma = \Gamma_u \bigcup \Gamma_p \bigcup \Gamma_h$ the temperature problem (**PT**) can be give by:

Given a heat flux $q^0 : \Gamma_p \mapsto I\!R$, *a surface conductance* $h : \Gamma_h \mapsto I\!R$, *a prescribed temperature* $T^o_{n+1} : \Gamma_u \mapsto I\!R$, *an initial temperature field* T_n *and pressure field* p_n, *an actual pressure field* p_{n+1}, *extra stress field* $\boldsymbol{\tau}$ *and strain rate* $\boldsymbol{D}$, *find* $T_{n+1} : \Omega \mapsto I\!R$ *such that*

$$\vec{\nabla} \cdot \lambda \vec{\nabla} T_{n+1} + tr(\boldsymbol{\tau} : \boldsymbol{D}) - 1/3tr(\boldsymbol{\tau})tr(\boldsymbol{D}) =$$

$$\beta(T_{n+1} - T_n)/\Delta t + \mu T_{n+1}(p_{n+1} - p_n)/\Delta t \tag{4.4}$$

and

$$(\vec{h} \cdot \vec{n} = q^0)_{n+1} \qquad on \ \Gamma_p \tag{4.5}$$

$$\vec{h} \cdot \vec{n} = h\,(T_{n+1} - T_\infty) \qquad on \ \Gamma_h \tag{4.6}$$

$$T_{n+1} = T^0_{n+1} \qquad on \ \Gamma_u \tag{4.7}$$

Where:

$$\beta = \rho c_p \tag{4.8}$$

$$\mu = \frac{1}{\rho}\frac{\partial \rho}{\partial T} \tag{4.9}$$

Calculating β and μ, the last estimate of the temperature is used. So equation (4.4) is assumed to be linear. On the boundary Γ_h a so-called Robin boundary condition is given. The term $1/3tr(\boldsymbol{\tau})tr(\boldsymbol{D})$ is only non-zero in case the extra stress tensor $\boldsymbol{\tau}$ is not deviatoric.

4.2 Visco-elastic problem

The visco-elastic problem will be derived from the momentum equation, the continuity equation and angular momentum equation using the constitutive equation for the Cauchy stress tensor. Due to the extremely high viscosity of the material compared to the velocities, inertia effects will be disregarded. Further, no body forces are assumed to be present. The momentum equation yields

$$\vec{\nabla} \cdot \boldsymbol{\sigma} = \vec{0} \tag{4.10}$$

Two constitutive equation for the Cauchy stress tensor are used; The generalized Newtonian Model and the generalized Multimode Maxwell Model dependent on the temperature in the material point.
With use of time discretization and reduced time the expression for the extra stress tensor of the Maxwell Model can be transformed:

$$\overline{\boldsymbol{\tau}}_{(n+1)i} = \int_0^{t_{n+1}} \frac{2\eta_{i0}}{\theta_{i0}} e^{-(\xi(t_{n+1})-\xi(s))/\theta_{i0}} \overline{\boldsymbol{D}}^d(s)ds \tag{4.11}$$

$$= e^{-\frac{\Delta\xi}{\theta_{i0}}} \int_0^{t_n} \frac{2\eta_{i0}}{\theta_{i0}} e^{-(\xi(t_n)-\xi(s))/\theta_{i0}} \overline{\boldsymbol{D}}^d(s)ds + \int_{t_n}^{t_{n+1}} \frac{2\eta_{i0}}{\theta_{i0}} e^{-(\xi(t_{n+1})-\xi(s))/\theta_{i0}} \overline{\boldsymbol{D}}^d(s)ds \tag{4.12}$$

$$= e^{-\frac{\Delta\xi}{\theta_{i0}}} \overline{\boldsymbol{\tau}}_{ni} + \int_{t_n}^{t_{n+1}} \frac{2\eta_{i0}}{\theta_{i0}} e^{-(\xi(t_{n+1})-\xi(s))/\theta_{i0}} \overline{\boldsymbol{D}}^d(s)ds \tag{4.13}$$

$$= e^{-\frac{\Delta\xi}{\theta_{i0}}} \overline{\boldsymbol{\tau}}_{ni} + \int_{t_n}^{t_{n+1}} \frac{2\eta_{i0}}{\theta_{i0}} e^{-(\xi(t_{n+1})-\xi(s))/\theta_{i0}} ds\, \overline{\boldsymbol{D}}^d_{n+\alpha} \tag{4.14}$$

Where:

$$\Delta\xi = \int_{t_n}^{t_{n+1}} \frac{1}{a_T(\tau)} d\tau \tag{4.15}$$

In the last step $\overline{\boldsymbol{D}}^d(s)$ is assumed to be constant in the time interval $[t_n, t_{n+1}]$ and is chosen at $t = t_{n+\alpha}$, $\alpha \in [0,1]$. This tensor will also be used in the Newtonian model. A constitutive equation for the Cauchy stress tensor including both models is defined by:

$$\boldsymbol{\sigma} = -p\boldsymbol{I} + \boldsymbol{\tau}^* + \sum_{i=1}^{m} \boldsymbol{\tau}_i \tag{4.16}$$

$$\boldsymbol{\tau}^* = 2\bar{\eta}\boldsymbol{D}^d \tag{4.17}$$

$$\overline{\boldsymbol{\tau}}_{(n+1)i} = G_{ni}\overline{\boldsymbol{\tau}}_{ni} + G_i\overline{\boldsymbol{D}}^d_{n+\alpha} \tag{4.18}$$

Where:

$$\overline{\eta} = \begin{cases} \overline{\eta}(\dot{\gamma}, \theta, \eta) & if\ T > T_g \\ 0 & if\ T \leq T_g \end{cases} \tag{4.19}$$

$$G_{ni} = \begin{cases} 0 & if\ T > T_g \\ e^{-\frac{\Delta\xi}{\theta_{i0}}} & if\ T \leq T_g\ (and\ T \leq T_g\ at\ t = t_n) \end{cases} \tag{4.20}$$

$$G_i = \begin{cases} 0 & if\ T > T_g \\ \int_{t_n}^{t_n+1} \frac{2\eta_{i0}}{\theta_{i0}} e^{-(\xi(t_{n+1})-\xi(\tau))/\theta_{i0}} ds & if\ T \leq T_g \end{cases} \tag{4.21}$$

The definition of the visco-elastic problem will continue in two different approaches from this point.

4.2.1 Infinitesimal strain theory

In the infinitesimal strain theory only small strains and rotations are permitted. Under these restrictions the strain rate tensor yields

$$\begin{aligned} \boldsymbol{D} &= \frac{1}{2}\left(\vec{\nabla}\vec{v} + (\vec{\nabla}\vec{v})^c\right) && (4.22) \\ &\approx \frac{1}{\Delta t}\frac{1}{2}\left(\vec{\nabla}_0(\vec{u}_{n+1} - \vec{u}_n) + (\vec{\nabla}_0(\vec{u}_{n+1} - \vec{u}_n))^c\right) && (4.23) \\ &= \frac{1}{\Delta t}\boldsymbol{\varepsilon}\left(\Delta\vec{u}\right) && (4.24) \end{aligned}$$

where

$$\Delta\vec{u} = \vec{u}_{n+1} - \vec{u}_n \tag{4.25}$$

The constants α, κ and $\overline{\eta}$ will be calculated using the last estimate of pressure, temperature and strain rate.
Using the domain Ω with boundary $\Gamma = \Gamma_u \bigcup \Gamma_p$ the linear visco-elastic problem (**PVE**) can be give by:

Given a boundary load $\vec{p}_{n+1} : \Gamma_p \mapsto I\!R^n$, a precribed displacement $\Delta\vec{u}^0 : \Gamma_u \mapsto I\!R^n$, an initial temperature field T_n, – pressure field p_n and extra stress field $\boldsymbol{\tau}_{ni}$ and an actual temperature field T_{n+1}, find $\Delta\vec{u} : \Omega \mapsto I\!R^n$ such that

$$\vec{\nabla} \cdot \Big(-p_{n+1}\boldsymbol{I} + 2\overline{\eta}\frac{1}{\Delta t}\boldsymbol{\varepsilon}^d(\Delta\vec{u}) + \sum_{i=1}^{m}(G_{ni}\boldsymbol{\tau}_{ni}^d) + (\sum_{i=1}^{m} G_i)\frac{1}{\Delta t}\boldsymbol{\varepsilon}^d(\Delta\vec{u}) \Big) = 0 \tag{4.26}$$

$$\alpha(T_{n+1} - T_n) + \kappa(p_{n+1} - p_n) + tr(\boldsymbol{\varepsilon}(\Delta\vec{u})) = 0 \tag{4.27}$$

$$\Delta\vec{u} = \Delta\vec{u}^0 \qquad \text{on } \Gamma_u \tag{4.28}$$

$$\boldsymbol{\sigma}_{n+1} \cdot \vec{n}_{n+1} = \vec{p}_{n+1} \qquad \text{on } \Gamma_p \tag{4.29}$$

4.2.2 Non-linear theory

In the non-linear theory finite strain and rotations are allowed. Recalling discretization of the time interval $\mathcal{S} = [0, T_e]$ in n_t intervals according to:

$$\mathcal{S} = \bigcup_{n=0}^{n_t} \mathcal{S}_n, \qquad \mathcal{S}_n = [t_n, t_{n+1}], \qquad \Delta t = t_{n+1} - t_n \tag{4.30}$$

Applying linear interpolation, the motion of a point with label $\vec{x}_0$ and $t \in \mathcal{S}_n$ can be given by:

$$\vec{\varphi}_{n+\alpha} = (1-\alpha)\vec{\varphi}_n + \alpha\vec{\varphi}_{n+1}, \qquad \alpha = \frac{t - t_n}{\Delta t} \in [0,1] \tag{4.31}$$

So, the deformation tensor in $\mathcal{S}_n$ can be given by:

$$\boldsymbol{F}_{n+\alpha} = (1-\alpha)\boldsymbol{F}_n + \alpha\boldsymbol{F}_{n+1} \tag{4.32}$$

Application of the generalized midpoint rule gives:

$$\dot{\boldsymbol{C}}_{n+\alpha} = \frac{\boldsymbol{C}_{n+1} - \boldsymbol{C}_n}{\Delta t} \tag{4.33}$$

Where:

$$\boldsymbol{C} = \boldsymbol{F}^c \cdot \boldsymbol{F} \tag{4.34}$$

Equation (4.33) is the basic approximation for deriving a relation for the strain rate tensor. The relation is given by [1] :

$$\boldsymbol{D}_{n+\alpha} = \frac{1}{2}\frac{1}{\Delta t}\Big(\boldsymbol{F}^{-c}_{n+\alpha}\cdot\boldsymbol{F}^{c}_{n+1}\cdot\boldsymbol{F}_{n+1}\cdot\boldsymbol{F}^{-1}_{n+\alpha} - \boldsymbol{F}^{-c}_{n+\alpha}\cdot\boldsymbol{F}^{c}_{n}\cdot\boldsymbol{F}_{n}\cdot\boldsymbol{F}^{-1}_{n+\alpha}\Big) \tag{4.35}$$

This approximation for the strain rate tensor is incrementally objective in $\mathcal{S}_n$, but only for $\alpha = \frac{1}{2}$ physically acceptable results can be obtained [2]. Using the theorem given in section 3.1.1 and the Truesdell proposition

$$\boldsymbol{A} = \boldsymbol{F}^{-1} \tag{4.36}$$

The relation for the Multimode Maxwell extra stress tensor yields:

$$\boldsymbol{\tau}_{(n+1)\,i} = \boldsymbol{F}_{n+1}\cdot\boldsymbol{F}^{-1}_{n}\cdot(G_{ni}\boldsymbol{\tau}_{ni})\cdot\boldsymbol{F}^{-c}_{n}\cdot\boldsymbol{F}^{c}_{n+1} + G_i\boldsymbol{F}_{n+1}\cdot\boldsymbol{F}^{-1}_{n+\frac{1}{2}}\cdot\boldsymbol{D}^{d}_{n+\frac{1}{2}}\cdot\boldsymbol{F}^{-c}_{n+\frac{1}{2}}\cdot\boldsymbol{F}^{c}_{n+1} \tag{4.37}$$

The relation (4.35) with $\alpha = \frac{1}{2}$ is also used in the Newtonian Fluid model. Using domain Ω the non-linear visco-elastic problem (**NPVE**) is given by:

Let the motion during $\mathcal{S}_n$ satisfy :

$$\vec{\varphi}_{n+\alpha} = (1-\alpha)\vec{\varphi}_n + \alpha\vec{\varphi}_{n+1}, \qquad \alpha = \frac{t-t_n}{\Delta t} \in [0,1] \tag{4.38}$$

and a boundary load $\vec{p}_{n+1} : \Gamma_p \mapsto \mathbb{R}^n$, a precribed motion $\vec{\varphi}^{\,0}_{n+1} : \Gamma_u \mapsto \mathbb{R}^n$, an initial temperature field T_n, – pressure field p_n, – deformation field $\boldsymbol{F}_n$ and extra stress field $\boldsymbol{\tau}_{ni}$ and an actual temperature field T_{n+1}, find $\vec{\varphi}_{n+1} : \Omega \mapsto \mathbb{R}$ such that

$$\vec{\nabla}\cdot\Bigg(-p_{n+1}\boldsymbol{I} + 2\overline{\eta}\boldsymbol{D}^{d}_{n+\frac{1}{2}} + \boldsymbol{F}_{n+1}\cdot\boldsymbol{F}^{-1}_{n}\cdot\sum_{i=1}^{m}(G_{ni}\boldsymbol{\tau}_{ni})\cdot\boldsymbol{F}^{-c}_{n}\cdot\boldsymbol{F}^{c}_{n+1} + (\sum_{i=1}^{m}G_i)\boldsymbol{F}_{n+1}\cdot\boldsymbol{F}^{-1}_{n+\frac{1}{2}}\cdot\boldsymbol{D}^{d}_{n+\frac{1}{2}}\cdot\boldsymbol{F}^{-c}_{n+\frac{1}{2}}\cdot\boldsymbol{F}^{c}_{n+1}\Bigg) = 0 \tag{4.39}$$

$$\alpha(T_{n+1}-T_n) + \kappa(p_{n+1}-p_n) + tr(\Delta t\boldsymbol{D}_{n+\frac{1}{2}}) = 0 \tag{4.40}$$

$$\vec{\varphi}_{n+1} = \vec{\varphi}^{\,0}_{n+1} \qquad on\ \Gamma_u \tag{4.41}$$

$$\boldsymbol{\sigma}_{n+1}\cdot\vec{n}_{n+1} = \vec{p}_{n+1} \qquad on\ \Gamma_p \tag{4.42}$$

The expression for the extra stress tensor (eq. (4.37)) is not deviatoric any more. In spite of this fact it's still assumed that the pressure term in the constitutive equation for the Cauchy stress tensor is the hydrostatic pressure (normaly defined by $p = -\frac{1}{3}tr(\boldsymbol{\sigma})$). Only in case of calculating pressure dependent constants the real hydrostatic pressure is used.

The constants α, κ and $\overline{\eta}$ will be calculated using the last estimates of pressure, temperature and strain rate.

4.2.3 Calculating G_{ni} and G_i

For the calculation of G_{ni} and G_i, appearing in the equation for extra stress tensor from the Maxwell model, some approximations have to be made. Recalling the definitions eq. (4.20), (4.21), (4.15), (3.15) and (3.11).
If $T \leq T_g$:

$$G_{ni} = e^{-\frac{\Delta\xi}{\theta_{i0}}} \tag{4.43}$$

$$G_i = \int_{t_n}^{t_n+1} \frac{2\eta_{i0}}{\theta_{i0}} e^{-(\xi(t_{n+1})-\xi(s))/\theta_{i0}} ds \tag{4.44}$$

$$\Delta\xi = \int_{t_n}^{t_n+1} \frac{1}{a_T(\tau)} d\tau \tag{4.45}$$

$$\xi(\tau) = \int_0^\tau \frac{1}{a_T} ds \tag{4.46}$$

$$a_T = e^{-c_3(T-T_0)} \tag{4.47}$$

First applying linear interpolation for the temperature on $\mathcal{S}_n$:

$$T(t) = T_n + \frac{T_{n+1} - T_n}{\Delta t}(t - t_n) \tag{4.48}$$

For G_{ni} this yields:

$$G_{ni} = e^{\frac{-\Delta t}{c_3(T_{n+1}-T_n)\theta_{i0}}\left\{e^{c_3(T_n+1-T_0)} - e^{c_3(T_n-T_0)}\right\}} \tag{4.49}$$

Because there is no analytical solution for the integral of G_i, a piecewise linear approximation for $\xi(\tau)$ is used. Defining the time domain $\mathcal{S}^* = [t_n, t_{n+1}]$, divided in k intervals according to:

$$\mathcal{S}^* = \bigcup_{j=0}^{k} \mathcal{S}_n^*, \qquad \mathcal{S}_n^* = [\tau_j, \tau_{j+1}], \qquad \Delta\tau = \tau_{j+1} - \tau_j \tag{4.50}$$

Applying piecewise linear approximation from $\xi(\tau)$ on $\mathcal{S}_n^*$:

$$\xi(\tau) = \xi(\tau_j) + \frac{\xi(\tau_{j+1}) - \xi(\tau_j)}{\Delta\tau}(\tau - \tau_j) \tag{4.51}$$

This yields:

$$\begin{aligned} G_i &= \sum_{j=1}^{k} \left\{ \int_{\tau_j}^{\tau_{j+1}} \frac{2\eta_{i0}}{\theta_{i0}} e^{-(\xi(\tau_{k+1}) - \xi(\tau_j) - \frac{\xi(\tau_{j+1}) - \xi(\tau_j)}{\Delta\tau}(\tau - \tau_j))/\theta_{i0}} d\tau \right\} & (4.52) \\ &= \sum_{j=1}^{k} \left\{ \frac{2\eta_{i0}\,\Delta\tau}{\xi(\tau_{j+1}) - \xi(\tau_j)} \left\{ e^{\frac{-(\xi(\tau_{k+1}) - \xi(\tau_{j+1}))}{\theta_{i0}}} - e^{\frac{-(\xi(\tau_{k+1}) - \xi(\tau_j))}{\theta_{i0}}} \right\} \right\} & (4.53) \end{aligned}$$

Where:

$$\begin{aligned} \xi(\tau_x) - \xi(\tau_z) &= \int_{\tau_x}^{\tau_z} e^{c_3(T_n + \frac{T_{n+1} - T_n}{\Delta t}(s - t_n) - T_0)} ds & (4.54) \\ &= \frac{\Delta t}{c_3(T_{n+1} - T_n)} \left\{ e^{c_3(T_n + \frac{T_{n+1} - T_n}{\Delta t}(\tau_z - t_n) - T_0)} - \right. \\ &\qquad \left. e^{c_3(T_n + \frac{T_{n+1} - T_n}{\Delta t}(\tau_x - t_n) - T_0)} \right\} & (4.55) \end{aligned}$$

The equations (4.49), (4.53) and (4.55) do not hold for $T_n = T_{n+1}$. In this special case simple equations for G_{ni} and G_i can be derived without using eq. (4.48) and (4.51). The constant k must be chosen dependent of the temperature change during time interval $\mathcal{S}_n$ (chosen was $k = 4 + int(\Delta T)$). Further extra attention must be paid to the calcalation of $e^x - e^y$ when x and y are near to zero. In that case the expansion of e^z is used.

Chapter 5

Application of the Finite Element Method

The FEM discretization of the temperature -, visco-elastic - and nonlinear visco-elastic problem is discussed in this chapter. Using this method the volume is divided into elements. In these elements the unknowns will be approximated with polynominals of a certain order.

The temperature - and visco-elastic problem will be solved separately to save computation time. This can be done because it is assumed that the dependence of the temperature problem on the displacement - and pressure field is weak. So, each time- or iteration-step the temperature problem is solved first, supplying a temperature field that is used in the visco-elastic problem.

5.1 The weak formulation

The system of equations **PT**, **PVE** and **NPVE** derived in the previous chapter are cast in a strong format by application of the weighted residual method. The equations are multiplied by a weighting function and integrated over the volume. The weak form is obtained by using integration by parts and transforming a volume integral into a boundary integral. The weak form of the problem imposes lower order of differentiability requirements on the solution than the original strong form. The weak forms, **PTW**, **PVEW** and **NPVEW**, are derived in appendix B. For the nonlinear visco-elastic problem the Updated Lagrange method is used. This means that as reference configuration of the time interval $\mathcal{S}_n$, the state at $t = t_n$ is chosen and implies that $\boldsymbol{F}_n = \boldsymbol{I}$.

5.2 Newton-Raphson solution method

The nonlinear visco-elastic problem will be solved using the Newton-Raphson iteration process. Therefor the system of equations has to be linearized. The weak form of the nonlinear visco-elastic problem in short notation:

$$A(\vec{w}, p, \vec{\varphi}) = L(\vec{w}, \vec{\varphi}) \tag{5.1}$$

$$B(q, p, \vec{\varphi}) = 0 \tag{5.2}$$

Let $\hat{\vec{\varphi}}$ be a estimate of the motion $\vec{\varphi}$, $\delta\vec{\varphi}$ the error in the estimate $\hat{\vec{\varphi}}$ and $\hat{p}$ be an estimate of the pressure p, with δp the error in the estimate $\hat{p}$:

$$\vec{\varphi} = \hat{\vec{\varphi}} + \delta\vec{\varphi} \tag{5.3}$$

$$p = \hat{p} + \delta p \tag{5.4}$$

The definition of the directional derivative of a functional $A(\ldots, \vec{\varphi})$ into the direction $\delta\vec{\varphi}$ with respect to $\vec{\varphi}$:

$$\delta_{\varphi} A(\ldots, \vec{\varphi}; \delta\vec{\varphi}) = \lim_{\theta \to 0} \frac{A(\ldots, \vec{\varphi} + \theta\delta\vec{\varphi}) - A(\ldots, \vec{\varphi})}{\theta} \tag{5.5}$$

Likewise

$$\delta_{p} A(\ldots, p; \delta p) = \lim_{\theta \to 0} \frac{A(\ldots, p + \theta\delta p) - A(\ldots, p)}{\theta} \tag{5.6}$$

Neglecting higher order terms the linearized system of equations is given by

$$A(\vec{w}, \hat{p}, \hat{\vec{\varphi}}) + \delta_{\varphi} A(\vec{w}, \hat{p}, \hat{\vec{\varphi}}; \delta\varphi) + \delta_{p} A(\vec{w}, \hat{p}, \hat{\vec{\varphi}}; \delta p) =$$

$$L(\vec{w}, \hat{\vec{\varphi}}) + \delta_{\varphi} L(\vec{w}, \hat{\vec{\varphi}}; \delta\varphi) \tag{5.7}$$

$$B(q, \hat{p}, \hat{\vec{\varphi}}) + \delta_{\varphi} B(q, \hat{p}, \hat{\vec{\varphi}}; \delta\varphi) + \delta_{p} B(q, \hat{p}, \hat{\vec{\varphi}}; \delta p) = 0 \tag{5.8}$$

For the derivation of this system of equations see appendix C.
Employing the Newton-Raphson iteration process this system of equations has to be solved each iteration step until convergence. After each iteration step the new estimates are calculated as follows:

$$\hat{\vec{\varphi}}^{i+1} = \hat{\vec{\varphi}}^{i} + \delta\vec{\varphi}^{i} \tag{5.9}$$

$$\hat{p}^{i+1} = \hat{p}^{i} + \delta p^{i} \tag{5.10}$$

where i denotes the i-th iteration step.

5.3 Discretization

The volume Ω will be divided into n_{el} element, such that

$$\Omega = \bigcup_{i=1}^{n_{el}} \Omega^e \tag{5.11}$$

Boundary elements are defined by

$$\Gamma^e = \Gamma \cap \Omega^e \tag{5.12}$$

Within each element there are a finite number of discrete points, the so-called nodes. In these nodes the unknowns, displacement and pressure or temperature, are calculated. The values of the unknown in any point of the element can be derived by interpolating between the nodes. This interpolating is done with use of shape functions. The weighting functions are also defined in the nodes and interpolated between them. According to the Galerkin method the same shape functions for the weighting function and the corresponding unknowns will be used. Further, the cartesian reference system will be introduced.

5.3.1 Discretization of the temperature problem

The temperature field and weighting function are interpolated over the element as follows

$$T(x,y,z) = \sum_{i=1}^{nT} T_i \varphi_i(x,y,z) \tag{5.13}$$

$$w(x,y,z) = \sum_{i=1}^{nT} w_i \varphi_i(x,y,z) \tag{5.14}$$

where nT is the number of temperature nodes in the element and $\varphi_i(x,y,z)$ is the shape function.
Interpolation on the boundary element

$$T(x,y,z) = \sum_{i=1}^{nTb} T_i \chi_i(x,y,z) \tag{5.15}$$

$$w(x,y,z) = \sum_{i=1}^{nTb} w_i \chi_i(x,y,z) \tag{5.16}$$

where nTb is the number of temperature nodes on the boundary element and $\chi_i(x,y,z)$ is the shape function.

The discretized temperature problem is worked out in appendix D. The result given by:

$$\underset{\sim}{w}^T \int_{\Omega^e} \left[\lambda \underline{A}^T \underline{A} + \underline{P}\{\beta + \mu(p - p_n)\}/\Delta t\right] d\Omega\, \underset{\sim}{T} + \underset{\sim b}{w}^T \int_{\Gamma_h^e} \underset{\sim}{\chi}\underset{\sim}{\chi}^T h\, d\Gamma \underset{\sim b}{T} =$$

$$\underset{\sim}{w}^T \int_{\Omega^e} \underset{\sim}{\varphi} \{trtd + \beta T_n/\Delta t\}\, d\Omega + \underset{\sim b}{w}^T \int_{\Gamma_h^e} \underset{\sim}{\chi} h T_\infty\, d\Gamma -$$

$$\underset{\sim b}{w}^T \int_{\Gamma_p^e} \underset{\sim}{\chi} q^0\, d\Gamma \qquad \forall\ \underset{\sim}{w} \tag{5.17}$$

These equations must hold for all admissible weighting functions. So, the contribution from one element in matrix form is given by

$$\boxed{\underline{S}^e\, \underset{\sim}{T} = \underset{\sim T}{f}} \tag{5.18}$$

where

$$\underline{S}^e = \int_{\Omega^e} \left[\lambda \underline{A}^T \underline{A} + \underline{P}\{\beta + \mu(p - p_n)\}/\Delta t\right] d\Omega + \int_{\Gamma_h^e} \underset{\sim}{\chi}\underset{\sim}{\chi}^T h\, d\Gamma \tag{5.19}$$

$$\underset{\sim T}{f} = \int_{\Omega^e} \underset{\sim}{\varphi} \{trtd + \beta T_n/\Delta t\}\, d\Omega + \int_{\Gamma_h^e} \underset{\sim}{\chi} h T_\infty\, d\Gamma - \int_{\Gamma_p^e} \underset{\sim}{\chi} q^0\, d\Gamma \tag{5.20}$$

5.3.2 Discretization of the visco-elastic problem

The displacement field and corresponding weighting function are interpolated over the element as follows:

$$\Delta\vec{u}(x, y, z) = \sum_{i=1}^{nv} \Delta\vec{u}_i \varphi_i(x, y, z) \tag{5.21}$$

$$\vec{w}(x, y, z) = \sum_{i=1}^{nv} \vec{w}_i \varphi_i(x, y, z) \tag{5.22}$$

where nv is the number of displacement nodes in the element and $\varphi_i(x, y, z)$ is the shape function.
Interpolation of the pressure field and the corresponding weighting function:

$$p(x, y, z) = \sum_{i=1}^{nvp} p_i \psi_i(x, y, z) \tag{5.23}$$

$$q(x,y,z) = \sum_{i=1}^{nvp} q_i \psi_i(x,y,z) \tag{5.24}$$

where nvp is the number of pressure nodes in the element and $\psi_i(x,y,z)$ is the shape function for the pressure.
Interpolation from the weighting function on the boundary element

$$\vec{w}(x,y,z) = \sum_{i=1}^{nvb} \vec{w}_i \chi_i(x,y,z) \tag{5.25}$$

where nvb is the number of displacement nodes in the boundary element and $\chi_i(x,y,z)$ is the shape function from the boundary element.
The discretized system of equations for the visco-elastic case is derived in appendix D. The result is given below

$$\underset{\sim}{w}^T \int_{\Omega^e} \underline{A}^T \left\{ 2\overline{\eta}\frac{1}{\Delta t}\underline{D}_{12} + (\sum_{i=1}^{m} G_i)\frac{1}{\Delta t}\underline{D}_{12} \right\} \underline{A}\, d\Omega \Delta \underset{\sim}{u} +$$

$$\underset{\sim}{w}^T \int_{\Omega^e} -\underline{Q}\, d\Omega \underset{\sim}{p} = \underset{\sim}{w}^T \int_{\Omega^e} -\underline{A}^T \underset{\sim}{c}_{10}\, d\Omega + \underset{\sim}{w}_b^T \int_{\Gamma^e} \underset{\sim}{\chi}^T \underset{\sim}{\chi}\, \underset{\sim}{b}\, d\Gamma \quad \forall\ \underset{\sim}{w} \tag{5.26}$$

and

$$\underset{\sim}{q}^T \int_{\Omega^e} \underset{\sim}{\psi}\, \underset{\sim}{c}_{11}^T \underline{A}\, d\Omega \Delta \underset{\sim}{u} + \underset{\sim}{q}^T \int_{\Omega^e} \kappa \underset{\sim}{\psi}\, \underset{\sim}{\psi}^T d\Omega \underset{\sim}{p} = \underset{\sim}{q}^T \int_{\Omega^e} -\underset{\sim}{\psi} c_{12}\, d\Omega \quad \forall\ \underset{\sim}{q} \tag{5.27}$$

These equations must hold for all admissible weighting functions. So, the contribution from one element in matrix formulation is given by

$$\boxed{\begin{bmatrix} \underline{K}^e & \underline{L} \\ \underline{Z} & \underline{M} \end{bmatrix} \begin{bmatrix} \Delta \underset{\sim}{u} \\ \underset{\sim}{p} \end{bmatrix} = \begin{bmatrix} \underset{\sim}{f}_v \\ \underset{\sim}{k}_v \end{bmatrix} \qquad (5.28)}$$

where

$$\underline{K}^e = \int_{\Omega^e} \underline{A}^T \left\{ 2\overline{\eta}\frac{1}{\Delta t}\underline{D}_{12} + (\sum_{i=1}^{m} G_i)\frac{1}{\Delta t}\underline{D}_{12} \right\} \underline{A}\, d\Omega \tag{5.29}$$

$$\underline{L} = \int_{\Omega^e} -\underline{Q}\, d\Omega \tag{5.30}$$

$$\underline{Z} = \int_{\Omega^e} \underset{\sim}{\psi}\, \underset{\sim}{c}_{11}^T \underline{A}\, d\Omega \tag{5.31}$$

$$\underline{M} = \int_{\Omega^e} \kappa \underset{\sim}{\psi} \underset{\sim}{\psi}^T \, d\Omega \tag{5.32}$$

$$\underset{\sim v}{f} = \int_{\Omega^e} -\underline{A}^T \underset{\sim 10}{c} \, d\Omega + \int_{\Gamma^e} \underset{\sim}{\chi}^T \underset{\sim}{\chi} \underset{\sim}{b} \, d\Gamma \tag{5.33}$$

$$\underset{\sim v}{k} = \int_{\Omega^e} -\underset{\sim}{\psi} c_{12} \, d\Omega \tag{5.34}$$

5.3.3 Discretization of nonlinear visco-elastic problem

The iterative motion (displacement) field and corresponding weighting function are interpolated over the element as follows:

$$\delta\vec{\varphi}(x,y,z) = \sum_{i=1}^{nnv} \delta\varphi_i \, \varphi_i(x,y,z) \tag{5.35}$$

$$\vec{w}(x,y,z) = \sum_{i=1}^{nnv} \vec{w}_i \varphi_i(x,y,z) \tag{5.36}$$

where nnv is the number of displacement nodes in the element and $\varphi_i(x,y,z)$ is the shape function for displacement.

Interpolation of the pressure field, the iterative pressure field and the corresponding weighting function:

$$p(x,y,z) = \sum_{i=1}^{nnvp} p_i \psi_i(x,y,z) \tag{5.37}$$

$$\delta p(x,y,z) = \sum_{i=1}^{nnvp} \delta p_i \psi_i(x,y,z) \tag{5.38}$$

$$q(x,y,z) = \sum_{i=1}^{nnvp} q_i \psi_i(x,y,z) \tag{5.39}$$

where nnvp is the number of pressure nodes in the element and $\psi_i(x,y,z)$ is the shape function for the pressure.

Interpolation from the weighting function on the boundary element

$$\vec{w}(x,y,z) = \sum_{i=1}^{nnvb} \vec{w}_i \chi_i(x,y,z) \tag{5.40}$$

where nnvb is the number of displacement nodes in the boundary element and $\chi_i(x,y,z)$ is the shape function for the boundary element.

The discretized system of equations for the nonlinear visco-elastic problem is derived in appendix D. The result is given below

$$\underset{\sim}{w}^T \int_{\Omega^e} \underline{A}^T \left\{ \underset{\sim}{\psi}^T \underset{\sim}{\hat{p}} \underline{C} + \underline{D} \right\} \underline{A} \, d\Omega \, \delta \underset{\sim}{\varphi} + \underset{\sim}{w}^T \int_{\Omega^e} -\underline{Q} \, d\Omega \, \delta \underset{\sim}{p} =$$

$$\underset{\sim}{w}^T \int_{\Omega^e} \left\{ \underline{Q} \underset{\sim}{p} - \underline{A}^T (\underset{\sim}{\hat{\tau}} + \underset{\sim}{\hat{\tau}}^*) \right\} d\Omega + \underset{\sim}{w}_b^T \int_{\Gamma^e} \underset{\sim}{\chi}^T \underset{\sim}{\chi} \underset{\sim}{b} \, d\Gamma \qquad \forall \ \underset{\sim}{w} \qquad (5.41)$$

and

$$\underset{\sim}{q}^T \int_{\Omega^e} \underset{\sim}{\psi} \left\{ \underset{\sim}{c}_3^T + c_{13} \underset{\sim}{c}_5^T \right\} \underline{A} \, d\Omega \delta \underset{\sim}{\varphi} + \underset{\sim}{q}^T \int_{\Omega^e} \kappa \underset{\sim}{\psi} \underset{\sim}{\psi}^T \, d\Omega \, \delta \underset{\sim}{p} =$$

$$\underset{\sim}{q}^T \int_{\Omega^e} -\underset{\sim}{\psi} c_{13} \, d\Omega \qquad \forall \ \underset{\sim}{q} \qquad (5.42)$$

These equations must hold for all admissible weighting functions. So, the contribution from one element in matrix formulation is given by

$$\begin{bmatrix} \underline{K}_n^e & \underline{L}_n \\ \underline{Z}_n & \underline{M}_n \end{bmatrix} \begin{bmatrix} \delta \underset{\sim}{\varphi} \\ \delta \underset{\sim}{p} \end{bmatrix} = \begin{bmatrix} \underset{\sim}{f}_{nv} \\ \underset{\sim}{k}_{nv} \end{bmatrix} \qquad (5.43)$$

where

$$\underline{K}_n^e = \int_{\Omega^e} \underline{A}^T \left\{ \underset{\sim}{\psi}^T \underset{\sim}{\hat{p}} \underline{C} + \underline{D} \right\} \underline{A} \, d\Omega \qquad (5.44)$$

$$\underline{L}_n = \int_{\Omega^e} -\underline{Q} \, d\Omega \qquad (5.45)$$

$$\underline{Z}_n = \int_{\Omega^e} \underset{\sim}{\psi} \left\{ \underset{\sim}{c}_3^T + c_{13} \underset{\sim}{c}_5^T \right\} \underline{A} \, d\Omega \qquad (5.46)$$

$$\underline{M}_n = \int_{\Omega^e} \kappa \underset{\sim}{\psi} \underset{\sim}{\psi}^T \, d\Omega \qquad (5.47)$$

$$\underset{\sim}{f}_{nv} = \int_{\Omega^e} \left\{ \underline{Q} \underset{\sim}{p} - \underline{A}^T (\underset{\sim}{\hat{\tau}} + \underset{\sim}{\hat{\tau}}^*) \right\} d\Omega + \int_{\Gamma^e} \underset{\sim}{\chi}^T \underset{\sim}{\chi} \underset{\sim}{b} \, d\Gamma \qquad (5.48)$$

$$\underset{\sim}{k}_{nv} = \int_{\Omega^e} -\underset{\sim}{\psi} c_{13} d\Omega \qquad (5.49)$$

5.4 The enriched trilinear element

The element that will be used for the temperature - and visco-elastic problem is the enriched trilinear element. This element is recommended by C.R. Beverly et al. [8] as a good compromise between solution accuracy, computation time and stability for mixed formulations.
The element has 15 displacement (or temperature) nodes and 4 pressure nodes. The displacements nodes are located a the corners of the hexahedral, the centre of the surfaces and one node at the centre of the hexahedral. See figure 5.1. The shape functions are defined using isoparametric coordinates.

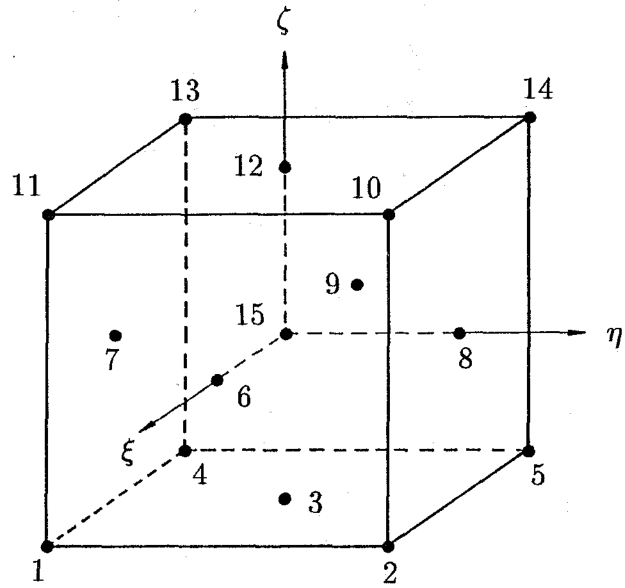

Figure 5.1: The enriched trilinear element.

The transformation to this, so-called $\underset{\sim}{\xi}$ -space with isoparametric coordinates leads to a cube with edges of length two. The shape functions are than derived by taking the trilinear element and adding bubble-functions at the surfaces and one bubble-function over the hole element. Also the derivatives of the shape functions are determined (see appendix E).
The shape functions for the pressure are defined in such way that the pressure field is linear (in the $\underset{\sim}{\xi}$ -space) over the element.
Also a boundary element is defined. This element has five displacement (or temperature) nodes. See appendix F.
The integrals over these elements will be calculated using numerical integration rules. These integration rules are given in appendix G.

5.5 Global system of equations

To obtain the global system of equations the element matrices and right hand sides have to be assembled. But first the element system of equations, can be simplified by elimination of the internal unknowns to save storage and computation time. These unknowns have no connection with other elements. For the temperature problem this is the temperature at the centre-node, for the visco-elastic problem the displacement at the centre-node and the four pressure values. The element system of equations, in general, is given by

$$\begin{bmatrix} \underline{Z}_1 & \underline{Z}_2 \\ \underline{Z}_3 & \underline{Z}_4 \end{bmatrix} \begin{bmatrix} \underset{\sim}{x} \\ \underset{\sim}{x}_{in} \end{bmatrix} = \begin{bmatrix} \underset{\sim}{f} \\ \underset{\sim}{f}_{in} \end{bmatrix} \tag{5.50}$$

where $\underset{\sim}{x}_{in}$ contains the internal unknowns.
The elimination leads to

$$\left(\underline{Z}_1 - \underline{Z}_2\,\underline{Z}_4^{-1}\,\underline{Z}_3\right) \underset{\sim}{x} = \underset{\sim}{f} - \underline{Z}_2\,\underline{Z}_4^{-1}\,\underset{\sim}{f}_{in} \tag{5.51}$$

The global system of equations is given by

$$\underset{\sim}{w}_g^T \left(\mathop{\mathrm{A}}_{e=1}^{n_{el}} \underline{K}^e \right) \underset{\sim}{x}_g = \underset{\sim}{w}_g^T \left(\mathop{\mathrm{A}}_{e=1}^{n_{el}} \underset{\sim}{f}^e \right) \tag{5.52}$$

where: $\mathop{\mathrm{A}}_{e=1}^{n_{el}}$ is the assemble operator

$\underset{\sim}{w}_g$ is the global weighting column
$\underset{\sim}{x}_g$ is the global column with unknowns
$\underline{K}^e$ is the element matrix
$\underset{\sim}{f}^e$ is the element right hand side

For all admissible weighting functions this yields

$$\boxed{\underline{K}\underset{\sim}{x}_g = \underset{\sim}{f}_g} \tag{5.53}$$

where:

$$\underline{K} = \mathop{\mathrm{A}}_{e=1}^{n_{el}} \underline{K}^e \tag{5.54}$$

$$\underset{\sim}{f}_g = \mathop{\mathrm{A}}_{e=1}^{n_{el}} \underset{\sim}{f}^e \tag{5.55}$$

Chapter 6

Numerical simulations

The equations derived in the previous chapter are implemented in the finite element package SEPRAN. Starting-point were a set of subroutines describing incompressible, isothermal visco-elastic behaviour based on a rate-form (Bever [5]). In this chapter the test cases and simulations of the cooling stage are discussed. Also the linear and nonlinear model are compared.

6.1 Test cases

To check the implementation some test cases are performed. For the visco-elastic problem a tension and simple shear test are derived analytical, see appendix H, and compared with simulations using the finite element model. The results are accurate within 0.01%. The displacement field in these tests are linear so this accuracy was expected. The approximation due to time discretization are not studied.
For the temperature problem a test case is obtained for the literature (see appendix H). Performing this test oscillations did occur within the elements. This may be caused by the fact that the approximation field of the enriched element is a combination between linear and quadratic. The oscillations seem to occur only in the nodes that are added to the linear element.

6.2 Simulation of the cooling stage

The model developed is capable of simulating the cooling stage under atmospheric pressure. The global matrix is solved by an iterative solver. Using this method memory usage can be reduced. Two different preconditioning methods are used: diagonal scaling and symmetric Gauss-Seidel.

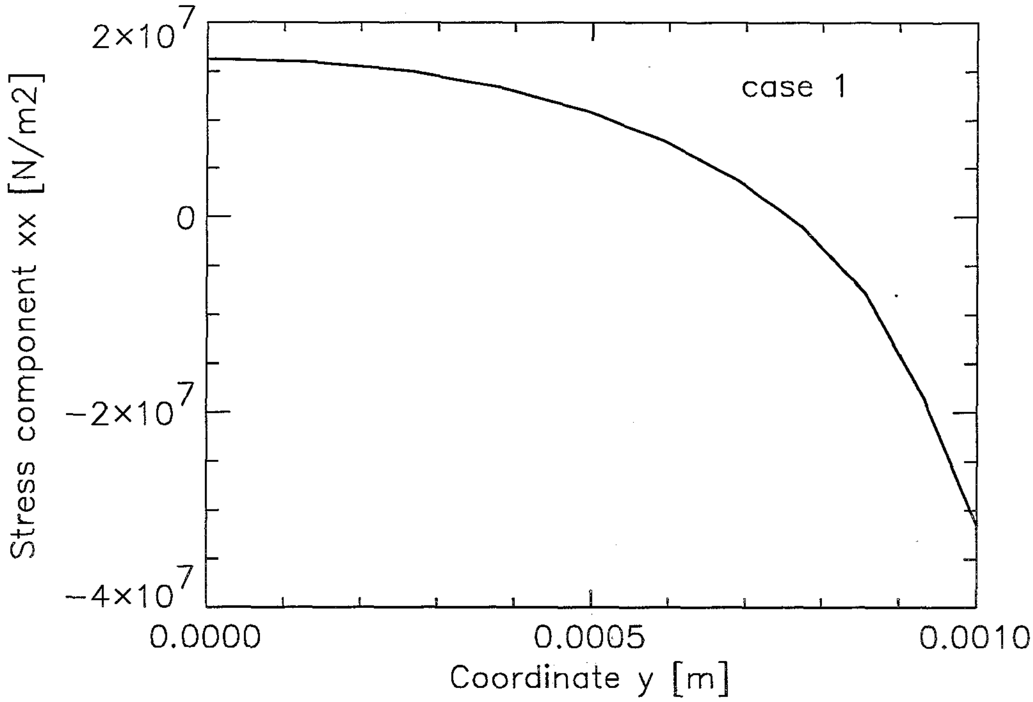

Figure 6.1: Stress component xx versus coordinate y.

At $t = 0$ the material is unloaded and the temperature field is homogeneous at a temperature above the glass transition temperature. A Robin boundary condition is applied on the boundary surfaces assuming the heat transfer to be linear with the temperature difference between boundary and at infinity. The simulations are performed on square or rectangular cubes. For reason of symmetry only one eighth part of the cube has to be simulated. The material used is polycarbonate Makrolon CD 2000. The material data is obtained from Douven [14], see appendix I. Seven cases are examined, detailed data and results are presented in appendix J. The results are discussed below.

Case 1

In this first case a cube is cooled down from 465K to 290K. This test was done to get an impression of the model and the phenomena that take place. The residual stress component xx over the y-axis is given in figure 6.1. A physical explanation for this result can be found in the differential shrinkage during the cooling. The outside surfaces solidify first followed by the middle of the cube. But the shrinkage of the middle of the cube is prevented by the already solidified outside. So in the outside surfaces compression develops and tension stresses develop in the middle of the cube.

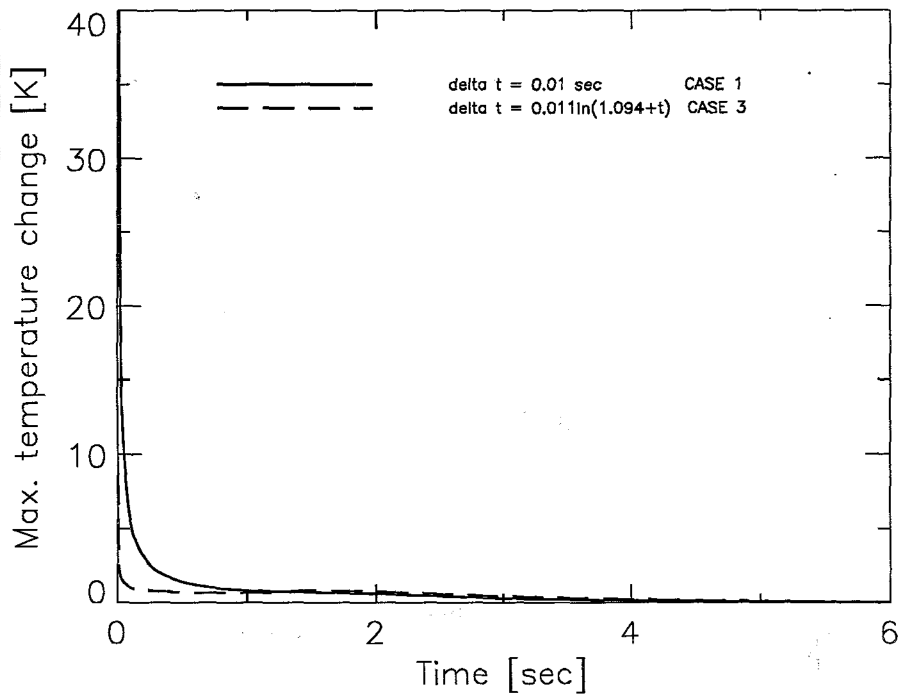

Figure 6.2: Temperature change versus time.

Case 2

In this case mesh refining is performed. Like in case 1, the mesh size is decreasing from the middle of the cube to the surfaces. This is done because the largest temperature gradients arise at the surfaces. The mesh refining from 6x6x6 to 10x10x10 shows that the accuracy of the first case was already quite good, the isobars have the same shape and minimum and maximum values differ only a few per cents. (The largest differences appear in the shear stresses.) In case of the 6x6x6 mesh the element size is 0.11mm at the surface and 0.23mm in the middle of the cube.

Case 3

Using a constant time step of 0.01 sec, the maximum temperature change during one time step starts with 40K, and decreases quickly. To prevent this large temperature change a logarithmic increasing time step is performed in case 3, starting with $\Delta t = 0.001$ to 0.02 sec. The maximum temperature change decreases to 9K, see figure 6.2. This is a more acceptable value. The changes in the results are very small. This may be explained by the fact that these large temperature changes occur in a very small area, the corner of the cube. A remark must be made on the temperature field. Due to the very small time steps oscillations within the elements occur. This may lead

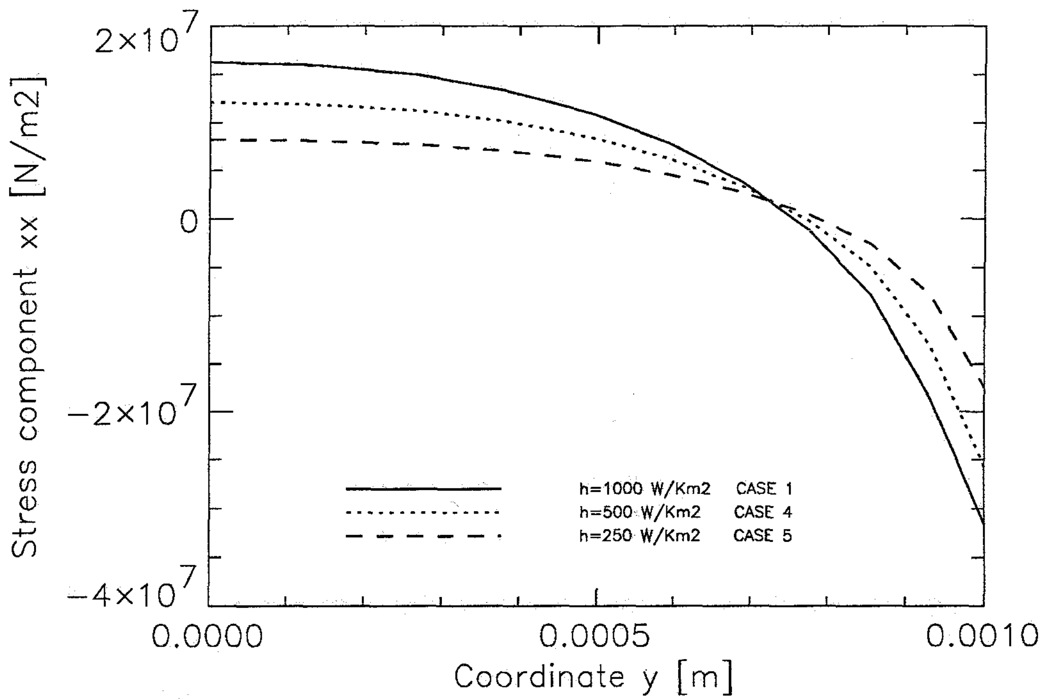

Figure 6.3: Effect of cooling rate on residual stress.

to loss of accuracy .

Case 4 and 5

According to Saffell [23] residual stresses are dependent on the cooling rate. Higher cooling rates give rise to higher residual stresses. In the simulations the cooling rate can be manipulated by the surface heat transfer coefficient h. Three different values of h are used to examen this effect. The residual stress components xx over the y-axis are presented in figure 6.3. The results are in agreement with the literature, also the minimum and maximum values of the residual stresses are in the same order of magnitude.

Case 6

This case is an example of the solidification of a rectangle cube

6.3 Non-linear application

The last case (7) is performed using the nonlinear model. The results are nearly the same as obtained in case 1. This could be expected because at temperatures below T_g, the deformations are small.

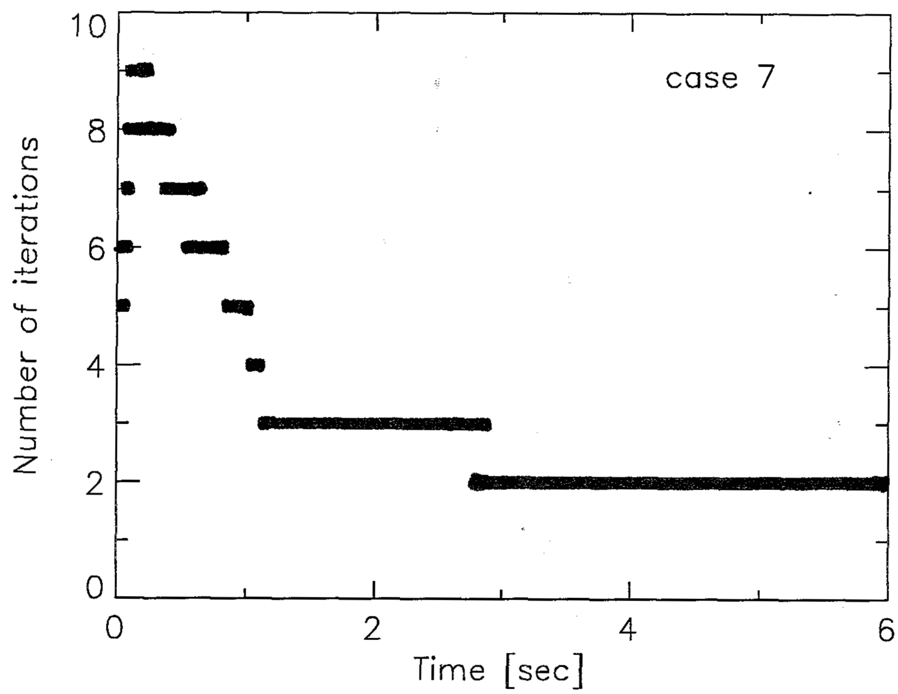

Figure 6.4: Number of iteration steps versus time.

In the beginning of the simulation up to 9 iteration steps are needed, see figure 6.4. Trying to improve the convergence speed some concepts were tested. First $\delta \boldsymbol{D}_{n+\frac{1}{2}}$ was implemented instead of $\delta \boldsymbol{D}_{n+1}$. No significant improvement was obtained. Further the solutions of the previous time steps (displacement and pressure) were taken as the starting values of the new step. With this concept convergence failed at $t = 0.5$ sec. The concept of taking only the pressure from the previous step turned out to be the best. The bad convergence speed at the beginning of the simulations may be caused by the existence of two quite different materials in the cube (melt and glassy state). After all the material in the cube is solidified (below $\pm$ 423K), the number of iterations decreases rapidly, see figure 6.5.

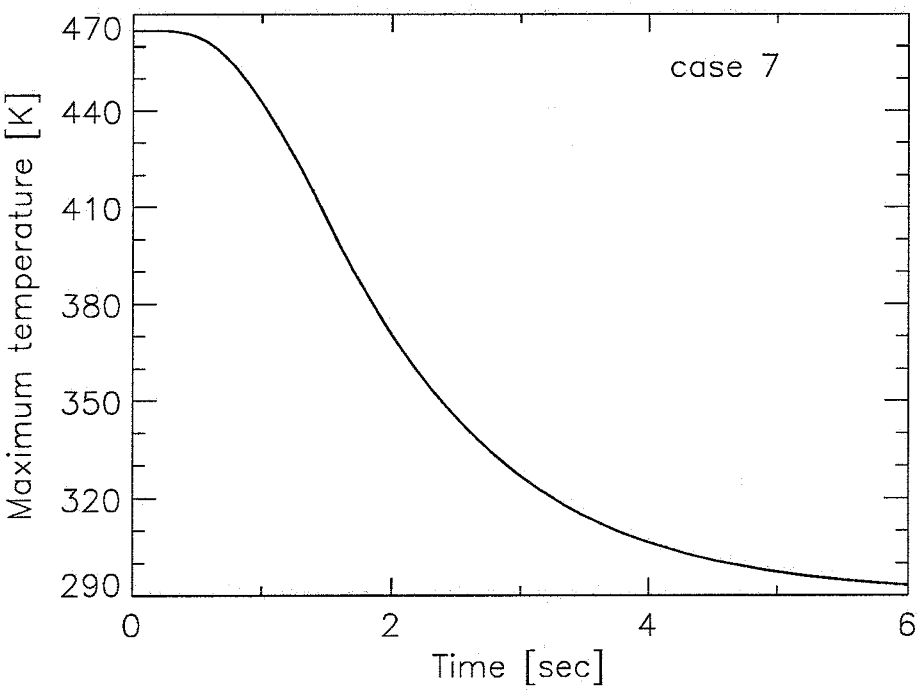

Figure 6.5: Maximum temperature versus time.

Chapter 7

Conclusions and recommendations

In this report a finite element model for the post-filling stage of the injection moulding process is presented. At this stage of development the model is capable of simulating the cooling stage under atmospheric pressure. The model is based on the lagrangian approach, using temperature and displacement as unknowns. The mechanical behaviour is described with the generalized Newtonian fluid model and the generalized multimode Maxwell model. For both models the linear and nonlinear application is given. The temperature and displacement field are solved separately.

A number of conclusions and recommendations for further research are summerized below.

- Compared to the literature available, the results of the presented model, concerning thermally induced residual stresses, are qualitatively good. The effect of the cooling rate is described quite well.

- Simulations with the nonlinear model give the same results as obtained with the linear model. This was expected because the cooling process is assumed to be close to linear. Further research on the nonlinear model is needed. Simulations on a real nonlinear problem should be performed. Instead of using the Truesdell proposition in the relation between the objective tensor $\boldsymbol{\sigma}$ and the invariant tensor $\overline{\boldsymbol{\sigma}}$, the rotation tensor $\boldsymbol{R}$ can be used. Doing this the extra stress tensor is deviatoric.

- In the temperature field oscillations occur. This is a limitation on the time step size. Further research could be done on the performance of other elements on this subject.

- The change from viscous model to visco-elastic model is deposited at the glass transition temperature. Taking into account the elastic effects of the melt stage the model-change temperature must be deposited at a higher value. This could be a topic of further research.

- Two iterative solvers did work for the simulations performed. Using this type of solver the memory usage reduces extremely, an important aspect in 3D simulations.

- The next step in the development of the model is the Updated ALE algorithm. This algorithm is needed in the packing and holding stage. In these stages extra material is pushed into the mould to compensate the shrinkage. Using a Lagrangian approach large mesh distortion arises. The Update ALE algorithm calculates the quantities of interest back to the original mesh each time step using the advection equation.

- Also the model could be based on the Eulerian description. The results to be obtained employing the two different descriptions could be compared. For implementation of mould elasticy the Lagrangian description is more suitable.

Bibliography

[1] Frank P.T. Baaijens. *Applied Computational Mechanics 1.* University of Technology Eindhoven, march 1991.

[2] Frank P.T. Baaijens. *An U-ALE formulation of 3-D unsteady visco-elastic flow.* University of Technology Eindhoven, july 1991.

[3] F.P.T. Baaijens. Calculation of residual stresses in injection molded products. *Rheologica Acta*, 30:284-299, 1991.

[4] A. Balfour and D.H. Marwick. *Programming in standard FORTRAN 77.* Heinemann educational books, London, 1979.

[5] J.J.M. Bever. *Three-dimensional Finite Element Modelling and Computer Simulation of a Visco-elastic Rubber Material.* WFW-report 91.027, Eindhoven, march 1991.

[6] Anniek de Bever. *Towards the computation of the dynamic behaviour of rubber materials.* WFW-report 92.007, Eindhoven, january 1992.

[7] Anniek de Bever. *Dynamic behaviour of rubber and rubberlike materials.* WFW-report 92.006 Eindhoven, january 1992.

[8] C.R. Beverly and R.I. Tanner. Numerical analysis of three-dimensional Newtonian extrudate swell. *Rheologica Acta*, 30:341-356, 1991.

[9] E. Bodewig. *Matrix calculus.* North-Holland Publishing Company, Amsterdam, 1959.

[10] F.J. du Chatenier. *Temperature distribution, heat fluxes, stored heat and thermal penetration depth in semi-infinite solids.* CFT-notitie 032/79, Eindhoven, june 1979.

[11] H.H. Chiang, C.A. Hieber and K.K. Wang. A unified simulation of the filling and postfilling stages in injection molding. part 1: Formulation. *Pol. Eng. and Sc.*, 31:116-124, 1991.

[12] H.H. Chiang, C.A. Hieber and K.K. Wang. A unified simulation of the filling and postfilling stages in injection molding. part 2: Experimental verification. *Pol. Eng. and Sc.*, 31:125-139, 1991.

[13] J.C.A.M. van Doormaal. *A Three-dimensional Finite Element Model for the Rolling Contact Problem in the Capstan Drive of a Video Recorder.* WFW-report 91.026, Eindhoven, april 1991.

[14] L.F.A. Douven. *Towards the computation of properties of injection moulding products.* PhD.thesis, Eindhoven, 1991.

[15] Michel Fortin. Old and new finite elements for incompressible flows. *Int. Journal for numerical methods in fluids*, 1:347-364, 1981.

[16] T.K. Heller. Effective quadrature rules for quadratic solid isoparametric finite elements. *Int. Journal for numerical methods in engineering*, 4:597-600, 1972.

[17] Thomas J.R. Hughes. *The finite element method. Linear static and dynamic finite element analysis.* Prentice-hall, New Jersey, 1987.

[18] Bruce M. Irons. Quadrature rules for brick based finite elements. *International Journal of Numerical Methodes in Engineering*, 2:293-294, 1971.

[19] K.K. Kabanemi and M.J. Crochet. Thermoviscoelastic Calculation of Residual Stresses and Residual Shapes of Injection Molded Parts. *Intern. Polymer Processing*, 7:60-70, 1992.

[20] Sangmoon Lee, Javier de la Vega and Donald C. Bogue. Residual Stresses and Birefringences in Large, Quenched Samples. *Journal of Applied Polymer Science*, 31:2791-2803, 1986.

[21] I. Müller. *Thermodynamics.* Pitman, London, 1985.

[22] C.W.J. Oomens. *Constitutieve Modellen.* University of Technology Eindhoven, january 1992.

[23] J.R. Saffell and A.H. Windle. The Influence of Thermal History on Internal Stress Distributions in Sheet of PMMA and Polycarbonate. *Journal of applied Polymer Science*, 25:1117-1129, 1980.

[24] P.J.G. Schreurs. *Continuumsmechanica.* University of Technology Eindhoven, 1990.

[25] Sepran manuals. *User manual, Programmers Guide and Standard Problems.* Ingenieursbureau SEPRA, Leidschendam 1984.

[26] C.W.M. Sitters. *Numerical Simulation of Injection Moulding.* PhD.thesis, University of Technology Eindhoven, 1988.

[27] Murray R. Spiegel. *Advanced Mathematics for Engineers and Scientists.* McGraw-Hill Book Company, New York, 1971.

[28] J.F.M. Verest. *Thermo-viscoelastische analyse voor een spuitgiet product.* WFW-report 87.043, Eindhoven, june 1987.

[29] C.J. Wust and D.C. Bogue. Stress Optical Behavior in Polystyrene; Residual Stresses and Birefringences in Large, Quenched Samples. *Journal of Applied Polymer Science*, 28:1931-1947, 1983.

[30] P. Zoller. A study of the pressure-volume-temperature relations of four related amorphous polymers: polycarbonate, polyarylate, phenoxy and polysulfone. *Jrnl. of Polymer Sc.*, 20:1453-1464, 1982.

Appendices to

Towards a three-dimensional Finite Element Model for the post-filling stage of Injection Moulding

WFW-report 92.124

J.H.A. Selen

Oktober 1992

Appendix A

Theory of reduced time

Reduced time is introduced to make the constitutive equation suitable for an arbitrary temperature history.

The basic constitutive equation, 1-dimensional and single-mode, is defined:

$$\sigma(t) = G(t)\,\epsilon \tag{A.1}$$

The relaxation function:

$$G(t) = \frac{2\eta}{\theta} e^{-t/\theta} \tag{A.2}$$

Where σ is the stress and ϵ is the strain.
The relaxation time and viscosity are temperature dependent, defining:

$$\theta(T) = a_T \theta_0 \tag{A.3}$$

$$\eta(T) = a_T \eta_0 \tag{A.4}$$

Where a_T is the time temperature shift factor.
For an arbitrary strain history eq. (A.1) yields [22]:

$$G(t) = \int_0^t G(t-\tau)\dot{\epsilon}(\tau)d\tau \tag{A.5}$$

Assuming the material is unloaded at time interval $(-\infty, 0]$. This equation only holds for constant temperature.

First step in the derivation is time discretization. At $t = \tau_i$ the temperature is T_i . The transformation from the relaxation function at reference temperature to T_i can be done by:

$$G_{T_i}(t) = G_{T_0}(t/a_{T_i}) \tag{A.6}$$

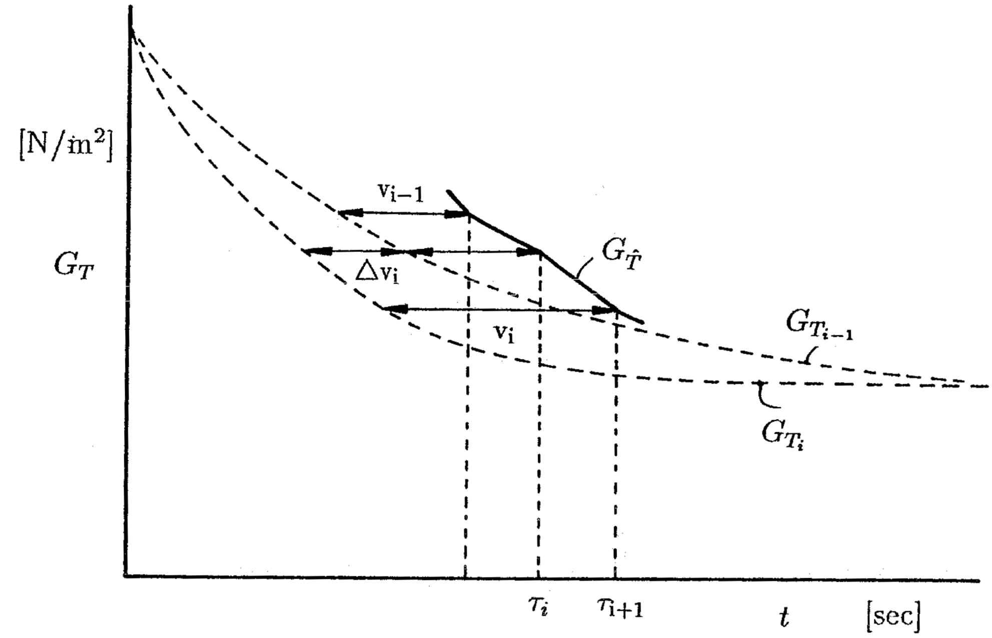

Figure A.1: Construction of $G_{\hat{T}}(t)$.

In figure A.1 the construction of the relaxation function for a given temperature history is shown. In this figure v_i expresses the horizontal shift of the curve. At $t = \tau_i$ the following equality must hold:

$$G_{\hat{T}}(\tau) = G_{T_{i-1}}(\tau_i - v_{i-1}) = G_{T_i}(\tau_i - v_i) \tag{A.7}$$

where:

$$G_{T_{i-1}} = G_{T_0}((\tau_i - v_{i-1})/a_{T_{i-1}}) \tag{A.8}$$

$$G_{T_i} = G_{T_0}((\tau_i - v_i)/a_{T_i}) \tag{A.9}$$

For $\tau_i \leq t \leq \tau_{i+1}$ this yields:

$$\tau_i \Delta a_i = v_i \Delta a_i - a_{T_i} \Delta v_i \tag{A.10}$$

where:

$$\Delta a_i = a_{T_i} - a_{T_{i-1}}, \qquad \Delta v_i = v_i - v_{i-1} \tag{A.11}$$

Transforming eq.(A.10) to a differential equation by decreasing the time interval yields:

$$\tau da = v(\tau) da - a(\tau) dv \tag{A.12}$$

Rearranging eq. (A.12) :

$$-\frac{\tau}{a^2(\tau)}da = d\frac{v}{a} \tag{A.13}$$

Integration and using $v(0) = 0$ yields:

$$v(t) = -a(t)\int_{\tau=0}^{t} \frac{\tau}{a^2(\tau)}da \tag{A.14}$$

Using eq. (A.7) :

$$\begin{aligned}
G_{\hat{T}}(t) &= G_{T_0}\left(\frac{t}{a(t)} + \int_{\tau=0}^{t} \frac{\tau}{a^2(\tau)}da\right) \\
&= G_{T_0}\left(\frac{\tau}{a(\tau)}\Big|_{\tau=0}^{t} + \int_{\tau=0}^{t} \tau d\frac{1}{a}\right) \\
&= G_{T_0}\left(\int_{\tau=0}^{t} \frac{1}{a(\tau)}d\tau\right)
\end{aligned} \tag{A.15}$$

Reduced time is now defined as:

$$\xi(t) = \int_{\tau=0}^{t} \frac{1}{a(\tau)}d\tau \tag{A.16}$$

The constitutive equation for an arbitrary temperature history:

$$\sigma(t) = \int_0^t G(\xi(t) - \xi(\tau))\dot{\epsilon}(\tau)d\tau \tag{A.17}$$

Appendix B

Derivation of the weak form

In this appendix the weak forms of the temperature -, visco-elastic - and nonlinear visco-elastic problem are derived.

B.1 The weak form of the temperature problem

The strong form (**PT**) is given by

Given a heat flux $q^0 : \Gamma_p \mapsto I\!R$, *a surface conductance* $h : \Gamma_h \mapsto I\!R$, *a prescribed temperature field* $T^o_{n+1} : \Gamma_u \mapsto I\!R$, *an initial temperature field* T_n *and pressure field* p_n, *an actual pressure field* p_{n+1}, *extra stress field* $\boldsymbol{\tau}$ *and strain rate* $\boldsymbol{D}$, *find* $T_{n+1} : \Omega \mapsto I\!R$ *such that*

$$\vec{\nabla} \cdot \lambda \vec{\nabla} T_{n+1} + tr(\boldsymbol{\tau} : \boldsymbol{D}) - 1/3 tr(\boldsymbol{\tau}) tr(\boldsymbol{D}) =$$

$$\beta (T_{n+1} - T_n)/\Delta t + \mu T_{n+1}(p_{n+1} - p_n)/\Delta t \tag{B.1}$$

and

$$(\vec{h} \cdot \vec{n} = q^0)_{n+1} \qquad on \ \Gamma_p \tag{B.2}$$

$$\vec{h} \cdot \vec{n} = h\,(T_{n+1} - T_\infty) \qquad on \ \Gamma_h \tag{B.3}$$

$$T_{n+1} = T^0_{n+1} \qquad on \ \Gamma_u \tag{B.4}$$

The weak form of the above problem is obtained by the following actions:

1. Multiplication of equation (B.1) by a weighting function w and integration over Ω.
2. Using integration by parts:

$$\vec{\nabla} \cdot (w \lambda \vec{\nabla} T) = \vec{\nabla} w \cdot \lambda \vec{\nabla} T + w \vec{\nabla} \cdot \lambda \vec{\nabla} T \tag{B.5}$$

3. Application of Gauss theorem:

$$\int_{\Omega} \vec{\nabla} \cdot (w \lambda \vec{\nabla} T) d\Omega = - \int_{\Gamma_p \cap \Gamma_h} wq \, d\Gamma \tag{B.6}$$

Defining the space of trial temperature fields

$$\mathcal{T} = \{T_{n+1} | T_{n+1} \in C^1, T_{n+1} = T^0_{n+1} \; on \; \Gamma_u\} \tag{B.7}$$

and the space of temperature weighting functions as

$$\mathcal{W} = \{w \,|\, w \in C^1, w = 0 \; on \; \Gamma_u\} \tag{B.8}$$

The weak form of the temperature problem (**PTW**) is now given by

Given see **PT**, *find* $T_{n+1} \in \mathcal{T}$ *such that for all* $w \in \mathcal{W}$

$$\begin{aligned} \int_{\Omega} \vec{\nabla} w \cdot \lambda \vec{\nabla} T_{n+1} \, d\Omega = \int_{\Omega} w \, \{ & tr(\boldsymbol{\tau} : \boldsymbol{D}) - 1/3 tr(\boldsymbol{\tau}) tr(\boldsymbol{D}) - \\ & \beta (T_{n+1} - T_n)/\Delta t - \mu T_{n+1} (p_{n+1} - p_n)/\Delta t \} \, d\Omega - \\ & \int_{\Gamma_p} w q^0 \, d\Gamma - \int_{\Gamma_h} w \, \{h(T_{n+1} - T_{\infty})\} \, d\Gamma \end{aligned} \tag{B.9}$$

B.2 The weak form of the linear visco-elastic problem

The strong form (**PVEL**) is given by

Given a boundary load $\vec{p}_{n+1} : \Gamma_p \mapsto \mathbb{R}^n$*, a precribed displacement field* $\Delta\vec{u}^0 : \Gamma_u \mapsto \mathbb{R}^n$*, an initial temperature field* T_n*, – pressure field* p_n *and extra stress field* $\boldsymbol{\tau}_{ni}$ *and an actual temperature field* T_{n+1}*, find* $\Delta\vec{u} : \Omega \mapsto \mathbb{R}^n$ *such that*

$$\vec{\nabla} \cdot \Big(-p_{n+1}\boldsymbol{I} + 2\overline{\eta}\frac{1}{\Delta t}\boldsymbol{\varepsilon}^d(\Delta\vec{u}) + \sum_{i=1}^{m}(G_{ni}\boldsymbol{\tau}^d_{ni}) + (\sum_{i=1}^{m} G_i)\frac{1}{\Delta t}\boldsymbol{\varepsilon}^d(\Delta\vec{u}) \Big) = 0 \tag{B.10}$$

$$\alpha(T_{n+1} - T_n) + \kappa(p_{n+1} - p_n) + tr(\boldsymbol{\varepsilon}(\Delta\vec{u})) = 0 \tag{B.11}$$

$$\Delta\vec{u} = \Delta\vec{u}^0 \qquad on\ \Gamma_u \tag{B.12}$$

$$\boldsymbol{\sigma}_{n+1} \cdot \vec{n}_{n+1} = \vec{p}^{\,0}_{n+1} \qquad on\ \Gamma_p \tag{B.13}$$

The weak form of the above problem is obtained by the following actions:
1. Multiplication of equation (B.10) by a weighting function $\vec{w}$ and integration over Ω.
2. Use of the symmetry of the Cauchy stress tensor and integrating by parts:

$$\vec{\nabla} \cdot \boldsymbol{\sigma} \cdot \vec{w} = (\vec{\nabla}\vec{w})^c : \boldsymbol{\sigma} + \vec{w} \cdot (\vec{\nabla} \cdot \boldsymbol{\sigma}) \tag{B.14}$$

3. Application of Gauss theorem:

$$\int_\Omega \vec{\nabla} \cdot \boldsymbol{\sigma} \cdot \vec{w}\, d\Omega = \int_{\Gamma_p} \vec{w}\vec{p}\, d\Gamma \tag{B.15}$$

4. Multiplication of equation (B.11) by a weighting function q and integration over Ω.

In the sequel the subscript $n+1$ will be omitted for notational simplification. Defining a set of trial solutions for the displacement field

$$\mathcal{U} = \{\Delta\vec{u} \,|\, \Delta\vec{u} \in [C^1]^n, \Delta\vec{u} = \Delta\vec{u}^0\ on\ \Gamma_u\} \tag{B.16}$$

The set of weighting functions is defined likewise by

$$\mathcal{W} = \{\vec{w} \,|\, \vec{w} \in [C^1]^n, \vec{w} = \vec{0} \; on \; \Gamma_u\} \tag{B.17}$$

The set of trial solutions for the pressure field by

$$\mathcal{P} = \{p \,|\, p \in C^0\} \tag{B.18}$$

The set of weighting functions is defined likewise by

$$\mathcal{Q} = \{q \,|\, q \in C^0\} \tag{B.19}$$

The weak form of the linear visco-elastic problem (**PVEW**) is given by

Given see **PVE**, *find* $\Delta\vec{u} \in \mathcal{U}$ *and* $p \in \mathcal{P}$ *such that for all resp.* $w \in \mathcal{W}$ *and* $q \in \mathcal{Q}$

$$\int_\Omega (\vec{\nabla}\vec{w})^c : \left\{ -p\boldsymbol{I} + 2\overline{\eta}\frac{1}{\Delta t}\boldsymbol{\varepsilon}^d(\Delta\vec{u}) + \sum_{i=1}^{m}(G_{ni}\boldsymbol{\tau}^d_{ni}) + \right.$$

$$\left. (\sum_{i=1}^{m} G_i)\frac{1}{\Delta t}\boldsymbol{\varepsilon}^d(\Delta\vec{u}) \right\} d\Omega = \int_{\Gamma_p} \vec{w}\vec{p}\, d\Gamma \tag{B.20}$$

$$\int_\Omega q\left\{\alpha(T - T_n) + \kappa(p - p_n) + tr(\boldsymbol{\varepsilon}(\Delta\vec{u}))\right\} d\Omega = 0 \tag{B.21}$$

B.3 The weak form of the nonlinear visco-elastic problem

The strong form (**NPVE**) is given by

Let the motion during S_n satisfy :

$$\vec{\varphi}_{n+\alpha} = (1-\alpha)\vec{\varphi}_n + \alpha\vec{\varphi}_{n+1}, \qquad \alpha = \frac{t-t_n}{\Delta t} \in [0,1] \tag{B.22}$$

and a boundary load $\vec{p}_{n+1} : \Gamma_p \mapsto I\!R^n$, a precribed motion field $\vec{\varphi}^{\,0}_{n+1} : \Gamma_u \mapsto I\!R^n$, an initial temperature field T_n, – pressure field p_n, – deformation field $\boldsymbol{F}_n$ and extra stress field $\boldsymbol{\tau}_{ni}$ and an actual temperature field T_{n+1}, find $\vec{\varphi}_{n+1} : \Omega \mapsto I\!R$ such that

$$\vec{\nabla} \cdot \Bigg(-p_{n+1}\boldsymbol{I} + 2\bar{\eta}\boldsymbol{D}^d_{n+\frac{1}{2}} + \boldsymbol{F}_{n+1} \cdot \boldsymbol{F}_n^{-1} \cdot \sum_{i=1}^{m} (G_{ni}\boldsymbol{\tau}_{ni}) \cdot \boldsymbol{F}_n^{-c} \cdot \boldsymbol{F}^c_{n+1} +$$

$$(\sum_{i=1}^{m} G_i)\boldsymbol{F}_{n+1} \cdot \boldsymbol{F}^{-1}_{n+\frac{1}{2}} \cdot \boldsymbol{D}^d_{n+\frac{1}{2}} \cdot \boldsymbol{F}^{-c}_{n+\frac{1}{2}} \cdot \boldsymbol{F}^c_{n+1} \Bigg) = 0 \tag{B.23}$$

$$\alpha(T_{n+1} - T_n) + \kappa(p_{n+1} - p_n) + tr(\Delta t \boldsymbol{D}_{n+\frac{1}{2}}) = 0 \tag{B.24}$$

$$\vec{\varphi}_{n+1} = \vec{\varphi}^{\,0}_{n+1} \qquad on\ \Gamma_u \tag{B.25}$$

$$\boldsymbol{\sigma}_{n+1} \cdot \vec{n}_{n+1} = \vec{p}_{n+1} \qquad on\ \Gamma_p \tag{B.26}$$

To obtain the weak form of the problem above the same actions as performed in the last paragraph have to be done. Using the Updated Lagrange method means in this case that $\boldsymbol{F}_n = \boldsymbol{I}$. For further purposes equation (B.23) will be split into two parts.
Defining the set of trial motion solutions

$$\mathcal{X} = \{\vec{\varphi} \,|\, \vec{\varphi} \in [C^1]^n, \vec{\varphi} = \vec{\varphi}^{\,0}\ on\ \Gamma_u\} \tag{B.27}$$

Using also the spaces $\mathcal{W}$, $\mathcal{P}$ and $\mathcal{Q}$ the formulation of the nonlinear visco-elastic problem (**NPVEW**) is given by

Let the motion during S_n *satisfy :*

$$\vec{\varphi}_{n+\alpha} = (1-\alpha)\vec{\varphi}_n + \alpha\vec{\varphi}_{n+1}, \qquad \alpha = \frac{t - t_n}{\Delta t} \in [0,1] \tag{B.28}$$

and see **NPVE**, *find* $\vec{\varphi} \in \mathcal{X}$ *and* $p \in \mathcal{P}$ *such that for all resp.* $w \in \mathcal{W}$ *and* $q \in \mathcal{Q}$

$$A(\vec{w}, p, \vec{\varphi}) = L(\vec{w}, \vec{\varphi}) \qquad \forall \vec{w} \in \mathcal{W} \tag{B.29}$$

$$B(q, p, \vec{\varphi}) = 0 \qquad \forall q \in \mathcal{Q} \tag{B.30}$$

with

$$A(\vec{w}, p, \vec{\varphi}) = \int_\Omega (\vec{\nabla}\vec{w})^c : \Big\{ -p\boldsymbol{I} + 2\overline{\eta}\boldsymbol{D}^d_{n+\frac{1}{2}} + \boldsymbol{F}\cdot\sum_{i=1}^m (G_{ni}\boldsymbol{\tau}_{ni})\cdot\boldsymbol{F}^c + (\sum_{i=1}^m G_i)\boldsymbol{F}\cdot\boldsymbol{F}^{-1}_{n+\frac{1}{2}}\cdot\boldsymbol{D}^d_{n+\frac{1}{2}}\cdot\boldsymbol{F}^{-c}_{n+\frac{1}{2}}\cdot\boldsymbol{F}^c \Big\}\, d\Omega \tag{B.31}$$

$$L(\vec{w}, \vec{\varphi}) = \int_{\Gamma_p} \vec{w}\,\vec{p}\,d\Gamma \tag{B.32}$$

$$B(q, p, \vec{\varphi}) = \int_\Omega q\left\{\alpha(T - T_n) + \kappa(p - p_n) + tr(\Delta t\boldsymbol{D}_{n+\frac{1}{2}})\right\} d\Omega \tag{B.33}$$

Remark on definition of spaces:
$[\ ]^n$: Means that every component must satisfy the condition.
C^k : is the class of functions that are at least k times differentiable.

Appendix C

Determination of the linearized system of equations

In this appendix the linearized system of equations is determined from the nonlinear visco-elastic problem. This system of equations will be used in the Newton-Raphson iteration process.

Starting-point is the following system of equations:

$$A(\vec{w},\hat{p},\hat{\vec{\varphi}}) + \delta_\varphi A(\vec{w},\hat{p},\hat{\vec{\varphi}};\delta\varphi) + \delta_p A(\vec{w},\hat{p},\hat{\vec{\varphi}};\delta p) = L(\vec{w},\hat{\vec{\varphi}}) + \delta_\varphi L(\vec{w},\hat{\vec{\varphi}};\delta\varphi) \tag{C.1}$$

$$B(q,\hat{p},\hat{\vec{\varphi}}) + \delta_\varphi B(q,\hat{p},\hat{\vec{\varphi}};\delta\varphi) + \delta_p B(q,\hat{p},\hat{\vec{\varphi}};\delta p) = 0 \tag{C.2}$$

where

$$A(\vec{w},\hat{p},\hat{\vec{\varphi}}) = \int_\Omega (\vec{\nabla}\vec{w})^c : \left\{ -\hat{p}_{n+1}\boldsymbol{I} + 2\overline{\eta}\boldsymbol{D}^d_{n+\frac{1}{2}} + \boldsymbol{F}_{n+1}\cdot\sum_{i=1}^{m}(G_{ni}\boldsymbol{\tau}_{ni})\cdot\boldsymbol{F}^c_{n+1} + (\sum_{i=1}^{m} G_i)\boldsymbol{F}_{n+1}\cdot\boldsymbol{F}^{-1}_{n+\frac{1}{2}}\cdot\boldsymbol{D}^d_{n+\frac{1}{2}}\cdot\boldsymbol{F}^{-c}_{n+\frac{1}{2}}\cdot\boldsymbol{F}^c_{n+1} \right\} d\Omega \tag{C.3}$$

$$L(\vec{w},\hat{\vec{\varphi}}) = \int_{\Gamma_p} \vec{w}\vec{p}\, d\Gamma \tag{C.4}$$

$$B(q,\hat{p},\hat{\vec{\varphi}}) = \int_\Omega q \left\{ \alpha(T_{n+1}-T_n) + \kappa(\hat{p}_{n+1}-p_n) + tr(\Delta t\boldsymbol{D}_{n+\frac{1}{2}}) \right\} d\Omega \tag{C.5}$$

The definition of the directional derivative of a functional $A(\vec{w}, p, \vec{\varphi})$ into the direction $\delta\vec{\varphi}$ with respect to the third variable

$$\delta_{\varphi} A(\vec{w}, p, \vec{\varphi}; \delta\vec{\varphi}) = \lim_{\theta \to 0} \frac{A(\vec{w}, p, \vec{\varphi} + \theta\delta\vec{\varphi}) - A(\vec{w}, p, \vec{\varphi})}{\theta} \tag{C.6}$$

likewise,

$$\delta_{p} A(\vec{w}, p, \vec{\varphi}; \delta p) = \lim_{\theta \to 0} \frac{A(\vec{w}, p + \theta\delta p, \vec{\varphi}) - A(\vec{w}, p, \vec{\varphi})}{\theta} \tag{C.7}$$

Analogously, the directional derivative of a tensor $\boldsymbol{A}(\vec{\varphi})$ into the direction $\delta\vec{\varphi}$ is defined as

$$\delta \boldsymbol{A}(\vec{\varphi}; \delta\vec{\varphi}) = \lim_{\theta \to 0} \frac{\boldsymbol{A}(\vec{\varphi} + \theta\delta\vec{\varphi}) - \boldsymbol{A}(\vec{\varphi})}{\theta} \tag{C.8}$$

In this appendix only $\delta_{\varphi} A$, $\delta_{p} A$, $\delta_{\varphi} B$ and $\delta_{p} B$ are calculated. The term $\delta_{\varphi} L$ is not calculated because this term is small compared to $\delta_{\varphi} A$ and $\delta_{p} A$, and thus can be neglected for that reason. Further for reason of simplicity, when calculating $\delta_{\varphi}(\boldsymbol{D}_{n+\frac{1}{2}})$, $\delta_{\varphi}(\boldsymbol{D}^{d}_{n+\frac{1}{2}})$ and $\delta_{\varphi}(\boldsymbol{F}_{n+1} \cdot \boldsymbol{F}^{-1}_{n+\frac{1}{2}} \cdot \boldsymbol{D}^{d}_{n+\frac{1}{2}} \cdot \boldsymbol{F}^{-c}_{n+\frac{1}{2}} \cdot \boldsymbol{F}^{c}_{n+1})$, $\alpha = 1$ is used instead of $\alpha = \frac{1}{2}$. Both assumptions can lead, at worse, to a lower speed of convergence of the Newton-Raphson iteration process.

First in the determination some transformations have to be carried out. The term $\vec{\nabla}\vec{w}$ must be made independent of the motion $\vec{\varphi}$ and the integration domain must be transformed to a known domain:

$$\vec{\nabla}\vec{w} = \boldsymbol{F} \cdot \vec{\nabla}_{\circ}\vec{w} \tag{C.9}$$

$$d\Omega = det(\boldsymbol{F}) d\Omega_{\circ} \tag{C.10}$$

So, eq.(C.3) and eq.(C.5) yield

$$\begin{aligned} A(\vec{w}, \hat{p}, \hat{\vec{\varphi}}) = \int_{\Omega_{\circ}} (\vec{\nabla}_{\circ}\vec{w})^{c} : \boldsymbol{F}^{-1}_{n+1} \cdot \Big\{ -p_{n+1}\boldsymbol{I} + 2\overline{\eta}\boldsymbol{D}^{d}_{n+\frac{1}{2}} + \\ \boldsymbol{F}_{n+1} \cdot \sum_{i=1}^{m} (G_{ni}\boldsymbol{\tau}_{ni}) \cdot \boldsymbol{F}^{c}_{n+1} + \\ (\sum_{i=1}^{m} G_{i}) \boldsymbol{F}_{n+1} \cdot \boldsymbol{F}^{-1}_{n+\frac{1}{2}} \cdot \boldsymbol{D}^{d}_{n+\frac{1}{2}} \cdot \boldsymbol{F}^{-c}_{n+\frac{1}{2}} \cdot \boldsymbol{F}^{c}_{n+1}) \Big\} det(\boldsymbol{F}_{n+1}) d\Omega_{0} \end{aligned} \tag{C.11}$$

$$\begin{aligned} B(q, \hat{p}, \hat{\vec{\varphi}}) = \int_{\Omega_{\circ}} q \left\{ \alpha(T_{n+1} - T_{n}) + \kappa(p_{n+1} - p_{n}) + \right. \\ \left. tr(\Delta t \boldsymbol{D}_{n+\frac{1}{2}}) \right\} det(\boldsymbol{F}_{n+1}) d\Omega_{0} \end{aligned} \tag{C.12}$$

In the sequel the subscript $n+1$ is omitted to simplify the notation.
Application of the definition eq. (C.6) on eq. (C.11) yields

$$\begin{aligned}\delta_\varphi A &= \int_{\Omega_0} (\vec{\nabla}_0 \vec{w})^c : \Big\{ \delta(\hat{\boldsymbol{F}}^{-1}) \cdot (-\hat{p}\boldsymbol{I} + \hat{\boldsymbol{\tau}}^* + \hat{\boldsymbol{\tau}})\, det(\hat{\boldsymbol{F}}) + \\ &\qquad \hat{\boldsymbol{F}}^{-1} \cdot (\delta\hat{\boldsymbol{\tau}}^* + \delta\hat{\boldsymbol{\tau}})\, det(\hat{\boldsymbol{F}}) + \\ &\qquad \hat{\boldsymbol{F}}^{-1} \cdot (-\hat{p}\boldsymbol{I} + \hat{\boldsymbol{\tau}}^* + \hat{\boldsymbol{\tau}})\, \delta(det(\hat{\boldsymbol{F}})) \Big\}\, d\Omega \qquad (C.13) \\ &= \int_{\Omega} (\vec{\nabla} \vec{w})^c : \Big\{ \hat{\boldsymbol{F}} \cdot \delta(\hat{\boldsymbol{F}}^{-1}) \cdot (-\hat{p}\boldsymbol{I} + \hat{\boldsymbol{\tau}}^* + \hat{\boldsymbol{\tau}}) + \\ &\qquad (\delta\hat{\boldsymbol{\tau}}^* + \delta\hat{\boldsymbol{\tau}}) + (-\hat{p}\boldsymbol{I} + \hat{\boldsymbol{\tau}}^* + \hat{\boldsymbol{\tau}}) \frac{\delta(det(\hat{\boldsymbol{F}}))}{det(\hat{\boldsymbol{F}})} \Big\}\, d\Omega \qquad (C.14)\end{aligned}$$

where the last estimate of the extra stress tensor from Maxwell model is defined

$$\hat{\boldsymbol{\tau}} = \hat{\boldsymbol{F}} \cdot \sum_{i=1}^{m} (G_{ni}\boldsymbol{\tau}_{ni}) \cdot \hat{\boldsymbol{F}}^c + (\sum_{i=1}^{m} G_i) \hat{\boldsymbol{F}} \cdot \hat{\boldsymbol{F}}^{-1}_{n+\frac{1}{2}} \cdot \boldsymbol{D}^d_{n+\frac{1}{2}} \cdot \hat{\boldsymbol{F}}^{-c}_{n+\frac{1}{2}} \cdot \hat{\boldsymbol{F}}^c \qquad (C.15)$$

and the last estimate from the Newtonian model

$$\hat{\boldsymbol{\tau}}^* = 2\overline{\eta}\boldsymbol{D}^d_{n+\frac{1}{2}} \qquad (C.16)$$

Application of the definition eq. (C.7) on eq. (C.12) yields

$$\delta_p A = \int_\Omega (\vec{\nabla}\vec{w})^c : (-\delta p \boldsymbol{I})\, d\Omega \qquad (C.17)$$

Defining

$$\boldsymbol{L}_{\delta\varphi} = \vec{\nabla}\delta\vec{\varphi} \qquad (C.18)$$

the following expressions can be obtained [1] :

$$\delta\hat{\boldsymbol{F}} = \boldsymbol{L}_{\delta\varphi} \cdot \hat{\boldsymbol{F}} \qquad (C.19)$$

$$\delta\hat{\boldsymbol{F}}^{-1} = -\hat{\boldsymbol{F}}^{-1} \cdot \boldsymbol{L}_{\delta\varphi} \qquad (C.20)$$

$$\delta(det(\hat{\boldsymbol{F}})) = det(\hat{\boldsymbol{F}}) tr(\boldsymbol{L}_{\delta\varphi}) \qquad (C.21)$$

Using eq. (C.8) and $\alpha = 1$:

$$\begin{aligned}\delta\hat{\boldsymbol{\tau}} &= \delta\hat{\boldsymbol{F}} \cdot \sum_{i=1}^{m} (G_{ni}\boldsymbol{\tau}_{ni}) \cdot \hat{\boldsymbol{F}}^c + \hat{\boldsymbol{F}} \cdot \sum_{i=1}^{m} (G_{ni}\boldsymbol{\tau}_{ni}) \cdot \delta(\hat{\boldsymbol{F}}^c) + \\ &\qquad \frac{1}{2}\frac{1}{\Delta \mathrm{t}} (\sum_{i=1}^{m} G_i) \Big\{ \frac{1}{3}\delta(\hat{\boldsymbol{F}}^{-c}) : \hat{\boldsymbol{F}}^{-1}\boldsymbol{I} + \frac{1}{3}\hat{\boldsymbol{F}}^{-c} : \delta(\hat{\boldsymbol{F}}^{-1})\boldsymbol{I} - \\ &\qquad \delta(\hat{\boldsymbol{F}}^{-c}) \cdot \hat{\boldsymbol{F}}^{-1} - \hat{\boldsymbol{F}}^{-c} \cdot \delta(\hat{\boldsymbol{F}}^{-1}) \Big\} \qquad (C.22) \\ &= \boldsymbol{L}_{\delta\varphi} \cdot \check{\boldsymbol{\tau}} + \check{\boldsymbol{\tau}} \cdot \boldsymbol{L}^c_{\delta\varphi} + \\ &\qquad \frac{1}{2}\frac{1}{\Delta t} (\sum_{i=1}^{m} G_i) \Big\{ \boldsymbol{L}^c_{\delta\varphi} \cdot \boldsymbol{B} + \boldsymbol{B} \cdot \boldsymbol{L}_{\delta\varphi} - \frac{2}{3} tr(\boldsymbol{L}^c_{\delta\varphi} \cdot \boldsymbol{B})\boldsymbol{I} \Big\} \qquad (C.23)\end{aligned}$$

and

$$
\begin{aligned}
\delta\hat{\boldsymbol{\tau}}^{*} &= \frac{\overline{\eta}}{\Delta t}\left\{\frac{1}{3}\delta(\hat{\boldsymbol{F}}^{-c}) : \hat{\boldsymbol{F}}^{-1}\boldsymbol{I} + \frac{1}{3}\hat{\boldsymbol{F}}^{-c} : \delta(\hat{\boldsymbol{F}}^{-1})\boldsymbol{I} - \right. \\
&\qquad \left. \delta(\hat{\boldsymbol{F}}^{-c}) \cdot \hat{\boldsymbol{F}}^{-1} - \hat{\boldsymbol{F}}^{-c} \cdot \delta(\hat{\boldsymbol{F}}^{-1})\right\} && \text{(C.24)} \\
&= \frac{\overline{\eta}}{\Delta t}\left\{\boldsymbol{L}_{\delta\varphi}^{c} \cdot \boldsymbol{B} + \boldsymbol{B} \cdot \boldsymbol{L}_{\delta\varphi} - \frac{2}{3}tr(\boldsymbol{L}_{\delta\varphi}^{c} \cdot \boldsymbol{B})\boldsymbol{I}\right\} && \text{(C.25)}
\end{aligned}
$$

where

$$
\breve{\boldsymbol{\tau}} = \hat{\boldsymbol{F}} \cdot \sum_{i=1}^{m}(G_{ni}\boldsymbol{\tau}_{ni}) \cdot \hat{\boldsymbol{F}}^{c} \tag{C.26}
$$

$$
\boldsymbol{B} = \hat{\boldsymbol{F}}^{-c} \cdot \hat{\boldsymbol{F}}^{-1} \tag{C.27}
$$

Using eq. (C.14), (C.21), (C.23) and (C.25) it follows that

$$
\begin{aligned}
\delta_{\varphi}A &= \int_{\Omega}(\vec{\nabla}\vec{w})^{c} : [-\boldsymbol{L}_{\delta\varphi} \cdot (-\hat{p}\boldsymbol{I} + \hat{\boldsymbol{\tau}}^{*} + \hat{\boldsymbol{\tau}}) + \\
&\quad \frac{\overline{\eta}}{\Delta t}\left\{\boldsymbol{L}_{\delta\varphi}^{c} \cdot \boldsymbol{B} + \boldsymbol{B} \cdot \boldsymbol{L}_{\delta\varphi} - \frac{2}{3}tr(\boldsymbol{L}_{\delta\varphi}^{c} \cdot \boldsymbol{B})\boldsymbol{I}\right\} + \\
&\quad \frac{1}{2}\frac{1}{\Delta t}(\sum_{i=1}^{m} G_{i})\left\{\boldsymbol{L}_{\delta\varphi}^{c} \cdot \boldsymbol{B} + \boldsymbol{B} \cdot \boldsymbol{L}_{\delta\varphi} - \frac{2}{3}tr(\boldsymbol{L}_{\delta\varphi}^{c} \cdot \boldsymbol{B})\boldsymbol{I}\right\} + \\
&\quad \boldsymbol{L}_{\delta\varphi} \cdot \breve{\boldsymbol{\tau}} + \breve{\boldsymbol{\tau}} \cdot \boldsymbol{L}_{\delta\varphi}^{c} + (-\hat{p}\boldsymbol{I} + \hat{\boldsymbol{\tau}}^{*} + \hat{\boldsymbol{\tau}}) \cdot tr(\boldsymbol{L}_{\delta\varphi})]\, d\Omega && \text{(C.28)}
\end{aligned}
$$

Application of the definition eq. (C.6) on eq. (C.11) yields

$$
\begin{aligned}
\delta_{\varphi}B &= \int_{\Omega_{o}} q\left[tr(\Delta t\delta\boldsymbol{D}_{n+\frac{1}{2}})det(\hat{\boldsymbol{F}}) + \right. \\
&\qquad \{\alpha(T - T_{n}) + \kappa(\hat{p} - p_{n}) + \\
&\qquad \left. tr(\Delta t\boldsymbol{D}_{n+\frac{1}{2}})\}\, \delta(det(\hat{\boldsymbol{F}}))\right] d\Omega && \text{(C.29)} \\
&= \int_{\Omega} q\left[tr(\Delta t\delta\boldsymbol{D}_{n+\frac{1}{2}}) + \right. \\
&\qquad \{\alpha(T - T_{n}) + \kappa(\hat{p} - p_{n}) + \\
&\qquad \left. tr(\Delta t\boldsymbol{D}_{n+\frac{1}{2}})\}\, \frac{\delta(det(\hat{\boldsymbol{F}}))}{det(\hat{\boldsymbol{F}})}\right] d\Omega && \text{(C.30)} \\
&= \int_{\Omega} q\left[tr(\boldsymbol{L}_{\delta\varphi}^{c} \cdot \boldsymbol{B}) + \left\{\, c_{6} + tr(\Delta t\boldsymbol{D}_{n+\frac{1}{2}})\,\right\} tr(\boldsymbol{L}_{\delta\varphi})\right] d\Omega && \text{(C.31)}
\end{aligned}
$$

where

$$
c_{6} = \alpha(T - T_{n}) + \kappa(\hat{p} - p_{n}) \tag{C.32}
$$

Application of the definition eq. (C.7) on eq. (C.5) yields

$$\delta_p B = \int_\Omega q \{\kappa \delta p\} \, d\Omega \tag{C.33}$$

With the use of equations (C.3), (C.4), (C.5), (C.17), (C.28) (C.31) and (C.33), equations (C.1) and (C.2) can be written as

$$\int_\Omega (\vec{\nabla}\vec{w})^c : \{-\hat{p}\boldsymbol{I} + \hat{\boldsymbol{\tau}}^* + \hat{\boldsymbol{\tau}}\} \, d\Omega + \int_\Omega (\vec{\nabla}\vec{w})^c : [-\boldsymbol{L}_{\delta\varphi} \cdot (-\hat{p}\boldsymbol{I} + \hat{\boldsymbol{\tau}}^* + \hat{\boldsymbol{\tau}}) +$$

$$\frac{\overline{\eta}}{\Delta t} \left\{ \boldsymbol{L}^c_{\delta\varphi} \cdot \boldsymbol{B} + \boldsymbol{B} \cdot \boldsymbol{L}_{\delta\varphi} - \frac{2}{3} tr(\boldsymbol{L}^c_{\delta\varphi} \cdot \boldsymbol{B}) \boldsymbol{I} \right\} + \boldsymbol{L}_{\delta\varphi} \cdot \check{\boldsymbol{\tau}} + \check{\boldsymbol{\tau}} \cdot \boldsymbol{L}^c_{\delta\varphi} +$$

$$\frac{1}{2}\frac{1}{\Delta t} (\sum_{i=1}^{m} G_i) \left\{ \boldsymbol{L}^c_{\delta\varphi} \cdot \boldsymbol{B} + \boldsymbol{B} \cdot \boldsymbol{L}_{\delta\varphi} - \frac{2}{3} tr(\boldsymbol{L}^c_{\delta\varphi} \cdot \boldsymbol{B}) \boldsymbol{I} \right\} + (-\hat{p}\boldsymbol{I} + \hat{\boldsymbol{\tau}}^* +$$

$$\hat{\boldsymbol{\tau}}) \cdot tr(\boldsymbol{L}_{\delta\varphi})] \, d\Omega + \int_\Omega (\vec{\nabla}\vec{w})^c : (-\delta p \boldsymbol{I}) \, d\Omega = \int_{\Gamma_p} \vec{w}\vec{p} \, d\Gamma \tag{C.34}$$

and

$$\int_\Omega q \left\{ c_6 + tr(\Delta t \boldsymbol{D}_{n+\frac{1}{2}}) \right\} d\Omega + \int_\Omega q \left[tr(\boldsymbol{L}^c_{\delta\varphi} \cdot \boldsymbol{B}) + \right.$$

$$\left. \left\{ c_6 + tr(\Delta t \boldsymbol{D}_{n+\frac{1}{2}}) \right\} tr(\boldsymbol{L}_{\delta\varphi}) \right] d\Omega + \int_\Omega q \{\kappa \delta p\} \, d\Omega = 0 \tag{C.35}$$

Denoted as the system of equations from **NPVEWL**.

Appendix D

Discretization

In this appendix the discretization equations of the temperature -, visco-elastic - and nonlinear visco-elastic problem are derived. The subscript $n+1$ will be omitted to simplify the notation.

D.1 Discretization of the temperature problem

Assume T and w approximated with piecewise polynomials of order k, $\mathcal{P}_k$. Let $\mathcal{T}^h$ and $\mathcal{W}^h$ be the finite dimensional approximations to $\mathcal{T}$ and $\mathcal{W}$

$$\mathcal{T}^h = \{T^h | T^h \in C^1, T^h \in \mathcal{P}_k(\Omega^e), T^h = T^0 \; on \; \Gamma_u^e\} \tag{D.1}$$

$$\mathcal{W}^h = \{w^h \,|\, w^h \in C^1, w^h \in \mathcal{P}_k(\Omega^e), w^h = 0 \; on \; \Gamma_u^e\} \tag{D.2}$$

The Galerkin finite element approximation of the temperature problem is now given by ($\mathbf{PTW}^h$)

Given q^0, h, T_n, p, p_n $\boldsymbol{\tau}$, and $\boldsymbol{D}$, find $T \in \mathcal{T}^h$ such that for all $w \in \mathcal{W}^h$

$$\begin{aligned}\int_{\Omega^e} \vec{\nabla} w \cdot \lambda \vec{\nabla} T_{n+1} \, d\Omega = \int_{\Omega^e} w \, \{tr(\boldsymbol{\tau} : \boldsymbol{D}) - 1/3 tr(\boldsymbol{\tau}) tr(\boldsymbol{D}) - \\ \beta(T - T_n)/\Delta t - \mu T(p - p_n)/\Delta t\} \, d\Omega - \\ \int_{\Gamma_p^e} w q^0 \, d\Gamma - \int_{\Gamma_h^e} w \, \{h(T - T_\infty)\} \, d\Gamma\end{aligned} \tag{D.3}$$

Where $\Gamma_p^e = \Gamma_p \bigcap \Gamma^e$ and $\Gamma_h^e = \Gamma_h \bigcap \Gamma^e$
Introducing a three-dimensional Cartesian reference system

$$\vec{\underset{\sim}{e}}^T = [\vec{e}_x \ \ \vec{e}_y \ \ \vec{e}_z] \tag{D.4}$$

So:

$$\vec{\nabla} = \vec{e}_x \frac{\partial}{\partial x} + \vec{e}_y \frac{\partial}{\partial y} + \vec{e}_z \frac{\partial}{\partial z} \tag{D.5}$$

Interpolation of the temperature field on each element

$$T|_{\Omega^e} = \begin{bmatrix} \varphi_1 & \cdots & \varphi_{nT} \end{bmatrix} \begin{bmatrix} T_1 \\ \vdots \\ T_{nT} \end{bmatrix} = \underset{\sim}{\varphi}^T \underset{\sim}{T} \tag{D.6}$$

Likewise the weighting functions

$$w|_{\Omega^e} = \begin{bmatrix} \varphi_1 & \cdots & \varphi_{nT} \end{bmatrix} \begin{bmatrix} w_1 \\ \vdots \\ w_{nT} \end{bmatrix} = \underset{\sim}{\varphi}^T \underset{\sim}{w} \tag{D.7}$$

Where nT is the number of temperature nodes on element.
Interpolation of the temperature field on boundary element

$$T|_{\Gamma^e} = \begin{bmatrix} \chi_1 & \cdots & \chi_{nTb} \end{bmatrix} \begin{bmatrix} T_1 \\ \vdots \\ T_{nTb} \end{bmatrix} = \underset{\sim}{\chi}^T \underset{\sim}{T}_b \tag{D.8}$$

Likewise the weighting functions

$$w|_{\Gamma^e} = \begin{bmatrix} \chi_1 & \cdots & \chi_{nTb} \end{bmatrix} \begin{bmatrix} w_1 \\ \vdots \\ w_{nTb} \end{bmatrix} = \underset{\sim}{\chi}^T \underset{\sim}{w}_b \tag{D.9}$$

Where nTb is the number of temperature nodes on boundary element.
Further defining:

$$\underline{A} = \begin{bmatrix} \frac{\partial}{\partial x} \\ \frac{\partial}{\partial y} \\ \frac{\partial}{\partial z} \end{bmatrix} \begin{bmatrix} \varphi_1 & \cdots & \varphi_{nT} \end{bmatrix} \tag{D.10}$$

The first term can be discretized as follows

$$\begin{aligned} \vec{\nabla} w \cdot \lambda \vec{\nabla} T &= (\underline{A}\underset{\sim}{w})^T \lambda \underline{A}\underset{\sim}{T} \\ &= \underset{\sim}{w}^T \lambda \underline{A}^T \underline{A} \underset{\sim}{T} \end{aligned} \tag{D.11}$$

The second part will first be rewritten and then discretized.
Introducing the abbreviation

$$trtd = tr(\boldsymbol{\tau} : \boldsymbol{D}) - 1/3tr(\boldsymbol{\tau})tr(\boldsymbol{D}) \tag{D.12}$$

Rewriting and discretizing the terms of this part

$$\begin{aligned}
& w\left[trtd - \beta(T - T_n)/\Delta t - \mu T(p - p_n)/\Delta t\right] \\
&= w\left[-T\left\{\beta/\Delta t + \mu(p - p_n)/\Delta t\right\} + trtd + \beta T_n/\Delta t\right] \\
&= \underset{\sim}{w}^T \underset{\sim}{\varphi}\left[-\varphi^T \underset{\sim}{T}\left\{\beta/\Delta t + \mu(p - p_n)/\Delta t\right\} + trtd + \beta T_n/\Delta t\right] \\
&= -\underset{\sim}{w}^T \underset{\sim}{\varphi}\underset{\sim}{\varphi}^T\left\{\beta/\Delta t + \mu(p - p_n)/\Delta t\right\}\underset{\sim}{T} + \underset{\sim}{w}^T \underset{\sim}{\varphi}(trtd + \beta T_n/\Delta t) \\
&= -\underset{\sim}{w}^T \underline{P}\{\beta + \mu(p - p_n)\}/\Delta t \underset{\sim}{T} + \underset{\sim}{w}^T \underset{\sim}{\varphi}(trtd + \beta T_n/\Delta t)
\end{aligned} \tag{D.13}$$

where

$$\underline{P} = \underset{\sim}{\varphi}\underset{\sim}{\varphi}^T \tag{D.14}$$

Discretizing the first boundary term

$$wq^0 = \underset{\sim}{w}_b^T \underset{\sim}{\chi} q^0 \tag{D.15}$$

The second term

$$\begin{aligned}
w\left\{h(T - T_\infty)\right\} &= \underset{\sim}{w}_b^T \underset{\sim}{\chi}\{h(\underset{\sim}{\chi}^T \underset{\sim}{T}_b - T_\infty)\} \\
&= \underset{\sim}{w}_b^T \underset{\sim}{\chi}\underset{\sim}{\chi}^T h \underset{\sim}{T}_b - \underset{\sim}{w}_b^T \underset{\sim}{\chi} h T_\infty
\end{aligned} \tag{D.16}$$

This leads to the discretized equation for the element:

$$\begin{aligned}
& \underset{\sim}{w}^T \int_{\Omega^e}\left[\lambda \underline{A}^T \underline{A} + \underline{P}\{\beta + \mu(p - p_n)\}/\Delta t\right] d\Omega\, \underset{\sim}{T} + \\
& \quad \underset{\sim}{w}_b^T \int_{\Gamma_h^e} \underset{\sim}{\chi}\underset{\sim}{\chi}^T h\, d\Gamma \underset{\sim}{T}_b = \underset{\sim}{w}^T \int_{\Omega^e} \underset{\sim}{\varphi}\left\{trtd + \beta T_n/\Delta t\right\} d\Omega + \\
& \quad\quad \underset{\sim}{w}_b^T \int_{\Gamma_h^e} \underset{\sim}{\chi} h T_\infty\, d\Gamma - \int_{\Gamma_p^e} \underset{\sim}{w}_b^T \underset{\sim}{\chi} q^0\, d\Gamma
\end{aligned} \tag{D.17}$$

D.2 Discretization of the linear visco-elastic problem

Defining the finite dimensional approximations to $\mathcal{U}$, $\mathcal{W}$, $\mathcal{P}$ and $\mathcal{Q}$

$$\mathcal{U}^h = \{\Delta\vec{u}^h \,|\, \Delta\vec{u}^h \in [C^1]^n,\ \Delta\vec{u}^h \in \mathcal{P}^k(\Omega^e),\ \Delta\vec{u}^h = \Delta\vec{u}^0 \ on\ \Gamma_u\} \tag{D.18}$$

$$\mathcal{W}^h = \{\vec{w}^h \,|\, \vec{w}^h \in [C^1]^n,\ \vec{w}^h \in \mathcal{P}^k(\Omega^e),\ \vec{w}^h = \vec{w}^0 \ on\ \Gamma_u\} \tag{D.19}$$

$$\mathcal{P}^h = \{p^h \,|\, p^h \in C^0,\ p^h \in \mathcal{P}^k(\Omega^e)\} \tag{D.20}$$

$$\mathcal{Q}^h = \{q^h \,|\, q^h \in C^0,\ q^h \in \mathcal{P}^k(\Omega^e)\} \tag{D.21}$$

The Galerkin finite element approximation of the visco-elastic problem is now given by $(\mathbf{PVEW}^h)$

Given $\vec{p}$, T_n, T, p_n and $\boldsymbol{\tau}_{ni}$, find $\Delta\vec{u} \in \mathcal{U}^h$ and $p \in \mathcal{P}^h$ such that for all resp. $w \in \mathcal{W}^h$ and $q \in \mathcal{Q}^h$

$$\int_{\Omega^e} (\vec{\nabla}\vec{w})^c : \left\{ -p\boldsymbol{I} + 2\overline{\eta}\frac{1}{\Delta t}\boldsymbol{\varepsilon}^d(\Delta\vec{u}) + \sum_{i=1}^{m}(G_{ni}\boldsymbol{\tau}^d_{ni}) + \right.$$
$$\left. (\sum_{i=1}^{m} G_i)\frac{1}{\Delta t}\boldsymbol{\varepsilon}^d(\Delta\vec{u}) \right\} d\Omega = \int_{\Gamma_p^e} \vec{w}\vec{p}\, d\Gamma \tag{D.22}$$

$$\int_{\Omega^e} q\,\{\alpha(T - T_n) + \kappa(p - p_n) + tr(\boldsymbol{\varepsilon}(\Delta\vec{u}))\}\ d\Omega = 0 \tag{D.23}$$

Where $\Gamma_p^e = \Gamma_p \bigcap \Gamma^e$. Introducing again a three-dimensional Cartesian reference system

$$\underset{\sim}{\vec{e}}^T = [\vec{e}_x \ \ \vec{e}_y \ \ \vec{e}_z] \tag{D.24}$$

So:

$$\vec{\nabla} = \vec{e}_x\frac{\partial}{\partial x} + \vec{e}_y\frac{\partial}{\partial y} + \vec{e}_z\frac{\partial}{\partial z} \tag{D.25}$$

$$\vec{w} = w^x\vec{e}_x + w^y\vec{e}_y + w^z\vec{e}_z \tag{D.26}$$

$$\Delta\vec{u} = \Delta u^x\vec{e}_x + \Delta u^y\vec{e}_y + \Delta u^z\vec{e}_z \tag{D.27}$$

Interpolation of the displacement field on each element

$$\Delta\vec{u}|_{\Omega^e} = \begin{bmatrix} \varphi_1 & 0 & 0 & \cdots & \varphi_{nv} & 0 & 0 \\ 0 & \varphi_1 & 0 & \cdots & 0 & \varphi_{nv} & 0 \\ 0 & 0 & \varphi_1 & \cdots & 0 & 0 & \varphi_{nv} \end{bmatrix} \begin{bmatrix} \Delta u_1^x \\ \Delta u_1^y \\ \Delta u_1^z \\ \vdots \\ \Delta u_{nv}^x \\ \Delta u_{nv}^y \\ \Delta u_{nv}^z \end{bmatrix} = \underline{\varphi}\Delta \underset{\sim}{u} \tag{D.28}$$

Interpolation of the weighting function on each element

$$\vec{w}|_{\Omega^e} = \begin{bmatrix} \varphi_1 & 0 & 0 & \cdots & \varphi_{nv} & 0 & 0 \\ 0 & \varphi_1 & 0 & \cdots & 0 & \varphi_{nv} & 0 \\ 0 & 0 & \varphi_1 & \cdots & 0 & 0 & \varphi_{nv} \end{bmatrix} \begin{bmatrix} w_1^x \\ w_1^y \\ w_1^z \\ \vdots \\ w_{nv}^x \\ w_{nv}^y \\ w_{nv}^z \end{bmatrix} = \underline{\varphi} \underset{\sim}{w} \tag{D.29}$$

Where nv is the number of displacement nodes in the element.
Interpolation of the weighting functions on the boundary element

$$\vec{w}|_{\Gamma^e} = \begin{bmatrix} \chi_1 & 0 & 0 & \cdots & \chi_{nvb} & 0 & 0 \\ 0 & \chi_1 & 0 & \cdots & 0 & \chi_{nvb} & 0 \\ 0 & 0 & \chi_1 & \cdots & 0 & 0 & \chi_{nvb} \end{bmatrix} \begin{bmatrix} w_1^x \\ w_1^y \\ w_1^z \\ \vdots \\ w_{nvb}^x \\ w_{nvb}^y \\ w_{nvb}^z \end{bmatrix} = \underline{\chi} \underset{\sim}{w}_b \tag{D.30}$$

Where nvb is the number of displacement nodes on the boundary element.
Interpolation of the pressure field on the element

$$p|_{\Omega^e} = \begin{bmatrix} p_1 & \cdots & p_{nvp} \end{bmatrix} \begin{bmatrix} \psi_1 \\ \vdots \\ \psi_{nvp} \end{bmatrix} = \underset{\sim}{p}^T \underset{\sim}{\psi} \tag{D.31}$$

Likewise the weighting functions

$$q|_{\Omega^e} = \begin{bmatrix} q_1 & \cdots & q_{nvp} \end{bmatrix} \begin{bmatrix} \psi_1 \\ \vdots \\ \psi_{nvp} \end{bmatrix} = \underset{\sim}{q}^T \underset{\sim}{\psi} \tag{D.32}$$

Where nvp is the number of pressure nodes in the element.
Matrix representation of the linear strain tensor

$$\underset{\sim}{\varepsilon}(\Delta\vec{u}) = \underset{\sim}{\vec{e}} \cdot \boldsymbol{\varepsilon}(\Delta\vec{u}) \cdot \underset{\sim}{\vec{e}}^T = \begin{bmatrix} \varepsilon_{xx} & \varepsilon_{xy} & \varepsilon_{xz} \\ \varepsilon_{xy} & \varepsilon_{yy} & \varepsilon_{yz} \\ \varepsilon_{xz} & \varepsilon_{yz} & \varepsilon_{zz} \end{bmatrix} \tag{D.33}$$

Where

$$\varepsilon_{xx} = \frac{\partial \Delta u^x}{\partial x} \tag{D.34}$$

$$\varepsilon_{xy} = \frac{1}{2}\left(\frac{\partial \Delta u^y}{\partial x} + \frac{\partial \Delta u^x}{\partial y}\right) \tag{D.35}$$

$$\varepsilon_{yy} = \frac{\partial \Delta u^y}{\partial y} \tag{D.36}$$

$$\varepsilon_{zz} = \frac{\partial \Delta u^z}{\partial z} \tag{D.37}$$

$$\varepsilon_{yz} = \frac{1}{2}\left(\frac{\partial \Delta u^z}{\partial y} + \frac{\partial \Delta u^y}{\partial z}\right) \tag{D.38}$$

$$\varepsilon_{xz} = \frac{1}{2}\left(\frac{\partial \Delta u^z}{\partial x} + \frac{\partial \Delta u^x}{\partial z}\right) \tag{D.39}$$

Introducing the column $\underset{\sim}{\varepsilon}$

$$\underset{\sim}{\varepsilon}^T = [\varepsilon_{xx} \quad 2\varepsilon_{xy} \quad \varepsilon_{yy} \quad \varepsilon_{zz} \quad 2\varepsilon_{yz} \quad 2\varepsilon_{xz}] \tag{D.40}$$

Using eq.(D.34) to (D.39) and discretizing

$$\underset{\sim}{\varepsilon} = \begin{bmatrix} \frac{\partial}{\partial x} & 0 & 0 \\ \frac{\partial}{\partial x} & \frac{\partial}{\partial y} & 0 \\ 0 & \frac{\partial}{\partial y} & 0 \\ 0 & 0 & \frac{\partial}{\partial z} \\ 0 & \frac{\partial}{\partial y} & \frac{\partial}{\partial z} \\ \frac{\partial}{\partial x} & 0 & \frac{\partial}{\partial z} \end{bmatrix} \begin{bmatrix} \Delta u^x \\ \Delta u^y \\ \Delta u^z \end{bmatrix} = \underline{A}\Delta\underset{\sim}{u} \tag{D.41}$$

In the last step eq.(D.28) is used, so

$$\underline{A} = \begin{bmatrix} \frac{\partial}{\partial x} & 0 & 0 \\ \frac{\partial}{\partial y} & \frac{\partial}{\partial x} & 0 \\ 0 & \frac{\partial}{\partial y} & 0 \\ 0 & 0 & \frac{\partial}{\partial z} \\ 0 & \frac{\partial}{\partial z} & \frac{\partial}{\partial y} \\ \frac{\partial}{\partial z} & 0 & \frac{\partial}{\partial x} \end{bmatrix} \begin{bmatrix} \varphi_1 & 0 & 0 & \cdots & \varphi_{nv} & 0 & 0 \\ 0 & \varphi_1 & 0 & \cdots & 0 & \varphi_{nv} & 0 \\ 0 & 0 & \varphi_1 & \cdots & 0 & 0 & \varphi_{nv} \end{bmatrix} \tag{D.42}$$

The term $(\vec{\nabla}\vec{w})^c$, denoted as $\boldsymbol{L}_w$, is treated likewise

$$\underline{L}_w = \underset{\sim}{e} \cdot \boldsymbol{L}_w \cdot \underset{\sim}{e}^T = \begin{bmatrix} L_{11} & L_{12} & L_{13} \\ L_{12} & L_{22} & L_{23} \\ L_{13} & L_{23} & L_{33} \end{bmatrix} \tag{D.43}$$

Introducing the column $\underset{\sim}{L}_w$

$$\underset{\sim}{L}_w^T = [L_{11} \quad 2L_{12} \quad L_{22} \quad L_{33} \quad 2L_{23} \quad 2L_{13}] \tag{D.44}$$

So, analogously to eq.(D.41)

$$\underset{\sim}{L}_w = \underline{A}\underset{\sim}{w} \tag{D.45}$$

Discretize the first term of eq.(D.22)

$$\begin{aligned} (\vec{\nabla}\vec{w})^c : -p\boldsymbol{I} &= \boldsymbol{L}_w : -p\boldsymbol{I} \\ &= -tr(\underline{L}_w)p \\ &= -\underset{\sim}{w}^T \underline{Q}\underset{\sim}{p} \end{aligned} \tag{D.46}$$

where

$$\underline{Q} = \begin{bmatrix} \frac{\partial}{\partial x}(\varphi_1) \\ \frac{\partial}{\partial y}(\varphi_1) \\ \frac{\partial}{\partial z}(\varphi_1) \\ \vdots \\ \frac{\partial}{\partial x}(\varphi_{nv}) \\ \frac{\partial}{\partial y}(\varphi_{nv}) \\ \frac{\partial}{\partial z}(\varphi_{nv}) \end{bmatrix} \begin{bmatrix} \psi_1 & \cdots & \psi_{nvp} \end{bmatrix} \tag{D.47}$$

Discretize the second term

$$
\begin{aligned}
(\vec{\nabla}\vec{w})^c : 2\overline{\eta}\frac{1}{\Delta t}\boldsymbol{\varepsilon}^d(\Delta\vec{u}) &= \boldsymbol{L}_w : 2\overline{\eta}\frac{1}{\Delta t}\boldsymbol{\varepsilon}^d(\Delta\vec{u}) \\
&= tr\left(\underline{L}_w : (2\overline{\eta}\frac{1}{\Delta t})\underline{\varepsilon}^d(\Delta\vec{u})\right) \\
&= \underset{\sim}{L}_w^T(2\overline{\eta}\frac{1}{\Delta t})\underline{D}_{12}\underset{\sim}{\varepsilon} \\
&= \underset{\sim}{w}^T\underline{A}^T(2\overline{\eta}\frac{1}{\Delta t})\underline{D}_{12}\underline{A}\Delta\underset{\sim}{u}
\end{aligned}
\tag{D.48}
$$

where

$$
\underline{D}_{12} = \begin{bmatrix} \frac{2}{3} & 0 & -\frac{1}{3} & -\frac{1}{3} & 0 & 0 \\ 0 & \frac{1}{2} & 0 & 0 & 0 & 0 \\ -\frac{1}{3} & 0 & \frac{2}{3} & -\frac{1}{3} & 0 & 0 \\ -\frac{1}{3} & 0 & -\frac{1}{3} & \frac{2}{3} & 0 & 0 \\ 0 & 0 & 0 & 0 & \frac{1}{2} & 0 \\ 0 & 0 & 0 & 0 & 0 & \frac{1}{2} \end{bmatrix}
\tag{D.49}
$$

Discretization of the third term

$$
\begin{aligned}
(\vec{\nabla}\vec{w})^c : \sum_{i=1}^{m}(G_{ni}\boldsymbol{\tau}_{ni}^d) &= \boldsymbol{L} : \tilde{\boldsymbol{\tau}} \\
&= tr\,(\underline{L}_w\,\underline{\tilde{\tau}}) \\
&= \underset{\sim}{L}_w^T\underset{\sim}{c}_{10} \\
&= \underset{\sim}{w}^T\underline{A}^T\underset{\sim}{c}_{10}
\end{aligned}
\tag{D.50}
$$

where

$$
\begin{aligned}
\underline{\tilde{\tau}} &= \underset{\sim}{\vec{e}}\cdot\tilde{\boldsymbol{\tau}}\cdot\underset{\sim}{\vec{e}}^T \\
&= \underset{\sim}{\vec{e}}\cdot\sum_{i=1}^{m}(G_{ni}\boldsymbol{\tau}_{ni}^d)\cdot\underset{\sim}{\vec{e}}^T \\
&= \begin{bmatrix} \tilde{\tau}_{11} & \tilde{\tau}_{12} & \tilde{\tau}_{13} \\ \tilde{\tau}_{12} & \tilde{\tau}_{22} & \tilde{\tau}_{23} \\ \tilde{\tau}_{13} & \tilde{\tau}_{23} & \tilde{\tau}_{33} \end{bmatrix}
\end{aligned}
\tag{D.51}
$$

and

$$
\underset{\sim}{c}_{10}^T = [\tilde{\tau}_{11} \quad \tilde{\tau}_{12} \quad \tilde{\tau}_{22} \quad \tilde{\tau}_{33} \quad \tilde{\tau}_{23} \quad \tilde{\tau}_{13}]
\tag{D.52}
$$

The fourth term can be discretized likewise the second term

$$
(\vec{\nabla}\vec{w})^c : (\sum_{i=1}^{m} G_i)\frac{1}{\Delta t}\boldsymbol{\varepsilon}^d(\Delta\vec{u}) = \underset{\sim}{w}^T\underline{A}^T(\sum_{i=1}^{m} G_i)\underline{D}_{12}\,\underline{A}\Delta\underset{\sim}{u}
\tag{D.53}
$$

In order to discretize the right hand side of eq.(D.22), the representation of $\vec{p}$ with respect to $\{\vec{e}_x \;\; \vec{e}_y \;\; \vec{e}_z\}$ is given by

$$\vec{p} = b^x\vec{e}_x + b^y\vec{e}_y + b^z\vec{e}_z \tag{D.54}$$

Discretizing the vector $\vec{p}$

$$\vec{p} = \underset{\sim}{\chi}\,\underset{\sim}{b} \tag{D.55}$$

where $\underset{\sim}{b}$ is the column with the components of the vector $\vec{p}$ in the element nodes. Thus discretizing the right hand side

$$\vec{w}\vec{p} = \underset{\sim b}{w}^T \underset{\sim}{\chi}^T \underset{\sim}{\chi}\,\underset{\sim}{b} \tag{D.56}$$

Before discretizing eq.(D.23) the terms in this equation are rearranged.
The first term

$$\begin{aligned} q\,\{\alpha(T - T_n) - \kappa p_n\} &= q\,c_{12} \\ &= \underset{\sim}{q}^T \underset{\sim}{\psi} c_{12} \end{aligned} \tag{D.57}$$

where

$$c_{12} = \alpha(T - T_n) - \kappa p_n \tag{D.58}$$

The second term

$$q\,\kappa\,p = \underset{\sim}{q}^T \kappa \underset{\sim}{\chi}\,\underset{\sim}{\chi}^T \underset{\sim}{p} \tag{D.59}$$

The third term

$$\begin{aligned} q\,tr(\boldsymbol{\varepsilon}(\Delta\vec{u})) &= \underset{\sim}{q}^T \underset{\sim}{\psi}\,\underset{\sim 11}{c}^T \underset{\sim}{\varepsilon} \\ &= \underset{\sim}{q}^T \underset{\sim}{\psi}\,\underset{\sim 11}{c}^T \underline{A}\Delta\underset{\sim}{u} \end{aligned} \tag{D.60}$$

where

$$\underset{\sim 11}{c}^T = [\,1 \;\; 0 \;\; 1 \;\; 1 \;\; 0 \;\; 0 \;\; 0\,] \tag{D.61}$$

The discretized system of equations for the element

$$\begin{aligned} &\underset{\sim}{w}^T \int_{\Omega^e} \underline{A}^T \left\{ 2\overline{\eta}\frac{1}{\Delta t}\underline{D}_{12} + \left(\sum_{i=1}^{m} G_i\right)\frac{1}{\Delta t}\underline{D}_{12} \right\} \underline{A}\, d\Omega \Delta \underset{\sim}{u} + \\ &\underset{\sim}{w}^T \int_{\Omega^e} -\underline{Q}\, d\Omega\, \underset{\sim}{p} = \underset{\sim}{w}^T \int_{\Omega^e} -\underline{A}^T \underset{\sim 10}{c}\, d\Omega + \underset{\sim b}{w}^T \int_{\Gamma_p^e} \underset{\sim}{\chi}^T \underset{\sim}{\chi}\,\underset{\sim}{b}\, d\Gamma \end{aligned} \tag{D.62}$$

and

$$\underset{\sim}{q}^T \int_{\Omega^e} \underset{\sim}{\psi}\,\underset{\sim 11}{c}^T \underline{A}\, d\Omega \Delta \underset{\sim}{u} + \underset{\sim}{q}^T \int_{\Omega^e} \kappa \underset{\sim}{\chi}\,\underset{\sim}{\chi}^T\, d\Omega\, \underset{\sim}{p} = \underset{\sim}{q}^T \int_{\Omega^e} -\underset{\sim}{\psi} c_{12}\, d\Omega \tag{D.63}$$

D.3 Discretization of the nonlinear visco-elastic problem

Defining the finite dimensional approximations to $\delta\mathcal{X}_0$, $\delta\mathcal{X}_{n+1}$, $\mathcal{W}$, $\mathcal{P}$ and $\mathcal{Q}$

$$\delta\mathcal{X}_0^h = \{\delta\vec{\varphi}^h \,|\, \delta\vec{\varphi}^h \in [C^1]^n,\ \delta\vec{\varphi}^h \in \mathcal{P}_k(\Omega^e),\ \delta\vec{\varphi}^h = \vec{0} \text{ on } \Gamma_u\} \tag{D.64}$$

$$\delta\mathcal{X}_{n+1}^h = \{\delta\vec{\varphi}^h \,|\, \delta\vec{\varphi}^h \in [C^1]^n,\ \delta\vec{\varphi}^h \in \mathcal{P}_k(\Omega^e),$$
$$\delta\vec{\varphi}^h = \vec{\varphi}^0(\vec{x}_0, t_{n+1}) - \vec{\varphi}^0(\vec{x}_0, t_n) \text{ on } \Gamma_u\} \tag{D.65}$$

$$\mathcal{W}^h = \{\vec{w}^h \,|\, \vec{w}^h \in [C^1]^n,\ \vec{w}^h \in \mathcal{P}_k(\Omega^e),\ \vec{w}^h = 0 \text{ on } \Gamma_u\} \tag{D.66}$$

$$\mathcal{P}^h = \{p^h \,|\, p^h \in C^0,\ p^h \in \mathcal{P}_k(\Omega^e)\} \tag{D.67}$$

$$\mathcal{Q}^h = \{q^h \,|\, q^h \in C^0,\ q^h \in \mathcal{P}_k(\Omega^e)\} \tag{D.68}$$

The first iteration step: $\delta\mathcal{X}_\alpha^h = \delta\mathcal{X}_{n+1}^h$, next iteration steps: $\delta\mathcal{X}_\alpha^h = \delta\mathcal{X}_0^h$. The Galerkin finite element approximation of the nonlinear visco-elastic problem is now given by (**NPVEWL**^{h})

Given $\vec{p}$, T_n, T, p_n, $\boldsymbol{\tau}_{ni}$, $\hat{p}$, and $\hat{\boldsymbol{F}}$, find $\delta\vec{\varphi} \in \delta\mathcal{X}_\alpha^h$ and $p \in \mathcal{P}^h$ such that for all resp. $w \in \mathcal{W}^h$ and $q \in \mathcal{Q}^h$

$$\int_{\Omega^c} (\vec{\nabla}\vec{w})^c : \{-\hat{p}\boldsymbol{I} + \hat{\boldsymbol{\tau}}^* + \hat{\boldsymbol{\tau}}\}\, d\Omega + \int_{\Omega^c} (\vec{\nabla}\vec{w})^c : [-\boldsymbol{L}_{\delta\varphi}\cdot(-\hat{p}\boldsymbol{I} + \hat{\boldsymbol{\tau}}^* + \hat{\boldsymbol{\tau}}) +$$
$$\frac{\overline{\eta}}{\Delta t}\left\{\boldsymbol{L}_{\delta\varphi}^c\cdot\boldsymbol{B} + \boldsymbol{B}\cdot\boldsymbol{L}_{\delta\varphi} - \frac{2}{3}tr(\boldsymbol{L}_{\delta\varphi}^c\cdot\boldsymbol{B})\boldsymbol{I}\right\} + \boldsymbol{L}_{\delta\varphi}\cdot\check{\boldsymbol{\tau}} + \check{\boldsymbol{\tau}}\cdot\boldsymbol{L}_{\delta\varphi}^c +$$
$$\frac{1}{2}\frac{1}{\Delta t}(\sum_{i=1}^m G_i)\left\{\boldsymbol{L}_{\delta\varphi}^c\cdot\boldsymbol{B} + \boldsymbol{B}\cdot\boldsymbol{L}_{\delta\varphi} - \frac{2}{3}tr(\boldsymbol{L}_{\delta\varphi}^c\cdot\boldsymbol{B})\boldsymbol{I}\right\} + (-\hat{p}\boldsymbol{I} + \hat{\boldsymbol{\tau}}^* +$$
$$\hat{\boldsymbol{\tau}})\cdot tr(\boldsymbol{L}_{\delta\varphi})]\, d\Omega + \int_{\Omega^c} (\vec{\nabla}\vec{w})^c : (-\delta p\boldsymbol{I})\, d\Omega = \int_{\Gamma_p^c} \vec{w}\vec{p}\, d\Gamma_p \tag{D.69}$$

and

$$\int_{\Omega^c} q\left\{c_6 + tr(\Delta t\boldsymbol{D}_{n+\frac{1}{2}})\right\} d\Omega + \int_{\Omega^c} q\left[tr(\boldsymbol{L}_{\delta\varphi}^c\cdot\boldsymbol{B}) +\right.$$
$$\left.\left\{c_6 + tr(\Delta t\boldsymbol{D}_{n+\frac{1}{2}})\right\} tr(\boldsymbol{L}_{\delta\varphi})\right] d\Omega + \int_{\Omega^c} q\{\kappa\delta p\}\, d\Omega = 0 \tag{D.70}$$

Where $\Gamma_p^e = \Gamma_p \bigcap \Gamma^e$. Introducing again a three-dimensional Cartesian reference system

$$\underset{\sim}{\vec{e}}^T = [\vec{e}_x \ \ \vec{e}_y \ \ \vec{e}_z] \tag{D.71}$$

So:

$$\vec{\nabla} = \vec{e}_x \frac{\partial}{\partial x} + \vec{e}_y \frac{\partial}{\partial y} + \vec{e}_z \frac{\partial}{\partial z} \tag{D.72}$$

$$\vec{w} = w^x \vec{e}_x + w^y \vec{e}_y + w^z \vec{e}_z \tag{D.73}$$

$$\delta\vec{\varphi} = \delta x \vec{e}_x + \delta y \vec{e}_y + \delta z \vec{e}_z \tag{D.74}$$

Interpolation of iterative motion (displacement) on each element

$$\delta\vec{\varphi}|_{\Omega^e} = \begin{bmatrix} \varphi_1 & 0 & 0 & \cdots & \varphi_{nnv} & 0 & 0 \\ 0 & \varphi_1 & 0 & \cdots & 0 & \varphi_{nnv} & 0 \\ 0 & 0 & \varphi_1 & \cdots & 0 & 0 & \varphi_{nnv} \end{bmatrix} \begin{bmatrix} \delta x_1 \\ \delta y_1 \\ \delta z_1 \\ \vdots \\ \delta x_{nnv} \\ \delta y_{nnv} \\ \delta z_{nnv} \end{bmatrix} = \underline{\varphi} \delta \underset{\sim}{\varphi} \tag{D.75}$$

Interpolation of the weighting function on each element

$$\vec{w}|_{\Omega^e} = \begin{bmatrix} \varphi_1 & 0 & 0 & \cdots & \varphi_{nnv} & 0 & 0 \\ 0 & \varphi_1 & 0 & \cdots & 0 & \varphi_{nnv} & 0 \\ 0 & 0 & \varphi_1 & \cdots & 0 & 0 & \varphi_{nnv} \end{bmatrix} \begin{bmatrix} w_1^x \\ w_1^y \\ w_1^z \\ \vdots \\ w_{nnv}^x \\ w_{nnv}^y \\ w_{nnv}^z \end{bmatrix} = \underline{\varphi} \underset{\sim}{w} \tag{D.76}$$

Where nnv is the number of displacement nodes in the element.
Interpolation of the weighting functions on the boundary element

$$\vec{w}|_{\Gamma^e} = \begin{bmatrix} \chi_1 & 0 & 0 & \cdots & \chi_{nnvb} & 0 & 0 \\ 0 & \chi_1 & 0 & \cdots & 0 & \chi_{nnvb} & 0 \\ 0 & 0 & \chi_1 & \cdots & 0 & 0 & \chi_{nnvb} \end{bmatrix} \begin{bmatrix} w_1^x \\ w_1^y \\ w_1^z \\ \vdots \\ w_{nnvb}^x \\ w_{nnvb}^y \\ w_{nnvb}^z \end{bmatrix} = \underline{\chi} \underset{\sim}{w}_b \tag{D.77}$$

Where *nnvb* is the number of displacement nodes on the boundary element.
Interpolation of the pressure field on the element

$$p|_{\Omega^e} = \begin{bmatrix} p_1 & \cdots & p_{nnvp} \end{bmatrix} \begin{bmatrix} \psi_1 \\ \vdots \\ \psi_{nnvp} \end{bmatrix} = \underset{\sim}{p}^T \underset{\sim}{\psi} \tag{D.78}$$

Interpolation of the iterative pressure field on the element

$$\delta p_{\Omega^e} = \begin{bmatrix} \delta p_1 & \cdots & \delta p_{nnvp} \end{bmatrix} \begin{bmatrix} \psi_1 \\ \vdots \\ \psi_{nnvp} \end{bmatrix} = \delta \underset{\sim}{p}^T \underset{\sim}{\psi} \tag{D.79}$$

Likewise the weighting functions

$$q|_{\Omega^e} = \begin{bmatrix} q_1 & \cdots & q_{nnvp} \end{bmatrix} \begin{bmatrix} \psi_1 \\ \vdots \\ \psi_{nnvp} \end{bmatrix} = \underset{\sim}{q}^T \underset{\sim}{\psi} \tag{D.80}$$

Where *nnvp* is the number of pressure nodes in the element.
Now the tensor $\boldsymbol{L}_{\delta\varphi}$ will be worked out. This tensor can be split into a symmetric and a skew symmetric part [13]

$$\boldsymbol{L}_{\delta\varphi} = \boldsymbol{D}_{\delta\varphi} + \boldsymbol{\Omega}_{\delta\varphi} \tag{D.81}$$

The matrix representation of $\boldsymbol{D}_{\delta\varphi}$ with respect to $\{\vec{e}_x \;\; \vec{e}_y \;\; \vec{e}_z\}$ is denoted by

$$\underline{D}_{\delta\varphi} = \underset{\sim}{\vec{e}} \cdot \boldsymbol{D}_{\delta\varphi} \cdot \underset{\sim}{\vec{e}}^T = \begin{bmatrix} D_{11}^{\delta\varphi} & D_{12}^{\delta\varphi} & D_{13}^{\delta\varphi} \\ D_{12}^{\delta\varphi} & D_{22}^{\delta\varphi} & D_{23}^{\delta\varphi} \\ D_{13}^{\delta\varphi} & D_{23}^{\delta\varphi} & D_{33}^{\delta\varphi} \end{bmatrix} \tag{D.82}$$

The matrix representation of $\boldsymbol{\Omega}_{\delta\varphi}$ with respect to $\{\vec{e}_x \;\; \vec{e}_y \;\; \vec{e}_z\}$ is denoted by

$$\underline{\Omega}_{\delta\varphi} = \underset{\sim}{\vec{e}} \cdot \boldsymbol{\Omega}_{\delta\varphi} \cdot \underset{\sim}{\vec{e}} = \begin{bmatrix} 0 & \Omega_{12}^{\delta\varphi} & -\Omega_{13}^{\delta\varphi} \\ -\Omega_{12}^{\delta\varphi} & 0 & \Omega_{23}^{\delta\varphi} \\ \Omega_{13}^{\delta\varphi} & -\Omega_{23}^{\delta\varphi} & 0 \end{bmatrix} \tag{D.83}$$

So,

$$\underline{L}_{\delta\varphi} = \begin{bmatrix} D_{11}^{\delta\varphi} & D_{12}^{\delta\varphi} + \Omega_{12}^{\delta\varphi} & D_{13}^{\delta\varphi} - \Omega_{13}^{\delta\varphi} \\ D_{12}^{\delta\varphi} - \Omega_{12}^{\delta\varphi} & D_{22}^{\delta\varphi} & D_{23}^{\delta\varphi} + \Omega_{23}^{\delta\varphi} \\ D_{13}^{\delta\varphi} + \Omega_{13}^{\delta\varphi} & D_{23}^{\delta\varphi} - \Omega_{23}^{\delta\varphi} & D_{33}^{\delta\varphi} \end{bmatrix} \tag{D.84}$$

where

$$D_{ij} = \frac{1}{2}\left(\frac{\partial \delta\varphi^i}{\partial \varphi^j} + \frac{\partial \delta\varphi^j}{\partial \varphi^i}\right) \tag{D.85}$$

$$\Omega_{ij} = \frac{1}{2}\left(\frac{\partial\delta\varphi^i}{\partial\varphi^j} + \frac{\partial\delta\varphi^j}{\partial\varphi^i}\right) \tag{D.86}$$

and $\varphi^i = x,\ y,\ z$ for resp. $i = 1,\ 2,\ 3$.
The term $(\vec{\nabla}\vec{w})^c$, denoted as $\boldsymbol{L}_w$, will be treated in the same way. So, the matrix representations, with respect to the Cartesian reference system, of the tensors $\boldsymbol{D}_w$, $\boldsymbol{\Omega}_w$ and $\boldsymbol{L}_w$

$$\underline{D}_w = \begin{bmatrix} D^w_{11} & D^w_{12} & D^w_{13} \\ D^w_{12} & D^w_{22} & D^w_{23} \\ D^w_{13} & D^w_{23} & D^w_{33} \end{bmatrix} \tag{D.87}$$

$$\underline{\Omega}_w = \begin{bmatrix} 0 & \Omega^w_{12} & -\Omega^w_{13} \\ -\Omega^w_{12} & 0 & \Omega^w_{23} \\ \Omega^w_{13} & -\Omega^w_{23} & 0 \end{bmatrix} \tag{D.88}$$

$$\underline{L}_w = \begin{bmatrix} D^w_{11} & D^w_{12} + \Omega^w_{12} & D^w_{13} - \Omega^w_{13} \\ D^w_{12} - \Omega^w_{12} & D^w_{22} & D^w_{23} + \Omega^w_{23} \\ D^w_{13} + \Omega^w_{13} & D^w_{23} - \Omega^w_{23} & D^w_{33} \end{bmatrix} \tag{D.89}$$

Now, introducing the column

$$\underset{\sim}{d}^T_{\delta\varphi} = \left[D^{\delta\varphi}_{11}\ \ 2D^{\delta\varphi}_{12}\ \ D^{\delta\varphi}_{22}\ \ D^{\delta\varphi}_{33}\ \ 2D^{\delta\varphi}_{23}\ \ 2D^{\delta\varphi}_{13}\ \ 2\Omega^{\delta\varphi}_{12}\ \ 2\Omega^{\delta\varphi}_{23}\ \ -2\Omega^{\delta\varphi}_{13}\right] \tag{D.90}$$

Likewise

$$\underset{\sim}{d}^T_{w} = \left[D^{w}_{11}\ \ 2D^{w}_{12}\ \ D^{w}_{22}\ \ D^{w}_{33}\ \ 2D^{w}_{23}\ \ 2D^{w}_{13}\ \ 2\Omega^{w}_{12}\ \ 2\Omega^{w}_{23}\ \ -2\Omega^{w}_{13}\right] \tag{D.91}$$

These columns will be worked out:

$$\underset{\sim}{d}_{\delta\varphi} = \begin{bmatrix} \frac{\partial}{\partial x}(\delta x) \\ \frac{\partial}{\partial y}(\delta x) + \frac{\partial}{\partial x}(\delta y) \\ \frac{\partial}{\partial y}(\delta y) \\ \frac{\partial}{\partial z}(\delta z) \\ \frac{\partial}{\partial z}(\delta y) + \frac{\partial}{\partial y}(\delta z) \\ \frac{\partial}{\partial z}(\delta x) + \frac{\partial}{\partial x}(\delta z) \\ \frac{\partial}{\partial y}(\delta x) - \frac{\partial}{\partial x}(\delta y) \\ \frac{\partial}{\partial z}(\delta y) - \frac{\partial}{\partial y}(\delta z) \\ \frac{\partial}{\partial x}(\delta z) - \frac{\partial}{\partial z}(\delta x) \end{bmatrix} = \begin{bmatrix} \frac{\partial}{\partial x} & 0 & 0 \\ \frac{\partial}{\partial y} & \frac{\partial}{\partial x} & 0 \\ 0 & \frac{\partial}{\partial y} & 0 \\ 0 & 0 & \frac{\partial}{\partial z} \\ 0 & \frac{\partial}{\partial z} & \frac{\partial}{\partial y} \\ \frac{\partial}{\partial z} & 0 & \frac{\partial}{\partial x} \\ \frac{\partial}{\partial y} & -\frac{\partial}{\partial x} & 0 \\ 0 & \frac{\partial}{\partial z} & -\frac{\partial}{\partial y} \\ -\frac{\partial}{\partial z} & 0 & \frac{\partial}{\partial x} \end{bmatrix} \begin{bmatrix} \delta x \\ \delta y \\ \delta z \end{bmatrix} \tag{D.92}$$

Discretizing $\delta\vec{\varphi}$ in eq.(D.92) yields

$$\underset{\sim}{d}_{\delta\varphi} = \underline{A}\,\delta\underset{\sim}{\varphi} \tag{D.93}$$

where

$$\underline{A} = \begin{bmatrix} \frac{\partial}{\partial x} & 0 & 0 \\ \frac{\partial}{\partial y} & \frac{\partial}{\partial x} & 0 \\ 0 & \frac{\partial}{\partial y} & 0 \\ 0 & 0 & \frac{\partial}{\partial z} \\ 0 & \frac{\partial}{\partial z} & \frac{\partial}{\partial y} \\ \frac{\partial}{\partial z} & 0 & \frac{\partial}{\partial x} \\ \frac{\partial}{\partial y} & -\frac{\partial}{\partial x} & 0 \\ 0 & \frac{\partial}{\partial z} & -\frac{\partial}{\partial y} \\ -\frac{\partial}{\partial z} & 0 & \frac{\partial}{\partial x} \end{bmatrix} \begin{bmatrix} \varphi_1 & 0 & 0 & \cdots & \varphi_{nnv} & 0 & 0 \\ 0 & \varphi_1 & 0 & \cdots & 0 & \varphi_{nnv} & 0 \\ 0 & 0 & \varphi_1 & \cdots & 0 & 0 & \varphi_{nnv} \end{bmatrix} \quad \text{(D.94)}$$

Likewise

$$\underset{\sim}{d}_w = \underline{A}\underset{\sim}{w} \qquad \text{(D.95)}$$

Discretizing the first term

$$\begin{aligned} (\vec{\nabla}\vec{w})^c : -\hat{p}\boldsymbol{I} &= \boldsymbol{L}_w : -\hat{p}\boldsymbol{I} \\ &= -tr(\underline{L}_w)\hat{p} \\ &= -\underset{\sim}{w}^T \underline{Q}\,\hat{\underset{\sim}{p}} \end{aligned} \qquad \text{(D.96)}$$

where

$$\underline{Q} = \begin{bmatrix} \frac{\partial}{\partial x}(\varphi_1) \\ \frac{\partial}{\partial y}(\varphi_1) \\ \frac{\partial}{\partial z}(\varphi_1) \\ \vdots \\ \frac{\partial}{\partial x}(\varphi_{nnv}) \\ \frac{\partial}{\partial y}(\varphi_{nnv}) \\ \frac{\partial}{\partial z}(\varphi_{nnv}) \end{bmatrix} \begin{bmatrix} \psi_1 & \cdots & \psi_{nnvp} \end{bmatrix} \qquad \text{(D.97)}$$

The third term

$$\begin{aligned} (\vec{\nabla}\vec{w})^c : \hat{\boldsymbol{\tau}} &= \boldsymbol{L}_w : \hat{\boldsymbol{\tau}} \\ &= tr(\underline{L}_w \hat{\underline{\tau}}) \\ &= \underset{\sim}{d}_w^T \hat{\underset{\sim}{\tau}} && \text{(D.98)} \\ &= \underset{\sim}{w}^T \underline{A}^T \hat{\underset{\sim}{\tau}} && \text{(D.99)} \end{aligned}$$

where (with respect to the Cartesian reference system)

$$\underline{\hat{\tau}} = \underset{\sim}{\vec{e}} \cdot \hat{\boldsymbol{\tau}} \cdot \underset{\sim}{\vec{e}}^T = \begin{bmatrix} \hat{\tau}_{11} & \hat{\tau}_{12} & \hat{\tau}_{13} \\ \hat{\tau}_{12} & \hat{\tau}_{22} & \hat{\tau}_{23} \\ \hat{\tau}_{13} & \hat{\tau}_{23} & \hat{\tau}_{33} \end{bmatrix} \tag{D.100}$$

and

$$\underset{\sim}{\hat{\tau}}^T = [\hat{\tau}_{11} \;\; \hat{\tau}_{12} \;\; \hat{\tau}_{22} \;\; \hat{\tau}_{33} \;\; \hat{\tau}_{23} \;\; \hat{\tau}_{13} \;\; 0 \;\; 0 \;\; 0] \tag{D.101}$$

The second term is now discretized likewise the third term

$$(\vec{\nabla}\vec{w})^c : \hat{\boldsymbol{\tau}}^* = \underset{\sim}{w}^T \underline{A}^T \underset{\sim}{\hat{\tau}}^* \tag{D.102}$$

where simulant to eq.(D.103) and eq.(D.101)

$$\underline{\hat{\tau}}^* = \begin{bmatrix} \hat{\tau}^*_{11} & \hat{\tau}^*_{12} & \hat{\tau}^*_{13} \\ \hat{\tau}^*_{12} & \hat{\tau}^*_{22} & \hat{\tau}^*_{23} \\ \hat{\tau}^*_{13} & \hat{\tau}^*_{23} & \hat{\tau}^*_{33} \end{bmatrix} \tag{D.103}$$

and

$$\underset{\sim}{\hat{\tau}}^{*T} = [\hat{\tau}^*_{11} \;\; \hat{\tau}^*_{12} \;\; \hat{\tau}^*_{22} \;\; \hat{\tau}^*_{33} \;\; \hat{\tau}^*_{23} \;\; \hat{\tau}^*_{13} \;\; 0 \;\; 0 \;\; 0] \tag{D.104}$$

The fourth term

$$\begin{aligned} (\vec{\nabla}\vec{w})^c : \boldsymbol{L}_{\delta\varphi} \cdot \hat{p}\boldsymbol{I} &= \boldsymbol{L}_w : \boldsymbol{L}_{\delta\varphi} \cdot \hat{p}\boldsymbol{I} \\ &= \hat{p}\, tr(\underline{L}_w \underline{L}_{\delta\varphi}) \\ &= \underset{\sim}{d}_w^T \underset{\sim}{\psi}^T \underset{\sim}{\hat{p}} \underline{C}_1 \underset{\sim}{d}_{\delta\varphi} \\ &= \underset{\sim}{w}^T \underline{A}^T \underset{\sim}{\psi}^T \underset{\sim}{\hat{p}} \underline{C}_1 \underline{A}\, \delta\underset{\sim}{\varphi} \end{aligned} \tag{D.105}$$

where

$$\underline{C}_1 = \begin{bmatrix} 1 & 0 & 0 & 0 & 0 & 0 & 0 & 0 & 0 \\ 0 & \frac{1}{2} & 0 & 0 & 0 & 0 & 0 & 0 & 0 \\ 0 & 0 & 1 & 0 & 0 & 0 & 0 & 0 & 0 \\ 0 & 0 & 0 & 1 & 0 & 0 & 0 & 0 & 0 \\ 0 & 0 & 0 & 0 & \frac{1}{2} & 0 & 0 & 0 & 0 \\ 0 & 0 & 0 & 0 & 0 & \frac{1}{2} & 0 & 0 & 0 \\ 0 & 0 & 0 & 0 & 0 & 0 & 0 & 0 & 0 \\ 0 & 0 & 0 & 0 & 0 & 0 & 0 & 0 & 0 \\ 0 & 0 & 0 & 0 & 0 & 0 & 0 & 0 & 0 \end{bmatrix} \tag{D.106}$$

Discretizing the sixth term

$$
\begin{aligned}
(\vec{\nabla}\vec{w})^c : -\boldsymbol{L}_{\delta\varphi}\cdot\hat{\boldsymbol{\tau}} &= -\boldsymbol{L}_w : \boldsymbol{L}_{\delta\varphi}\cdot\hat{\boldsymbol{\tau}} \\
&= -tr(\underline{L}_w\,\underline{L}_{\delta\varphi}\,\underline{\hat{\tau}}) \\
&= \underset{\sim}{d}_w^T\,\underline{D}_1\,\underset{\sim}{d}_{\delta\varphi} \\
&= \underset{\sim}{w}^T\underline{A}^T\underline{D}_1\underline{A}\,\delta\underset{\sim}{\varphi}
\end{aligned}
\tag{D.107}
$$

where

$$
\underline{D}_1 = - \tag{D.108}
$$

$$
\begin{bmatrix}
\hat{\tau}_{11} & \frac{1}{2}\hat{\tau}_{12} & 0 & 0 & 0 & \frac{1}{2}\hat{\tau}_{13} & \frac{1}{2}\hat{\tau}_{12} & 0 & \frac{1}{2}\hat{\tau}_{13} \\
\frac{1}{2}\hat{\tau}_{12} & \frac{(\hat{\tau}_{11}+\hat{\tau}_{22})}{4} & \frac{1}{2}\hat{\tau}_{12} & 0 & \frac{1}{4}\hat{\tau}_{13} & \frac{1}{4}\hat{\tau}_{23} & \frac{(-\hat{\tau}_{11}+\hat{\tau}_{22})}{4} & \frac{1}{4}\hat{\tau}_{13} & \frac{1}{4}\hat{\tau}_{23} \\
0 & \frac{1}{2}\hat{\tau}_{12} & a_{22} & 0 & \frac{1}{2}\hat{\tau}_{23} & 0 & -\frac{1}{2}\hat{\tau}_{12} & \frac{1}{2}\hat{\tau}_{23} & 0 \\
0 & 0 & 0 & \hat{\tau}_{33} & \frac{1}{2}\hat{\tau}_{23} & \frac{1}{2}\hat{\tau}_{13} & 0 & -\frac{1}{2}\hat{\tau}_{23} & -\frac{1}{2}\hat{\tau}_{13} \\
0 & \frac{1}{4}\hat{\tau}_{13} & \frac{1}{2}\hat{\tau}_{23} & \frac{1}{2}\hat{\tau}_{23} & \frac{(\hat{\tau}_{22}+\hat{\tau}_{33})}{4} & \frac{1}{4}\hat{\tau}_{12} & -\frac{1}{4}\hat{\tau}_{13} & \frac{(-\hat{\tau}_{22}+\hat{\tau}_{33})}{4} & -\frac{1}{4}\hat{\tau}_{12} \\
\frac{1}{2}\hat{\tau}_{13} & \frac{1}{4}\hat{\tau}_{23} & 0 & \frac{1}{2}\hat{\tau}_{13} & \frac{1}{4}\hat{\tau}_{12} & \frac{(\hat{\tau}_{11}+\hat{\tau}_{33})}{4} & \frac{1}{4}\hat{\tau}_{23} & -\frac{1}{4}\hat{\tau}_{12} & \frac{(-\hat{\tau}_{11}+\hat{\tau}_{33})}{4} \\
-\frac{1}{2}\hat{\tau}_{12} & \frac{(\hat{\tau}_{11}-\hat{\tau}_{22})}{4} & \frac{1}{2}\hat{\tau}_{12} & 0 & \frac{1}{4}\hat{\tau}_{13} & -\frac{1}{4}\hat{\tau}_{23} & \frac{(-\hat{\tau}_{11}-\hat{\tau}_{22})}{4} & \frac{1}{4}\hat{\tau}_{13} & -\frac{1}{4}\hat{\tau}_{23} \\
0 & -\frac{1}{4}\hat{\tau}_{13} & -\frac{1}{2}\hat{\tau}_{23} & \frac{1}{2}\hat{\tau}_{23} & \frac{(\hat{\tau}_{22}-\hat{\tau}_{33})}{4} & \frac{1}{4}\hat{\tau}_{12} & \frac{1}{4}\hat{\tau}_{13} & \frac{(-\hat{\tau}_{22}-\hat{\tau}_{33})}{4} & -\frac{1}{4}\hat{\tau}_{12} \\
-\frac{1}{2}\hat{\tau}_{13} & -\frac{1}{4}\hat{\tau}_{23} & 0 & \frac{1}{2}\hat{\tau}_{13} & \frac{1}{4}\hat{\tau}_{12} & \frac{(\hat{\tau}_{11}-\hat{\tau}_{33})}{4} & -\frac{1}{4}\hat{\tau}_{23} & -\frac{1}{4}\hat{\tau}_{12} & \frac{(-\hat{\tau}_{11}-\hat{\tau}_{33})}{4}
\end{bmatrix}
$$

The fifth term is treated likewise the sixth term

$$
(\vec{\nabla}\vec{w})^c : -\boldsymbol{L}_{\delta\varphi}\cdot\hat{\boldsymbol{\tau}}^* = \underset{\sim}{w}^T\underline{A}^T\underline{D}_1^*\underline{A}\,\delta\underset{\sim}{\varphi} \tag{D.109}
$$

Where $\underline{D}_1^*$ is the same as $\underline{D}_1$ only with respect to $\hat{\boldsymbol{\tau}}^*$ instead of $\hat{\boldsymbol{\tau}}$.
Discretizing term 7, equal to term 12 (except the constant)

$$
\begin{aligned}
(\vec{\nabla}\vec{w})^c : \boldsymbol{L}^c_{\delta\varphi}\cdot\boldsymbol{B} &= \boldsymbol{L}_w : \boldsymbol{L}^c_{\delta\varphi}\cdot\boldsymbol{B} \\
&= tr(\underline{L}_w\underline{L}^c_{\delta\varphi}\underline{B}) \\
&= \underset{\sim}{d}_w^T\,\underline{D}_4\,\underset{\sim}{d}_{\delta\varphi} \\
&= \underset{\sim}{w}^T\underline{A}^T\underline{D}_4\,\underline{A}\,\delta\underset{\sim}{\varphi}
\end{aligned}
\tag{D.110}
$$

where

$$
\underline{B} = \underset{\sim}{\vec{e}}\cdot\boldsymbol{B}\cdot\underset{\sim}{\vec{e}}^T = \begin{bmatrix} B_{11} & B_{12} & B_{13} \\ B_{12} & B_{22} & B_{23} \\ B_{13} & B_{23} & B_{33} \end{bmatrix} \tag{D.111}
$$

and

$$\underline{D}_4 = \tag{D.112}$$

$$\begin{bmatrix} B_{11} & \frac{1}{2}B_{12} & 0 & 0 & 0 & \frac{1}{2}B_{13} & -\frac{1}{2}B_{12} & 0 & -\frac{1}{2}B_{13} \\ \frac{1}{2}B_{12} & \frac{(B_{11}+B_{22})}{4} & \frac{1}{2}B_{12} & 0 & \frac{1}{4}B_{13} & \frac{1}{4}B_{23} & \frac{(B_{11}-B_{22})}{4} & -\frac{1}{4}B_{13} & -\frac{1}{4}B_{23} \\ 0 & \frac{1}{2}B_{12} & B_{22} & 0 & \frac{1}{2}B_{23} & 0 & \frac{1}{2}B_{12} & -\frac{1}{2}B_{23} & 0 \\ 0 & 0 & 0 & B_{33} & \frac{1}{2}B_{23} & \frac{1}{2}B_{13} & 0 & \frac{1}{2}B_{23} & \frac{1}{2}B_{13} \\ 0 & \frac{1}{4}B_{13} & \frac{1}{2}B_{23} & \frac{1}{2}B_{23} & \frac{(B_{22}+B_{33})}{4} & \frac{1}{4}B_{12} & \frac{1}{4}B_{13} & \frac{(B_{22}-B_{33})}{4} & \frac{1}{4}B_{12} \\ \frac{1}{2}B_{13} & \frac{1}{4}B_{23} & 0 & \frac{1}{2}B_{13} & \frac{1}{4}B_{12} & \frac{(B_{11}+B_{33})}{4} & -\frac{1}{4}B_{23} & \frac{1}{4}B_{12} & \frac{(B_{11}-B_{33})}{4} \\ -\frac{1}{2}B_{12} & \frac{(B_{11}-B_{22})}{4} & \frac{1}{2}B_{12} & 0 & \frac{1}{4}B_{13} & -\frac{1}{4}B_{23} & \frac{(B_{11}+B_{22})}{4} & -\frac{1}{4}B_{13} & \frac{1}{4}{}_{23} \\ 0 & -\frac{1}{4}B_{13} & -\frac{1}{2}B_{23} & \frac{1}{2}B_{23} & \frac{(B_{22}-B_{33})}{4} & \frac{1}{4}B_{12} & -\frac{1}{4}B_{13} & \frac{(B_{22}+B_{33})}{4} & \frac{1}{4}B_{12} \\ -\frac{1}{2}B_{13} & -\frac{1}{4}B_{23} & 0 & \frac{1}{2}B_{13} & \frac{1}{4}B_{12} & \frac{(B_{11}-B_{33})}{4} & \frac{1}{4}B_{23} & \frac{1}{4}B_{12} & \frac{(B_{11}+B_{33})}{4} \end{bmatrix}$$

Discretizing term 8, equal to term 13 (except the constant)

$$\begin{aligned} (\vec{\nabla}\vec{w})^c : \boldsymbol{B} \cdot \boldsymbol{L}_{\delta\varphi} &= \boldsymbol{L}_w : \boldsymbol{B} \cdot \boldsymbol{L}_{\delta\varphi} \\ &= tr(\underline{L}_w \, \underline{B} \, \underline{L}_{\delta\varphi}) \\ &= \underset{\sim}{d}_w^T \underline{D}_5 \underset{\sim}{d}_{\delta\varphi} \\ &= \underset{\sim}{w}^T \underline{A}^T \underline{D}_5 \, \underline{A} \, \delta\underset{\sim}{\varphi} \end{aligned} \tag{D.113}$$

where

$$\underline{D}_5 = \tag{D.114}$$

$$\begin{bmatrix} B_{11} & \frac{1}{2}B_{12} & 0 & 0 & 0 & \frac{1}{2}B_{13} & -\frac{1}{2}B_{12} & 0 & -\frac{1}{2}B_{13} \\ \frac{1}{2}B_{12} & \frac{B_{11}+B_{22}}{4} & \frac{1}{2}B_{12} & 0 & \frac{1}{4}B_{13} & \frac{1}{4}B_{23} & \frac{B_{11}-B_{22}}{4} & -\frac{1}{4}B_{13} & -\frac{1}{4}B_{23} \\ 0 & \frac{1}{2}B_{12} & B_{22} & 0 & \frac{1}{2}B_{23} & 0 & \frac{1}{2}B_{12} & -\frac{1}{2}B_{23} & 0 \\ 0 & 0 & 0 & B_{33} & \frac{1}{2}B_{23} & \frac{1}{2}B_{13} & 0 & \frac{1}{2}B_{23} & \frac{1}{2}B_{13} \\ 0 & \frac{1}{4}B_{13} & \frac{1}{2}B_{23} & \frac{1}{2}B_{23} & \frac{B_{22}+B_{33}}{4} & \frac{1}{4}B_{12} & \frac{1}{4}B_{13} & \frac{B_{22}-B_{33}}{4} & \frac{1}{4}B_{12} \\ \frac{1}{2}B_{13} & \frac{1}{4}B_{23} & 0 & \frac{1}{2}B_{13} & \frac{1}{4}B_{12} & \frac{B_{11}+B_{33}}{4} & -\frac{1}{4}B_{23} & \frac{1}{4}B_{12} & \frac{B_{11}-B_{33}}{4} \\ \frac{1}{2}B_{12} & \frac{-B_{11}+B_{22}}{4} & -\frac{1}{2}B_{12} & 0 & -\frac{1}{4}B_{13} & \frac{1}{4}B_{23} & \frac{-B_{11}-B_{22}}{4} & \frac{1}{4}B_{13} & -\frac{1}{4}{}_{23} \\ 0 & \frac{1}{4}B_{13} & \frac{1}{2}B_{23} & -\frac{1}{2}B_{23} & \frac{B_{22}+B_{33}}{4} & -\frac{1}{4}B_{12} & \frac{1}{4}B_{13} & \frac{-B_{22}-B_{33}}{4} & -\frac{1}{4}B_{12} \\ \frac{1}{2}B_{13} & \frac{1}{4}B_{23} & 0 & -\frac{1}{2}B_{13} & -\frac{1}{4}B_{12} & \frac{-B_{11}+B_{33}}{4} & -\frac{1}{4}B_{23} & -\frac{1}{4}B_{12} & \frac{-B_{11}-B_{33}}{4} \end{bmatrix}$$

Discretizing term 9, equal to term 14 (except the constant)

$$
\begin{aligned}
(\vec{\nabla}\vec{w})^c : -\frac{2}{3}tr(\boldsymbol{L}^c_{\delta\varphi}\cdot\boldsymbol{B})\boldsymbol{I} &= -\frac{2}{3}\boldsymbol{L}_w : \boldsymbol{I}\,tr(\boldsymbol{L}^c_{\delta\varphi}\cdot\boldsymbol{B}) \\
&= -\frac{2}{3}tr(\underline{L}_w)tr(\underline{L}^c_{\delta\varphi}\underline{B}) \\
&= \underset{\sim}{d}^T_w\underline{D}_7\underset{\sim}{d}_{\delta\varphi} \\
&= \underset{\sim}{w}^T\underline{A}^T\underline{D}_7\underline{A}\delta\underset{\sim}{\varphi}
\end{aligned}
\tag{D.115}
$$

where

$$
\underline{D}_7 = -\frac{2}{3}\begin{bmatrix}
B_{11} & B_{12} & B_{22} & B_{33} & B_{23} & B_{13} & 0 & 0 & 0 \\
0 & 0 & 0 & 0 & 0 & 0 & 0 & 0 & 0 \\
B_{11} & B_{12} & B_{22} & B_{33} & B_{23} & B_{13} & 0 & 0 & 0 \\
B_{11} & B_{12} & B_{22} & B_{33} & B_{23} & B_{13} & 0 & 0 & 0 \\
0 & 0 & 0 & 0 & 0 & 0 & 0 & 0 & 0 \\
0 & 0 & 0 & 0 & 0 & 0 & 0 & 0 & 0 \\
0 & 0 & 0 & 0 & 0 & 0 & 0 & 0 & 0 \\
0 & 0 & 0 & 0 & 0 & 0 & 0 & 0 & 0 \\
0 & 0 & 0 & 0 & 0 & 0 & 0 & 0 & 0
\end{bmatrix}
\tag{D.116}
$$

Discretizing term 10

$$
\begin{aligned}
(\vec{\nabla}\vec{w})^c : \boldsymbol{L}_{\delta\varphi}\cdot\breve{\boldsymbol{\tau}} &= \boldsymbol{L}_w : \boldsymbol{L}_{\delta\varphi}\cdot\breve{\boldsymbol{\tau}} \\
&= tr(\underline{L}_w)\underline{L}_{\delta\varphi}\underline{\breve{\tau}}) \\
&= \underset{\sim}{d}^T_w\underline{D}_2\underset{\sim}{d}_{\delta\varphi} \\
&= \underset{\sim}{w}^T\underline{A}^T\underline{D}_2\underline{A}\delta\underset{\sim}{\varphi}
\end{aligned}
\tag{D.117}
$$

where

$$
\underline{\breve{\tau}} = \begin{bmatrix}
\breve{\tau}_{11} & \breve{\tau}_{12} & \breve{\tau}_{13} \\
\breve{\tau}_{12} & \breve{\tau}_{22} & \breve{\tau}_{23} \\
\breve{\tau}_{13} & \breve{\tau}_{23} & \breve{\tau}_{33}
\end{bmatrix}
\tag{D.118}
$$

and

$$\underline{D}_2 = \tag{D.119}$$

$$\begin{bmatrix}
\breve{\tau}_{11} & \frac{1}{2}\breve{\tau}_{12} & 0 & 0 & 0 & \frac{1}{2}\breve{\tau}_{13} & \frac{1}{2}\breve{\tau}_{12} & 0 & \frac{1}{2}\breve{\tau}_{13} \\
\frac{1}{2}\breve{\tau}_{12} & \frac{(\breve{\tau}_{11}+\breve{\tau}_{22})}{4} & \frac{1}{2}\breve{\tau}_{12} & 0 & \frac{1}{4}\breve{\tau}_{13} & \frac{1}{4}\breve{\tau}_{23} & \frac{(-\breve{\tau}_{11}+\breve{\tau}_{22})}{4} & \frac{1}{4}\breve{\tau}_{13} & \frac{1}{4}\breve{\tau}_{23} \\
0 & \frac{1}{2}\breve{\tau}_{12} & a_{22} & 0 & \frac{1}{2}\breve{\tau}_{23} & 0 & -\frac{1}{2}\breve{\tau}_{12} & \frac{1}{2}\breve{\tau}_{23} & 0 \\
0 & 0 & 0 & \breve{\tau}_{33} & \frac{1}{2}\breve{\tau}_{23} & \frac{1}{2}\breve{\tau}_{13} & 0 & -\frac{1}{2}\breve{\tau}_{23} & -\frac{1}{2}\breve{\tau}_{13} \\
0 & \frac{1}{4}\breve{\tau}_{13} & \frac{1}{2}\breve{\tau}_{23} & \frac{1}{2}\breve{\tau}_{23} & \frac{(\breve{\tau}_{22}+\breve{\tau}_{33})}{4} & \frac{1}{4}\breve{\tau}_{12} & -\frac{1}{4}\breve{\tau}_{13} & \frac{(-\breve{\tau}_{22}+\breve{\tau}_{33})}{4} & -\frac{1}{4}\breve{\tau}_{12} \\
\frac{1}{2}\breve{\tau}_{13} & \frac{1}{4}\breve{\tau}_{23} & 0 & \frac{1}{2}\breve{\tau}_{13} & \frac{1}{4}\breve{\tau}_{12} & \frac{(\breve{\tau}_{11}+\breve{\tau}_{33})}{4} & \frac{1}{4}\breve{\tau}_{23} & -\frac{1}{4}\breve{\tau}_{12} & \frac{(-\breve{\tau}_{11}+\breve{\tau}_{33})}{4} \\
-\frac{1}{2}\breve{\tau}_{12} & \frac{(\breve{\tau}_{11}-\breve{\tau}_{22})}{4} & \frac{1}{2}\breve{\tau}_{12} & 0 & \frac{1}{4}\breve{\tau}_{13} & -\frac{1}{4}\breve{\tau}_{23} & \frac{(-\breve{\tau}_{11}-\breve{\tau}_{22})}{4} & \frac{1}{4}\breve{\tau}_{13} & -\frac{1}{4}\breve{\tau}_{23} \\
0 & -\frac{1}{4}\breve{\tau}_{13} & -\frac{1}{2}\breve{\tau}_{23} & \frac{1}{2}\breve{\tau}_{23} & \frac{(\breve{\tau}_{22}-\breve{\tau}_{33})}{4} & \frac{1}{4}\breve{\tau}_{12} & \frac{1}{4}\breve{\tau}_{13} & \frac{(-\breve{\tau}_{22}-\breve{\tau}_{33})}{4} & -\frac{1}{4}\breve{\tau}_{12} \\
-\frac{1}{2}\breve{\tau}_{13} & -\frac{1}{4}\breve{\tau}_{23} & 0 & \frac{1}{2}\breve{\tau}_{13} & \frac{1}{4}\breve{\tau}_{12} & \frac{(\breve{\tau}_{11}-\breve{\tau}_{33})}{4} & -\frac{1}{4}\breve{\tau}_{23} & -\frac{1}{4}\breve{\tau}_{12} & \frac{(-\breve{\tau}_{11}-\breve{\tau}_{33})}{4}
\end{bmatrix}$$

Discretizing term 11

$$\begin{aligned}
(\vec{\nabla}\vec{w})^c : \boldsymbol{L}_{\delta\varphi} \cdot \breve{\boldsymbol{\tau}} &= \boldsymbol{L}_w : \breve{\boldsymbol{\tau}} \cdot \boldsymbol{L}_{\delta\varphi} \\
&= tr(\underline{L}_w \, \underline{\breve{\tau}} \, \underline{L}_{\delta\varphi}) \\
&= \underset{\sim}{d}_w^T \, \underline{D}_3 \, \underset{\sim}{d}_{\delta\varphi} \\
&= \underset{\sim}{w}^T \, \underline{A}^T \, \underline{D}_3 \, \underline{A} \, \delta\underset{\sim}{\varphi}
\end{aligned} \tag{D.120}$$

where

$$\underline{D}_3 = \tag{D.121}$$

$$\begin{bmatrix}
\breve{\tau}_{11} & \frac{1}{2}\breve{\tau}_{12} & 0 & 0 & 0 & \frac{1}{2}\breve{\tau}_{13} & \frac{1}{2}\breve{\tau}_{12} & 0 & \frac{1}{2}\breve{\tau}_{13} \\
\frac{1}{2}\breve{\tau}_{12} & \frac{\breve{\tau}_{11}+\breve{\tau}_{22}}{4} & \frac{1}{2}\breve{\tau}_{12} & 0 & \frac{1}{4}\breve{\tau}_{13} & \frac{1}{4}\breve{\tau}_{23} & \frac{-\breve{\tau}_{11}+\breve{\tau}_{22}}{4} & \frac{1}{4}\breve{\tau}_{13} & \frac{1}{4}\breve{\tau}_{23} \\
0 & \frac{1}{2}\breve{\tau}_{12} & a_{22} & 0 & \frac{1}{2}\breve{\tau}_{23} & 0 & -\frac{1}{2}\breve{\tau}_{12} & \frac{1}{2}\breve{\tau}_{23} & 0 \\
0 & 0 & 0 & \breve{\tau}_{33} & \frac{1}{2}\breve{\tau}_{23} & \frac{1}{2}\breve{\tau}_{13} & 0 & -\frac{1}{2}\breve{\tau}_{23} & -\frac{1}{2}\breve{\tau}_{13} \\
0 & \frac{1}{4}\breve{\tau}_{13} & \frac{1}{2}\breve{\tau}_{23} & \frac{1}{2}\breve{\tau}_{23} & \frac{\breve{\tau}_{22}+\breve{\tau}_{33}}{4} & \frac{1}{4}\breve{\tau}_{12} & -\frac{1}{4}\breve{\tau}_{13} & \frac{-\breve{\tau}_{22}+\breve{\tau}_{33}}{4} & -\frac{1}{4}\breve{\tau}_{12} \\
\frac{1}{2}\breve{\tau}_{13} & \frac{1}{4}\breve{\tau}_{23} & 0 & \frac{1}{2}\breve{\tau}_{13} & \frac{1}{4}\breve{\tau}_{12} & \frac{\breve{\tau}_{11}+\breve{\tau}_{33}}{4} & \frac{1}{4}\breve{\tau}_{23} & -\frac{1}{4}\breve{\tau}_{12} & \frac{-\breve{\tau}_{11}+\breve{\tau}_{33}}{4} \\
\frac{1}{2}\breve{\tau}_{12} & \frac{-\breve{\tau}_{11}+\breve{\tau}_{22}}{4} & -\frac{1}{2}\breve{\tau}_{12} & 0 & -\frac{1}{4}\breve{\tau}_{13} & \frac{1}{4}\breve{\tau}_{23} & \frac{(\breve{\tau}_{11}+\breve{\tau}_{22})}{4} & -\frac{1}{4}\breve{\tau}_{13} & \frac{1}{4}\breve{\tau}_{23} \\
0 & \frac{1}{4}\breve{\tau}_{13} & \frac{1}{2}\breve{\tau}_{23} & -\frac{1}{2}\breve{\tau}_{23} & \frac{(-\breve{\tau}_{22}+\breve{\tau}_{33})}{4} & -\frac{1}{4}\breve{\tau}_{12} & -\frac{1}{4}\breve{\tau}_{13} & \frac{(\breve{\tau}_{22}+\breve{\tau}_{33})}{4} & \frac{1}{4}\breve{\tau}_{12} \\
\frac{1}{2}\breve{\tau}_{13} & \frac{1}{4}\breve{\tau}_{23} & 0 & -\frac{1}{2}\breve{\tau}_{13} & -\frac{1}{4}\breve{\tau}_{12} & \frac{-\breve{\tau}_{11}+\breve{\tau}_{33}}{4} & \frac{1}{4}\breve{\tau}_{23} & \frac{1}{4}\breve{\tau}_{12} & \frac{\breve{\tau}_{11}+\breve{\tau}_{33}}{4}
\end{bmatrix}$$

Discretizing term 15

$$
\begin{aligned}
(\vec{\nabla}\vec{w})^c : -\hat{p}\boldsymbol{I}\,tr(\boldsymbol{L}_{\delta\varphi}) &= \boldsymbol{L}_w : -\hat{p}\boldsymbol{I}\,tr(\boldsymbol{L}_{\delta\varphi}) \\
&= -\hat{p}\,tr(\underline{L}_w)\,tr(\underline{L}_{\delta\varphi}) \\
&= \underset{\sim}{d}_w^T \underset{\sim}{\psi}^T \underset{\sim}{\hat{p}}\,\underline{C}_2\,\underset{\sim}{d}_{\delta\varphi} \\
&= \underset{\sim}{w}^T \underline{A}^T \underset{\sim}{\psi}^T \underset{\sim}{\hat{p}}\,\underline{C}_2\,\underline{A}\,\delta\underset{\sim}{\varphi}
\end{aligned} \tag{D.122}
$$

where

$$
\underline{C}_2 = -\begin{bmatrix}
1 & 0 & 1 & 1 & 0 & 0 & 0 & 0 & 0 \\
0 & 0 & 0 & 0 & 0 & 0 & 0 & 0 & 0 \\
1 & 0 & 1 & 1 & 0 & 0 & 0 & 0 & 0 \\
1 & 0 & 1 & 1 & 0 & 0 & 0 & 0 & 0 \\
0 & 0 & 0 & 0 & 0 & 0 & 0 & 0 & 0 \\
0 & 0 & 0 & 0 & 0 & 0 & 0 & 0 & 0 \\
0 & 0 & 0 & 0 & 0 & 0 & 0 & 0 & 0 \\
0 & 0 & 0 & 0 & 0 & 0 & 0 & 0 & 0 \\
0 & 0 & 0 & 0 & 0 & 0 & 0 & 0 & 0
\end{bmatrix} \tag{D.123}
$$

Discretizing term 17

$$
\begin{aligned}
(\vec{\nabla}\vec{w})^c : \hat{\boldsymbol{\tau}}\,tr(\boldsymbol{L}_{\delta\varphi}) &= \boldsymbol{L}_w : \hat{\boldsymbol{\tau}}\,tr(\boldsymbol{L}_{\delta\varphi}) \\
&= tr(\underline{L}_w\,\underline{\hat{\tau}})tr(\underline{L}_{\delta\varphi}) \\
&= \underset{\sim}{d}_w^T \underline{D}_6\,\underset{\sim}{d}_{\delta\varphi} \\
&= \underset{\sim}{w}^T \underline{A}^T \underline{D}_6\,\underline{A}\delta\underset{\sim}{\varphi}
\end{aligned} \tag{D.124}
$$

where

$$
\underline{D}_6 = \begin{bmatrix}
\hat{\tau}_{11} & 0 & \hat{\tau}_{11} & \hat{\tau}_{11} & 0 & 0 & 0 & 0 & 0 \\
\hat{\tau}_{12} & 0 & \hat{\tau}_{12} & \hat{\tau}_{12} & 0 & 0 & 0 & 0 & 0 \\
\hat{\tau}_{22} & 0 & \hat{\tau}_{22} & \hat{\tau}_{22} & 0 & 0 & 0 & 0 & 0 \\
\hat{\tau}_{33} & 0 & \hat{\tau}_{33} & \hat{\tau}_{33} & 0 & 0 & 0 & 0 & 0 \\
\hat{\tau}_{23} & 0 & \hat{\tau}_{23} & \hat{\tau}_{23} & 0 & 0 & 0 & 0 & 0 \\
\hat{\tau}_{13} & 0 & \hat{\tau}_{13} & \hat{\tau}_{13} & 0 & 0 & 0 & 0 & 0 \\
0 & 0 & 0 & 0 & 0 & 0 & 0 & 0 & 0 \\
0 & 0 & 0 & 0 & 0 & 0 & 0 & 0 & 0 \\
0 & 0 & 0 & 0 & 0 & 0 & 0 & 0 & 0
\end{bmatrix} \tag{D.125}
$$

Discretizing term 16 likewise term 17

$$
(\vec{\nabla}\vec{w})^c : \hat{\boldsymbol{\tau}}^* tr(\boldsymbol{L}_{\delta\varphi}) = \underset{\sim}{w}^T \underline{A}^T \underline{D}_6^*\,\underline{A}\delta\underset{\sim}{\varphi} \tag{D.126}
$$

Where $\underline{D}_6^*$ is the same as $\underline{D}_6$ only with respect to $\hat{\boldsymbol{\tau}}^*$ instead of $\hat{\boldsymbol{\tau}}$.
Discretizing term 18

$$\begin{aligned}(\vec{\nabla}\vec{w})^c : -\delta p\boldsymbol{I} &= -\boldsymbol{L}_w : \delta p\boldsymbol{L} \\ &= -tr(\underline{L}_w)\delta p \\ &= -tr(\underline{L}_w)\underset{\sim}{\psi}^T\delta\underset{\sim}{p} \\ &= -\underset{\sim}{w}^T\underline{Q}\,\delta\underset{\sim}{p}\end{aligned} \tag{D.127}$$

Representation of $\vec{p}$ with respect to $\{\vec{e}_x\ \ \vec{e}_y\ \ \vec{e}_z\}$ and discretizing

$$\vec{p} = b^x\vec{e}_x + b^y\vec{e}_y + b^z\vec{e}_z = \underset{\sim}{\chi}\,\underset{\sim}{b} \tag{D.128}$$

So discretizing the boundary term

$$\vec{w}\vec{p} = \underset{\sim b}{w}^T\,\underset{\sim}{\chi}^T\,\underset{\sim}{\chi}\,\underset{\sim}{b} \tag{D.129}$$

Now discretizing equation (D.70). The first term

$$\begin{aligned}q\{c_6 + tr(\Delta t\,\boldsymbol{D}_{n+\frac{1}{2}})\} &= q\{c_6 + tr(\Delta t\underline{D}_{n+\frac{1}{2}})\} \\ &= \underset{\sim}{q}^T\underset{\sim}{\psi}\{c_6 + tr(\Delta t\underline{D}_{n+\frac{1}{2}})\}\end{aligned} \tag{D.130}$$

The second term

$$\begin{aligned}q\,tr(\boldsymbol{L}_{\delta\varphi}^c\cdot\boldsymbol{B}) &= q\,tr(\underline{L}_{\delta\varphi}^c\,\underline{B}) \\ &= \underset{\sim}{q}^T\underset{\sim}{\psi}\,\underset{\sim 3}{c}^T\underline{A}\,\delta\underset{\sim}{\varphi}\end{aligned} \tag{D.131}$$

where

$$\underset{\sim 3}{c}^T = [B_{11}\ \ B_{12}\ \ B_{22}\ \ B_{33}\ \ B_{23}\ \ B_{13}\ \ 0\ \ 0\ \ 0] \tag{D.132}$$

The third term

$$\begin{aligned}q\{c_6 + tr(\Delta t\,\boldsymbol{D}_{n+\frac{1}{2}})\}\,tr(\boldsymbol{L}_{\delta\varphi}) &= q\{c_6 + tr(\Delta t\underline{D}_{n+\frac{1}{2}})\}\,tr(\underline{L}_{\delta\varphi}) \\ &= \underset{\sim}{q}^T\underset{\sim}{\psi}(c_6 + tr(\Delta t\underline{D}_{n+\frac{1}{2}}))\,\underset{\sim 5}{c}^T\underline{A}\,\delta\underset{\sim}{\varphi}\end{aligned} \tag{D.133}$$

where

$$\underset{\sim 5}{c}^T = [1\ \ 0\ \ 1\ \ 1\ \ 0\ \ 0\ \ 0\ \ 0\ \ 0] \tag{D.134}$$

The last term

$$q\,\kappa\,\delta p = \underset{\sim}{q}^T\,\kappa\,\underset{\sim}{\psi}\,\underset{\sim}{\psi}^T\,\delta\underset{\sim}{p} \tag{D.135}$$

So, the discretized system of equations yields

$$\underset{\sim}{w}^T \int_{\Omega^e} \underline{A}^T \left\{ \underset{\sim}{\psi}^T \hat{\underset{\sim}{p}}\, \underline{C} + \underline{D} \right\} \underline{A}\, d\Omega\, \delta\underset{\sim}{\varphi} + \underset{\sim}{w}^T \int_{\Omega^e} -\underline{Q}\, d\Omega\, \delta \underset{\sim}{p} =$$

$$\underset{\sim}{w}^T \int_{\Omega^e} \left\{ \underline{Q}\,\underset{\sim}{p} - \underline{A}^T(\hat{\underset{\sim}{\tau}} + \hat{\underset{\sim}{\tau}}^*) \right\} d\Omega + \underset{\sim}{w}_b^T \int_{\Gamma^e} \underset{\sim}{\chi}^T \underset{\sim}{\chi}\, \underset{\sim}{b}\, d\Gamma \tag{D.136}$$

and

$$\underset{\sim}{q}^T \int_{\Omega^e} \underset{\sim}{\psi} \left\{ \underset{\sim}{c}_3^T + c_{13}\, \underset{\sim}{c}_5^T \right\} \underline{A}\, d\Omega \delta\underset{\sim}{\varphi} + \underset{\sim}{q}^T \int_{\Omega^e} \kappa \underset{\sim}{\psi}\, \underset{\sim}{\psi}^T\, d\Omega\, \delta\underset{\sim}{p} =$$

$$\underset{\sim}{q}^T \int_{\Omega^e} -\underset{\sim}{\psi}\, c_{13}\, d\Omega \tag{D.137}$$

where

$$\underline{D} = \underline{D}_1 + \underline{D}_1^* + \underline{D}_2 + \underline{D}_3 + \left\{ \frac{\overline{\eta}}{\Delta t} + \frac{1}{2}\frac{1}{\Delta t}\left(\sum_{i=1}^{m} G_i \right) \right\} (\underline{D}_4 + \underline{D}_5 + \underline{D}_7)$$

$$+\underline{D}_6 + \underline{D}_6^* \tag{D.138}$$

$$\underline{C} = \underline{C}_1 + \underline{C}_2 \tag{D.139}$$

$$c_{13} = c_6 + tr(\Delta t \underline{D}_{n+\frac{1}{2}}) \tag{D.140}$$

Appendix E

Enriched trilinear element

In this appendix the shape functions and the $x-$, $y-$ and $z-$derivatives of an arbitrary enriched trilinear element will de derived.

This element has 15 displacement nodes and 4 pressure nodes. In order to derive the shape functions isoparametric coordinates are used. This so called $\underset{\sim}{\xi}$ - space is an orthonormal space with ξ, η and ζ as independent coordinates. The basic idea of deriving the shape functions for the displacement is adding bubble-functions at the surfaces and midpoint of a trilinear hexahedral element. The shape functions of the trilinear hexahedral element are given by [13] :

$$N_1(\underset{\sim}{\xi}) = \frac{1}{8}(1+\xi)(1-\eta)(1-\zeta) \tag{E.1}$$

$$N_2(\underset{\sim}{\xi}) = \frac{1}{8}(1+\xi)(1+\eta)(1-\zeta) \tag{E.2}$$

$$N_4(\underset{\sim}{\xi}) = \frac{1}{8}(1-\xi)(1-\eta)(1-\zeta) \tag{E.3}$$

$$N_5(\underset{\sim}{\xi}) = \frac{1}{8}(1-\xi)(1+\eta)(1-\zeta) \tag{E.4}$$

$$N_{10}(\underset{\sim}{\xi}) = \frac{1}{8}(1+\xi)(1-\eta)(1+\zeta) \tag{E.5}$$

$$N_{11}(\underset{\sim}{\xi}) = \frac{1}{8}(1+\xi)(1+\eta)(1+\zeta) \tag{E.6}$$

$$N_{13}(\underset{\sim}{\xi}) = \frac{1}{8}(1-\xi)(1-\eta)(1+\zeta) \tag{E.7}$$

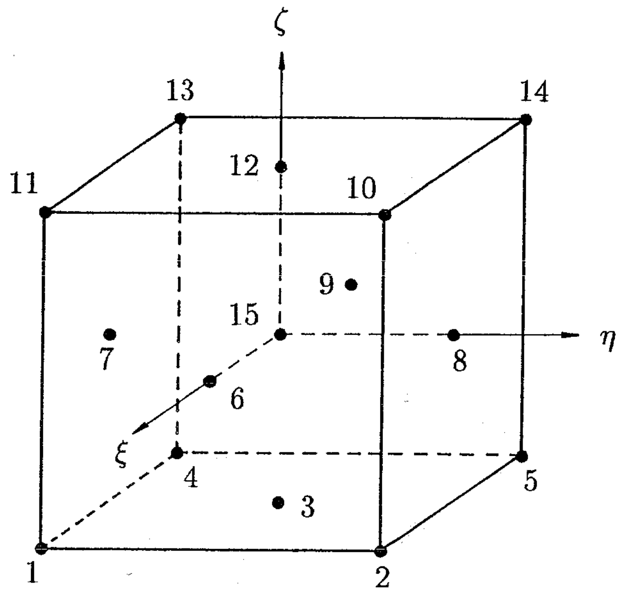

Figure E.1: The enriched trilinear element.

$$N_{14}(\underset{\sim}{\xi}) = \frac{1}{8}(1-\xi)(1+\eta)(1+\zeta) \tag{E.8}$$

The bubble-function added to the surface with node 3:

$$N_3(\underset{\sim}{\xi}) = \frac{1}{2}(1-\zeta)(1-\xi^2)(1-\eta^2) \tag{E.9}$$

Surface with node 12:

$$N_{12}(\underset{\sim}{\xi}) = \frac{1}{2}(1+\zeta)(1-\xi^2)(1-\eta^2) \tag{E.10}$$

Surface with node 7:

$$N_7(\underset{\sim}{\xi}) = \frac{1}{2}(1-\eta)(1-\xi^2)(1-\zeta^2) \tag{E.11}$$

Surface with node 8:

$$N_8(\underset{\sim}{\xi}) = \frac{1}{2}(1+\eta)(1-\xi^2)(1-\zeta^2) \tag{E.12}$$

Surface with node 6:

$$N_6(\underset{\sim}{\xi}) = \frac{1}{2}(1-\xi)(1-\eta^2)(1-\zeta^2) \tag{E.13}$$

Surface with node 9:

$$N_9(\underset{\sim}{\xi}) = \frac{1}{2}(1+\xi)(1-\eta^2)(1-\zeta^2) \tag{E.14}$$

i	ξ	η	ζ
1	1	-1	-1
2	1	1	-1
3	0	0	-1
4	-1	-1	-1
5	-1	1	-1
6	1	0	0
7	0	-1	0
8	0	1	0
9	-1	0	0
10	1	-1	1
11	1	1	1
12	0	0	1
13	-1	-1	1
14	-1	1	1
15	0	0	0

Table E.1: Isoparametric coordinates of nodal points

The bubble-function added to the midpoint:

$$N_{15}(\underset{\sim}{\xi}) = (1-\xi^2)(1-\eta^2)(1-\zeta^2) \tag{E.15}$$

The shape functions $\varphi_i(\xi,\eta,\zeta)$ must be assembled out of the functions $N_j(\xi,\eta,\zeta)$ in such way that they satisfy the following equations:

$$x(\underset{\sim}{\xi}) = \sum_{i=1}^{15} \varphi_i(\underset{\sim}{\xi}) x_i^e \tag{E.16}$$

$$y(\underset{\sim}{\xi}) = \sum_{i=1}^{15} \varphi_i(\underset{\sim}{\xi}) y_i^e \tag{E.17}$$

$$z(\underset{\sim}{\xi}) = \sum_{i=1}^{15} \varphi_i(\underset{\sim}{\xi}) z_i^e \tag{E.18}$$

This yields:

$$\varphi_1(\xi,\eta,\zeta) = N_1 - \frac{1}{4}(N_3+N_6+N_7) + \frac{1}{4}N_{15} \tag{E.19}$$

$$\varphi_2(\xi,\eta,\zeta) = N_2 - \frac{1}{4}(N_3+N_6+N_8) + \frac{1}{4}N_{15} \tag{E.20}$$

$$\varphi_3(\xi,\eta,\zeta) = N_3 - \frac{1}{2}N_{15} \tag{E.21}$$

$$\varphi_4(\xi,\eta,\zeta) = N_4 - \frac{1}{4}(N_3+N_7+N_9) + \frac{1}{4}N_{15} \tag{E.22}$$

$$\varphi_5(\xi,\eta,\zeta) = N_5 - \frac{1}{4}(N_3 + N_8 + N_9) + \frac{1}{4}N_{15} \tag{E.23}$$

$$\varphi_6(\xi,\eta,\zeta) = N_6 - \frac{1}{2}N_{15} \tag{E.24}$$

$$\varphi_7(\xi,\eta,\zeta) = N_7 - \frac{1}{2}N_{15} \tag{E.25}$$

$$\varphi_8(\xi,\eta,\zeta) = N_8 - \frac{1}{2}N_{15} \tag{E.26}$$

$$\varphi_9(\xi,\eta,\zeta) = N_9 - \frac{1}{2}N_{15} \tag{E.27}$$

$$\varphi_{10}(\xi,\eta,\zeta) = N_{10} - \frac{1}{4}(N_6 + N_7 + N_{12}) + \frac{1}{4}N_{15} \tag{E.28}$$

$$\varphi_{11}(\xi,\eta,\zeta) = N_{11} - \frac{1}{4}(N_6 + N_8 + N_{12}) + \frac{1}{4}N_{15} \tag{E.29}$$

$$\varphi_{12}(\xi,\eta,\zeta) = N_{12} - \frac{1}{2}N_{15} \tag{E.30}$$

$$\varphi_{13}(\xi,\eta,\zeta) = N_{13} - \frac{1}{4}(N_7 + N_9 + N_{12}) + \frac{1}{4}N_{15} \tag{E.31}$$

$$\varphi_{14}(\xi,\eta,\zeta) = N_{14} - \frac{1}{4}(N_8 + N_9 + N_{12}) + \frac{1}{4}N_{15} \tag{E.32}$$

$$\varphi_{15}(\xi,\eta,\zeta) = N_{15} \tag{E.33}$$

The $\xi-$, $\eta-$ and $\zeta-$derivatives of these shape functions are calculated by first deriving the derivatives of the functions $N_i(\xi,\eta,\zeta)$ and then assemble them with the same factors as use to assemble the shape functions. The $\xi-$, $\eta-$ and $\zeta-$derivatives of the shape functions can be calculated easily but the $x-$, $y-$ and $z-$derivatives are needed [13]. They are given by:

$$\varphi_{i,x} = \varphi_{i,\xi}\xi_{,x} + \varphi_{i,\eta}\eta_{,x} + \varphi_{i,\zeta}\zeta_{,x} \tag{E.34}$$

$$\varphi_{i,y} = \varphi_{i,\xi}\xi_{,y} + \varphi_{i,\eta}\eta_{,y} + \varphi_{i,\zeta}\zeta_{,y} \tag{E.35}$$

$$\varphi_{i,z} = \varphi_{i,\xi}\xi_{,z} + \varphi_{i,\eta}\eta_{,z} + \varphi_{i,\zeta}\zeta_{,z} \tag{E.36}$$

In matrix formulation:

$$\begin{bmatrix} \varphi_{i,x} \\ \varphi_{i,y} \\ \varphi_{i,z} \end{bmatrix} = \begin{bmatrix} \xi_{,x} & \eta_{,x} & \zeta_{,x} \\ \xi_{,y} & \eta_{,y} & \zeta_{,y} \\ \xi_{,z} & \eta_{,z} & \zeta_{,z} \end{bmatrix} \begin{bmatrix} \varphi_{i,\xi} \\ \varphi_{i,\eta} \\ \varphi_{i,\zeta} \end{bmatrix} \tag{E.37}$$

As ξ, η and ζ are not known as a function of x, y and z the inverse relation must be used:

$$x(\underset{\sim}{\xi}) = \sum_{i=1}^{15} \varphi_i(\underset{\sim}{\xi}) x_i^e \tag{E.38}$$

$$y(\underset{\sim}{\xi}) = \sum_{i=1}^{15} \varphi_i(\underset{\sim}{\xi}) y_i^e \tag{E.39}$$

$$z(\underset{\sim}{\xi}) = \sum_{i=1}^{15} \varphi_i(\underset{\sim}{\xi}) z_i^e \tag{E.40}$$

The matrix $\underset{\sim}{x}_{,\underset{\sim}{\xi}}$, containing the $\xi-$, $\eta-$ and $\zeta-$derivatives of x, y and z can be determined out of these inverse relations:

$$\underset{\sim}{x}_{,\underset{\sim}{\xi}} = \begin{bmatrix} x_{,\xi} & x_{,\eta} & x_{,\zeta} \\ y_{,\xi} & y_{,\eta} & y_{,\zeta} \\ z_{,\xi} & z_{,\eta} & z_{,\zeta} \end{bmatrix} \tag{E.41}$$

Where:

$$x_{,\xi} = \sum_{i=1}^{15} \varphi_{i,\xi} x_i^e \tag{E.42}$$

$$x_{,\eta} = \sum_{i=1}^{15} \varphi_{i,\eta} x_i^e \tag{E.43}$$

$$x_{,\zeta} = \sum_{i=1}^{15} \varphi_{i,\zeta} x_i^e \tag{E.44}$$

Corresponding expressions for the derivatives of x, y and z are valid. The matrix $\underset{\sim}{\xi}_{,\underset{\sim}{x}}$, which is called the Jacobian matrix, can be computed by inverting the matrix $\underset{\sim}{x}_{,\underset{\sim}{\xi}}$:

$$\underset{\sim}{\xi}_{\underset{\sim}{x}} = \begin{bmatrix} \xi_{,x} & \xi_{,y} & \xi_{,z} \\ \eta_{,x} & \eta_{,y} & \eta_{,z} \\ \zeta_{,x} & \zeta_{,y} & \zeta_{,z} \end{bmatrix} = (\underset{\sim}{x}_{,\underset{\sim}{\xi}})^{-1} \tag{E.45}$$

This leads to the expression for the $x-$, $y-$ and $z-$derivatives of the shape functions:

$$\varphi_{i,\underset{\sim}{x}} = (\underset{\sim}{x}_{,\underset{\sim}{\xi}})^{-T} \varphi_{i,\underset{\sim}{\xi}} \tag{E.46}$$

The shape functions for the pressure nodes are defined as follows:

$$\psi_1(\xi, \eta, \zeta) = 1 \tag{E.47}$$

$$\psi_2(\xi, \eta, \zeta) = \xi \tag{E.48}$$

$$\psi_3(\xi, \eta, \zeta) = \eta \tag{E.49}$$

$$\psi_4(\xi, \eta, \zeta) = \zeta \tag{E.50}$$

Appendix F

Five node boundary element

In this appendix the shape functions of an arbitrary five node boundary element will be obtained.

In order to derive the shape functions isoparametric coordinates are used. This so called $\underset{\sim}{\xi}^*$ - space has two independent coordinates: ξ and η. Simulant

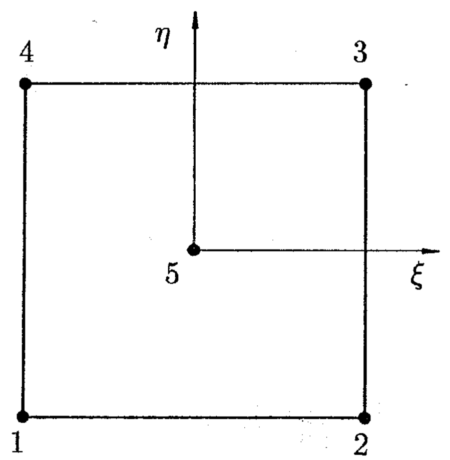

Figure F.1: Five node boundary element

to the enriched trilinear element the shape functions are derived by taking the shape functions of an bilinear element and adding a bubble-function on the surface. The bilinear shape functions [13]:

$$N_1(\xi,\eta) = \frac{1}{4}(1-\xi)(1-\eta) \tag{F.1}$$

$$N_2(\xi,\eta) = \frac{1}{4}(1+\xi)(1-\eta) \tag{F.2}$$

$$N_3(\xi,\eta) = \frac{1}{4}(1+\xi)(1+\eta) \tag{F.3}$$

$$N_4(\xi,\eta) = \frac{1}{4}(1-\xi)(1+\eta) \tag{F.4}$$

The bubble function:

$$N_5(\xi,\eta) = \frac{1}{4}(1-\xi^2)(1-\eta^2) \tag{F.5}$$

i	ξ	η
1	-1	-1
2	1	-1
3	1	1
4	-1	1
5	0	0

Table F.1: Isoparametric coordinates of nodal points

The shape functions $\varphi_i(\underset{\sim}{\xi}^*)$ have to be assembled out of the functions $N_j(\underset{\sim}{\xi}^*)$ in such way that they satisfy the following equations:

$$x(\underset{\sim}{\xi}^*) = \sum_{i=1}^{5} \varphi_i(\underset{\sim}{\xi}^*) x_i^e \tag{F.6}$$

$$y(\underset{\sim}{\xi}^*) = \sum_{i=1}^{5} \varphi_i(\underset{\sim}{\xi}^*) y_i^e \tag{F.7}$$

$$z(\underset{\sim}{\xi}^*) = \sum_{i=1}^{5} \varphi_i(\underset{\sim}{\xi}^*) z_i^e \tag{F.8}$$

This yields:

$$\chi_1(\xi,\eta) = N_1 - \frac{1}{4}N_5 \tag{F.9}$$

$$\chi_2(\xi,\eta) = N_2 - \frac{1}{4}N_5 \tag{F.10}$$

$$\chi_3(\xi,\eta) = N_3 - \frac{1}{4}N_5 \tag{F.11}$$

$$\chi_4(\xi,\eta) = N_4 - \frac{1}{4}N_5 \tag{F.12}$$

$$\chi_5(\xi,\eta) = N_5 \tag{F.13}$$

Appendix G

Numerical integration

To obtain the element matrices, volume - and surface integrals have to be calculated. The integrals must be transformed to the $\underset{\sim}{\xi}$ - resp. $\underset{\sim}{\xi}^*$ - space and integration rules have to be applied.

G.1 Volume integrals

General appearance:

$$I = \int_{\Omega^e} \mathcal{F}(\underset{\sim}{x}) d\Omega \tag{G.1}$$

This integral can be transformed to the $\underset{\sim}{\xi}$ - space [17]:

$$I = \int_{-1}^{1}\int_{-1}^{1}\int_{-1}^{1} \mathcal{F}(x(\xi,\eta,\zeta), y(\xi,\eta,\zeta), z(\xi,\eta,\zeta)) j(\xi,\eta,\zeta)\, d\xi\, d\eta\, d\zeta \tag{G.2}$$

where:

$$j = \begin{vmatrix} \frac{\partial x}{\partial \xi} & \frac{\partial x}{\partial \eta} & \frac{\partial x}{\partial \zeta} \\ \frac{\partial y}{\partial \xi} & \frac{\partial y}{\partial \eta} & \frac{\partial y}{\partial \zeta} \\ \frac{\partial z}{\partial \xi} & \frac{\partial z}{\partial \eta} & \frac{\partial z}{\partial \zeta} \end{vmatrix} \tag{G.3}$$

Approximation of this integral with a numerical integration rule:

$$I \approx \sum_{i=1}^{n_{int}} \mathcal{F}\left(x(\underset{\sim}{\xi}_i), y(\underset{\sim}{\xi}_i), z(\underset{\sim}{\xi}_i)\right) * j(\underset{\sim}{\xi}_i) * w_i \tag{G.4}$$

Integration rule, 15 points [18]:

$$\int_{-1}^{1}\int_{-1}^{1}\int_{-1}^{1} \mathcal{F}(x,y,z) dx dy dz \approx$$

$$
\begin{array}{lll}
A_1 * \mathcal{F}(0,0,0)+ & & (1\ term) \\
B_6 * \{\mathcal{F}(-b,0,0)+\mathcal{F}(b,0,0)+ & ...\}+ & (6\ terms) \\
C_8 * \{\mathcal{F}(-c,-c,-c)+\mathcal{F}(c,-c,-c)+ & ...\} & (8\ terms)
\end{array}
\tag{G.5}
$$

where:

$$
\begin{array}{llllll}
A_1 & = & 0.712137436 & & & \\
B_6 & = & 0.686227234 & b & = & 0.848418011 \\
C_8 & = & 0.396312395 & c & = & 0.727662441
\end{array}
\tag{G.6}
$$

G.2 Surface integrals

General appearance:

$$
I = \int_{\Gamma^e} \mathcal{G}(x,y,z)dS \tag{G.7}
$$

The transformation equations:

$$
x = f(\xi,\eta), \qquad y = g(\xi,\eta), \qquad z = h(\xi,\eta) \tag{G.8}
$$

In vector notation:

$$
\begin{aligned}
\mathbf{r} &= x\mathbf{i} + y\mathbf{j} + z\mathbf{k} \\
&= f(\xi,\eta)\mathbf{i} + g(\xi,\eta)\mathbf{j} + h(\xi,\eta)\mathbf{k}
\end{aligned}
\tag{G.9}
$$

The surface integral is given by [27]:

$$
dS = \left| \frac{\partial r}{\partial \xi} * \frac{\partial r}{\partial \eta} \right| d\xi d\eta \tag{G.10}
$$

where:

$$
\begin{aligned}
\frac{\partial r}{\partial \xi} * \frac{\partial r}{\partial \eta} &= \begin{vmatrix} \mathbf{i} & \mathbf{j} & \mathbf{k} \\ \frac{\partial x}{\partial \xi} & \frac{\partial y}{\partial \xi} & \frac{\partial z}{\partial \xi} \\ \frac{\partial x}{\partial \eta} & \frac{\partial y}{\partial \eta} & \frac{\partial z}{\partial \eta} \end{vmatrix} \\
&= \begin{vmatrix} \frac{\partial y}{\partial \xi} & \frac{\partial z}{\partial \xi} \\ \frac{\partial y}{\partial \eta} & \frac{\partial z}{\partial \eta} \end{vmatrix} \mathbf{i} + \begin{vmatrix} \frac{\partial x}{\partial \xi} & \frac{\partial z}{\partial \xi} \\ \frac{\partial x}{\partial \eta} & \frac{\partial z}{\partial \eta} \end{vmatrix} \mathbf{j} + \begin{vmatrix} \frac{\partial x}{\partial \xi} & \frac{\partial y}{\partial \xi} \\ \frac{\partial x}{\partial \eta} & \frac{\partial y}{\partial \eta} \end{vmatrix} \mathbf{k} \\
&= \frac{\partial(y,z)}{\partial(\xi,\eta)}\mathbf{i} + \frac{\partial(x,z)}{\partial(\xi,\eta)}\mathbf{j} + \frac{\partial(x,y)}{\partial(\xi,\eta)}\mathbf{k}
\end{aligned}
\tag{G.11}
$$

This yields:

$$
dS = j^* d\xi d\eta \tag{G.12}
$$

where:

$$j^* = \sqrt{\left(\frac{\partial(y,z)}{\partial(\xi,\eta)}\right)^2 + \left(\frac{\partial(x,z)}{\partial(\xi,\eta)}\right)^2 + \left(\frac{\partial(x,y)}{\partial(\xi,\eta)}\right)^2} \tag{G.13}$$

The transformation of the integral to the $\underset{\sim}{\xi}^*$ - space yields:

$$I = \int_{-1}^{1}\int_{-1}^{1} \mathcal{G}(x(\xi,\eta), y(\xi,\eta), z(\xi,\eta)) j^*(\xi,\eta)\, d\xi\, d\eta \tag{G.14}$$

Approximation of this integral with a numerical integration rule:

$$I \approx \sum_{i=1}^{n_int} \mathcal{G}\left(x(\underset{\sim}{\xi}_i^*), y(\underset{\sim}{\xi}_i^*), z(\underset{\sim}{\xi}_i^*)\right) * j(\underset{\sim}{\xi}_i^*) * w_i \tag{G.15}$$

Integration rule, 9 points [1]:

$$\int_{-1}^{1}\int_{-1}^{1} \mathcal{G}(x,y)dxdy \approx$$

$$\begin{array}{llll} A_1 * \mathcal{G}(0,0)+ & & (1\ term) & \\ B_4 * \{\mathcal{G}(b,b) + \mathcal{G}(-b,b) + & ...\}+ & (4\ terms) & \\ C_4 * \{\mathcal{G}(c,0) + \mathcal{G}(-c,0) + & ...\} & (4\ terms) & \end{array} \tag{G.16}$$

where:

$$\begin{array}{lllllll} A_1 & = & 0.7901234686 & & & \\ B_6 & = & 0.3086420047 & b & = & 0.7745966692 \\ C_8 & = & 0.4938271818 & c & = & 0.7745966692 \end{array} \tag{G.17}$$

Appendix H

Test cases

In this appendix the test cases, tension and simple shear, for checking the visco-elastic element will be worked out. For the thermal element a test case obtained from the literature (Chatenier [10]) is given.

H.1 The tension test

The tension test is worked out for both linear and nonlinear theory. The material is assumed to be unloaded at the beginning of the tests and tests are carried out isothermal. The tension bar is given in figure H.1. Defining

$$\lambda_1 = \frac{L}{L_0} \tag{H.1}$$

$$\lambda_2 = \frac{h}{h_0} \tag{H.2}$$

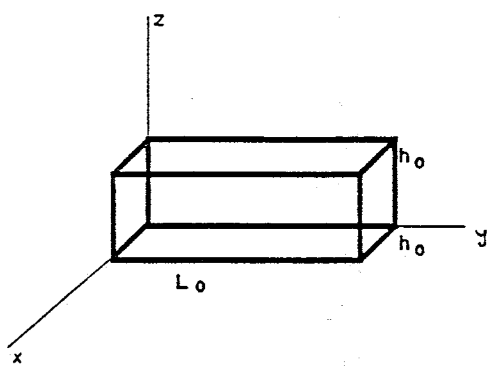

Figure H.1: The tension bar

Linear theory

The strain matrix is given by

$$\underline{\varepsilon}(\Delta\vec{u}) = \begin{bmatrix} \lambda_2 - 1 & 0 & 0 \\ 0 & \lambda_1 - 1 & 0 \\ 0 & 0 & \lambda_2 - 1 \end{bmatrix} \tag{H.3}$$

The trace of this matrix

$$tr(\underline{\varepsilon}(\Delta\vec{u})) = \lambda_1 + 2\lambda_2 - 3 \tag{H.4}$$

For this tension test the following must hold

$$\sigma_{(n+1)xx} = \sigma_{(n+1)zz} = 0 \tag{H.5}$$

Visco-elastic material behaviour:

$$\underline{\sigma}_{n+1} = -p_{n+1}\underline{I} + \underline{\tau}_{n+1} \tag{H.6}$$

$$\underline{\tau}_{n+1} = \sum_{i=1}^{m}(G_{ni}\underline{\tau}_{ni}) + \left(\sum_{i=1}^{m} G_i\right)\frac{1}{\Delta t}\underline{\varepsilon}^d(\Delta\vec{u}) \tag{H.7}$$

$$\alpha\Delta T + \kappa\Delta p + tr(\underline{\varepsilon}(\Delta\vec{u})) = 0 \tag{H.8}$$

For the given strain matrix equation H.7 yields (only non-zero terms)

$$\tau_{(n+1)xx} = \sum_{i=1}^{m}(G_{ni}\tau_{(ni)xx}) + \left(\sum_{i=1}^{m} G_i\right)\frac{1}{\Delta t}\frac{1}{3}(\lambda_2 - \lambda_1) \tag{H.9}$$

$$\tau_{(n+1)yy} = \sum_{i=1}^{m}(G_{ni}\tau_{(ni)yy}) + \left(\sum_{i=1}^{m} G_i\right)\frac{1}{\Delta t}\frac{2}{3}(\lambda_1 - \lambda_2) \tag{H.10}$$

$$\tau_{(n+1)zz} = \tau_{(n+1)xx} \tag{H.11}$$

Equation H.8 yields

$$\kappa(p_{n+1} - p_n) + \lambda_1 + 2\lambda_2 - 3 = 0 \tag{H.12}$$

Applying equation H.5 yields

$$p_{n+1} = \tau_{(n+1)xx} = \tau_{(n+1)zz} \tag{H.13}$$

For a given λ_1, λ_2 can be calculated as follows

$$\lambda_2 = \frac{\kappa(p_n - \sum_{i=1}^{m}(G_{ni}\tau_{(ni)xx}) + (\sum_{i=1}^{m} G_i)\,\frac{1}{\Delta t}\frac{1}{3}\lambda_1) - \lambda_1 + 3}{\kappa\,(\sum_{i=1}^{m} G_i)\,\frac{1}{\Delta t}\frac{1}{3} + 2} \tag{H.14}$$

Newtonian material behaviour:

$$\underline{\sigma}_{n+1} = -p_{n+1}\underline{I} + \underline{\tau}_{n+1} \tag{H.15}$$

$$\underline{\tau}_{n+1} = 2\overline{\eta}\frac{1}{\Delta t}\underline{\varepsilon}^d(\Delta\vec{u}) \tag{H.16}$$

$$\alpha\Delta T + \kappa\Delta p + tr(\underline{\varepsilon}(\Delta\vec{u})) = 0 \tag{H.17}$$

For the given strain matrix equation H.16 yields (only non-zero terms)

$$\tau_{(n+1)xx} = \overline{\eta}\frac{1}{\Delta t}\frac{2}{3}(\lambda_2 - \lambda_1) \tag{H.18}$$

$$\tau_{(n+1)yy} = \overline{\eta}\frac{1}{\Delta t}\frac{4}{3}(\lambda_1 - \lambda_2) \tag{H.19}$$

$$\tau_{(n+1)zz} = \tau_{(n+1)xx} \tag{H.20}$$

Equation H.17 yields

$$\kappa(p_{n+1} - p_n) + \lambda_1 + 2\lambda_2 - 3 = 0 \tag{H.21}$$

Applying equation H.5 yields

$$p_{n+1} = \tau_{(n+1)xx} = \tau_{(n+1)zz} \tag{H.22}$$

For a given λ_1, λ_2 can be calculated as follows

$$\lambda_2 = \frac{\kappa(p_n + \frac{2}{3}\overline{\eta}\frac{1}{\Delta t}\lambda_1) - \lambda_1 + 3}{\kappa\frac{2}{3}\overline{\eta}\frac{1}{\Delta t} + 2} \tag{H.23}$$

Nonlinear theory

For the tension bar the deformation matrix is given by

$$\underline{F}_{n+1} = \begin{bmatrix} \lambda_2 & 0 & 0 \\ 0 & \lambda_1 & 0 \\ 0 & 0 & \lambda_2 \end{bmatrix} \tag{H.24}$$

The deformation rate matrix is given by

$$\underline{D}_{n+\frac{1}{2}} = \frac{2}{\Delta t}\begin{bmatrix} \frac{\lambda_2-1}{\lambda_2+1} & 0 & 0 \\ 0 & \frac{\lambda_1-1}{\lambda_1+1} & 0 \\ 0 & 0 & \frac{\lambda_2-1}{\lambda_2+1} \end{bmatrix} \tag{H.25}$$

The trace of the deformation rate matrix is given by

$$tr(\underline{D}_{n+\frac{1}{2}}) = \frac{1}{\Delta t}\left\{2\frac{\lambda_1 - 1}{\lambda_1 + 1} + 4\frac{\lambda_2 - 1}{\lambda_2 + 1}\right\} \tag{H.26}$$

Visco-elastic material behaviour:

$$\underline{\sigma}_{n+1} = -p_{n+1}\underline{I} + \underline{\tau}_{n+1} \tag{H.27}$$

$$\begin{aligned}\underline{\tau}_{n+1} = \underline{F}_{n+1}\sum_{i=1}^{m}(G_{ni}\underline{\tau}_{ni})\,\underline{F}^{T}_{n+1} + \\ \left(\sum_{i=1}^{m} G_i\right)\underline{F}_{n+1}\underline{F}^{-1}_{n+\frac{1}{2}}\underline{D}^{d}_{n+\frac{1}{2}}\underline{F}^{-T}_{n+\frac{1}{2}}\underline{F}^{T}_{n+1}\end{aligned} \tag{H.28}$$

$$\alpha\Delta T + \kappa\Delta p + tr(\Delta t\,\underline{D}_{n+\frac{1}{2}}) = 0 \tag{H.29}$$

For the given deformation and deformation rate matrix equation H.28 yields (only non-zero terms)

$$\begin{aligned}\tau_{(n+1)xx} &= \lambda_2^2\sum_{i=1}^{m}(G_{ni}\underline{\tau}_{(ni)xx}) + \left(\sum_{i=1}^{m} G_i\right)\frac{8}{3}\frac{1}{\Delta t}\left\{\frac{\lambda_2^2(\lambda_2-1)}{(\lambda_2+1)^3} - \right. \\ &\qquad \left.\frac{\lambda_2^2(\lambda_1-1)}{(\lambda_2+1)^2(\lambda_1+1)}\right\}\end{aligned} \tag{H.30}$$

$$\begin{aligned}\tau_{(n+1)yy} &= \lambda_1^2\sum_{i=1}^{m}(G_{ni}\underline{\tau}_{(ni)yy}) + \left(\sum_{i=1}^{m} G_i\right)\frac{16}{3}\frac{1}{\Delta t}\left\{\frac{\lambda_1^2(\lambda_1-1)}{(\lambda_1+1)^3} - \right. \\ &\qquad \left.\frac{\lambda_1^2(\lambda_2-1)}{(\lambda_1+1)^2(\lambda_2+1)}\right\}\end{aligned} \tag{H.31}$$

$$\tau_{(n+1)zz} = \tau_{(n+1)xx} \tag{H.32}$$

Equation H.29 yields

$$\kappa(p_{n+1} - p_n) + 2\frac{\lambda_1 - 1}{\lambda_1 + 1} + 4\frac{\lambda_2 - 1}{\lambda_2 + 1} = 0 \tag{H.33}$$

Applying equation H.5 yields

$$p_{n+1} = \tau_{(n+1)xx} = \tau_{(n+1)zz} \tag{H.34}$$

Numerical solving this set of equations (given λ_1) :
- calculate λ_2 with last estimate of p_{n+1} (using eq. H.33)
- calculate new estimate of p_{n+1} (using eq.H.30 and eq.H.34)
- repeat until convergence.

Newtonian material behaviour:

$$\underline{\sigma}_{n+1} = -p_{n+1}\underline{I} + \underline{\tau}_{n+1} \tag{H.35}$$

$$\underline{\tau}_{n+1} = 2\overline{\eta}\underline{D}^{d}_{n+\frac{1}{2}} \tag{H.36}$$

$$\alpha\Delta T + \kappa\Delta p + tr(\Delta t\underline{D}_{n+\frac{1}{2}}) = 0 \tag{H.37}$$

For the given deformation rate matrix equation H.36 yields (only non-zero terms)

$$\tau_{(n+1)xx} = \eta\frac{1}{\Delta t}\frac{4}{3}\left\{\frac{(\lambda_2-1)}{(\lambda_2+1)} - \frac{(\lambda_1-1)}{(\lambda_1+1)}\right\} \tag{H.38}$$

$$\tau_{(n+1)yy} = \eta\frac{1}{\Delta t}\frac{8}{3}\left\{\frac{(\lambda_1-1)}{(\lambda_1+1)} - \frac{(\lambda_2-1)}{(\lambda_2+1)}\right\} \tag{H.39}$$

$$\tau_{(n+1)zz} = \tau_{(n+1)xx} \tag{H.40}$$

Equation H.37 yields

$$\kappa(p_{n+1}-p_n) + 2\frac{(\lambda_1-1)}{(\lambda_1+1)} + 4\frac{(\lambda_2-1)}{(\lambda_2+1)} = 0 \tag{H.41}$$

Applying equation H.5 yields

$$p_{n+1} = \tau_{(n+1)xx} = \tau_{(n+1)zz} \tag{H.42}$$

For the numerical solving see above.

H.2 The simple shear test

The simple shear test is worked out for both linear and nonlinear theory. The material is assumed to be unloaded at the beginning of the tests and tests are carried out isothermal. The cube on which the test is performed is given in figure H.2. Defining

$$\gamma = \frac{b}{c} \tag{H.43}$$

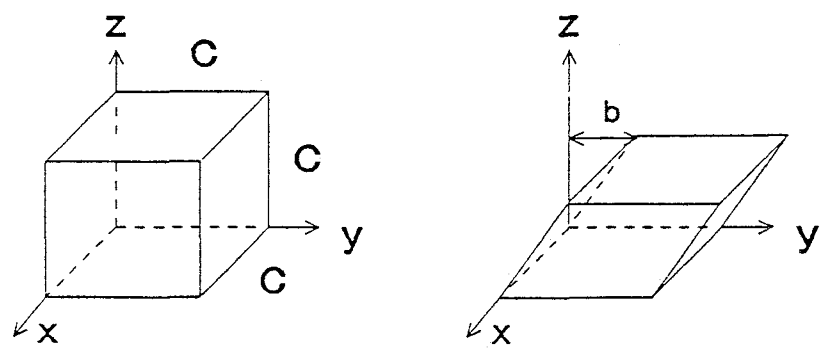

Figure H.2: Simple shear

Linear theory

The strain matrix is given by

$$\underline{\varepsilon}(\Delta\vec{u}) = \begin{bmatrix} 0 & 0 & 0 \\ 0 & 0 & \frac{1}{2}\gamma \\ 0 & \frac{1}{2}\gamma & 0 \end{bmatrix} \tag{H.44}$$

The trace of this matrix is zero.

Visco-elastic material behaviour:
See equation H.6, H.7 and H.8. For the given strain matrix equation H.7 yields (only non-zero terms)

$$\tau_{(n+1)yz} = \sum_{i=1}^{m}(G_{ni}\tau_{(ni)yz}) + \left(\sum_{i=1}^{m} G_i\right)\frac{1}{\Delta t}\frac{1}{2}\gamma \tag{H.45}$$

Equation H.8 yields

$$p_{n+1} = 0 \tag{H.46}$$

Newtonian material behaviour:
See equation H.15, H.16 and H.17. For the given strain matrix equation H.16 yields (only non-zero terms)

$$\tau_{(n+1)yz} = \overline{\eta}\frac{1}{\Delta t}\gamma \tag{H.47}$$

Equation H.17 yields

$$p_{n+1} = 0 \tag{H.48}$$

Nonlinear theory

The deformation matrix is given by

$$\underline{F}_{n+1} = \begin{bmatrix} 1 & 0 & 0 \\ 0 & 1 & \gamma \\ 0 & 0 & 1 \end{bmatrix} \tag{H.49}$$

The deformation rate matrix is given by

$$\underline{D}_{n+\frac{1}{2}} = \frac{1}{\Delta t}\begin{bmatrix} 0 & 0 & 0 \\ 0 & 0 & \frac{1}{2}\gamma \\ 0 & \frac{1}{2}\gamma & 0 \end{bmatrix} \tag{H.50}$$

The trace of the deformation rate matrix is zero.

Visco-elastic material behaviour:
See equation H.27, H.28 and H.29. For the given deformation - and deformation rate matrix equation H.28 yields (only non-zero terms)

$$\tau_{(n+1)yx} = \sum_{i=1}^{m}(G_{ni}\underline{\tau}_{(ni)yz}) + \left(\sum_{i=1}^{m} G_i\right)\frac{1}{2}\frac{1}{\Delta t}\gamma \tag{H.51}$$

$$\tau_{(n+1)yy} = 2\gamma\sum_{i=1}^{m}(G_{ni}\underline{\tau}_{(ni)yz}) \tag{H.52}$$

$$\tag{H.53}$$

Equation H.29 yields

$$p_{n+1} = 0 \tag{H.54}$$

Newtonian material behaviour:
See equation H.35, H.36 and H.37. For the given deformation rate matrix equation H.36 yields (only non-zero terms)

$$\tau_{(n+1)yz} = \overline{\eta}\frac{1}{\Delta t}\gamma \tag{H.55}$$

Equation H.29 yields

$$p_{n+1} = 0 \tag{H.56}$$

H.3 Temperature test case

Starting-point is the following equation

$$\frac{\partial T}{\partial t} = k\frac{\partial^2 T}{\partial x^2} \tag{H.57}$$

Assuming a half body with boundary conditions $T(x = 0, t = 0) = T_0$.
Analytical solution

$$T(x,t) = T_0\left\{1 - erf\left(\frac{x}{2\sqrt{kt}}\right)\right\} \tag{H.58}$$

where

$$erf(z) = \frac{2}{\sqrt{\pi}}\int_0^z e^{-x^2}\,dx \tag{H.59}$$

(Chatenier [10])

Appendix I

Material data of Makrolon CD 2000

In this appendix the material data of a polycarbonate, Makrolon CD 2000 from Bayer, are given. This data is obtained from Douven [14].
The following data are given:
- Relaxation times and viscosities for melt state, table I.1.
- Relaxation times and viscosities for the glassy state, table I.2.
- WLF parameters, table I.3.
- Parameters in shift function for glassy state, table I.4.
- Parameters in Tait equation (melt and glassy state), table I.5.
- Parameters for c_p, table I.6.
- The thermal conductivity, table I.7.

mode-no.	Maxwell	
	$\eta_{r0} = 0.678$ Pas	
i	θ_i s	η_i Pas
1	$9.238 \cdot 10^{-3}$	$3.101 \cdot 10^{2}$
2	$9.548 \cdot 10^{-4}$	$2.596 \cdot 10^{2}$
3	$1.852 \cdot 10^{-4}$	$6.846 \cdot 10^{1}$
4	$4.817 \cdot 10^{-5}$	$1.135 \cdot 10^{1}$
5	$1.804 \cdot 10^{-5}$	4.254
6	$2.019 \cdot 10^{-6}$	1.377

Table I.1: Linear visco-elastic parameters for melt state.

mode-no.	Maxwell	
i	θ_i s	η_i Pas
1	6.323	$1.019 \cdot 10^9$
2	$3.528 \cdot 10^{-1}$	$1.085 \cdot 10^8$
3	$1.968 \cdot 10^{-2}$	$2.332 \cdot 10^6$
4	$1.098 \cdot 10^{-3}$	$5.307 \cdot 10^4$
5	$6.125 \cdot 10^{-5}$	$1.225 \cdot 10^3$
6	$3.417 \cdot 10^{-6}$	$4.261 \cdot 10^1$
7	$1.906 \cdot 10^{-7}$	3.137

Table I.2: Linear visco-elastic parameters for glassy state.

c_1		3.05
c_2	K	134.72
T_0	K	511

Table I.3: WLF parameters (melt state).

c_3		0.6015
T_0	K	413

Table I.4: Parameters shift function (glassy state).

		melt	glass
a_0	m^3/kg	$8.68 \cdot 10^{-4}$	$8.68 \cdot 10^{-4}$
a_1	$m^3/(kgK)$	$5.77 \cdot 10^{-7}$	$2.2 \cdot 10^{-7}$
B_0	Pa	$3.161 \cdot 10^8$	$3.954 \cdot 10^8$
B_1	K^{-1}	$4.078 \cdot 10^{-3}$	$2.609 \cdot 10^{-3}$
$T_g(0)$	K	423.4	
s	K/Pa	$5.2 \cdot 10^{-7}$	

Table I.5: Parameters in Tait-equation.

c_{p1}	$J/(kgK)$	1700
c_{p2}	$J/(kgK^2)$	2.2
c_{p3}	$J/(kgK)$	120
c_{p4}	K^{-1}	0.2
c_{p5}	K	412

Table I.6: Parameters for c_p.

λ	W/mK	0.27

Table I.7: The thermal conductivity coefficient.

Appendix J

Results of numerical simulations

In this appendix the results of cases 1 to 7 are presented.

J.1 Case 1

Material		:	polycarbonate Makrolon CD 2000
Size of cube		:	2x2x2mm
$T(t=0)$	[K]	=	465.0
T_∞	[K]	=	290.0
t_{end}	[sec]	=	6.0
Δt	[sec]	=	0.01
h	[W/Km^2]	=	1000.0
Mesh size		:	6x6x6 elements

At $t = t_{end}$:

T, min.	[K]	=	290.11
T, max.	[K]	=	293.19
σ_{xx}, min.	[N/m^2]	=	-3.09E+07
σ_{xx}, max.	[N/m^2]	=	1.66E+07
σ_{xy}, min.	[N/m^2]	=	-7.94E+05
σ_{xy}, max.	[N/m^2]	=	6.73E+06
Hydrostatic pressure, min.	[N/m^2]	=	-1.66E+07
Hydrostatic pressure, max.	[N/m^2]	=	2.06E+07

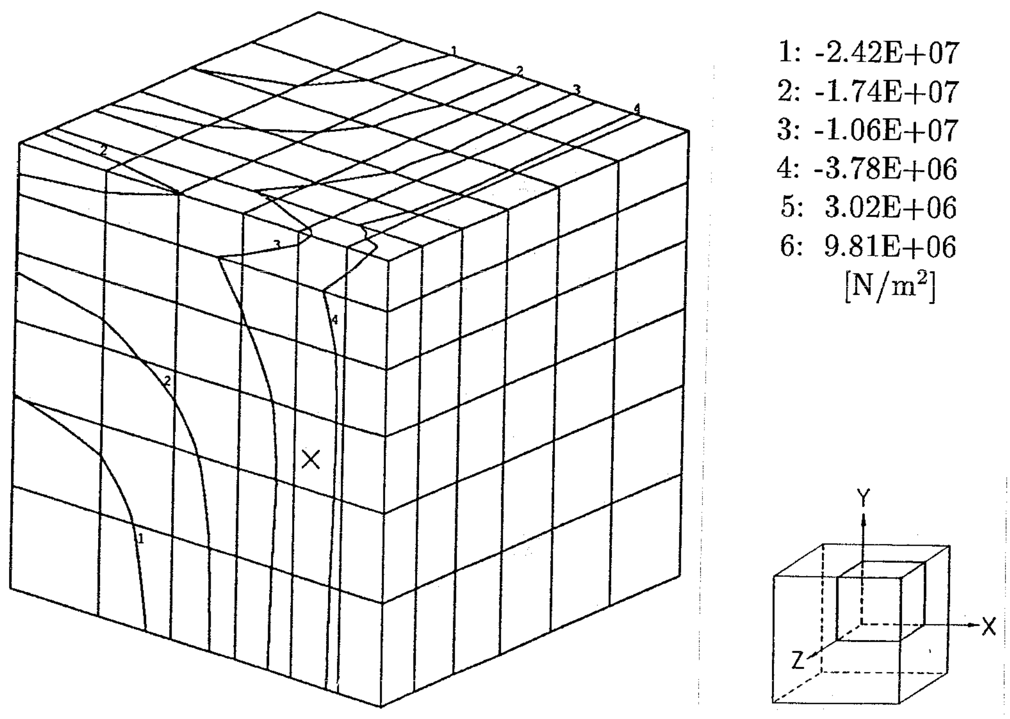

Figure J.1: Case 1, stress component σ_{xx}, outside surfaces.

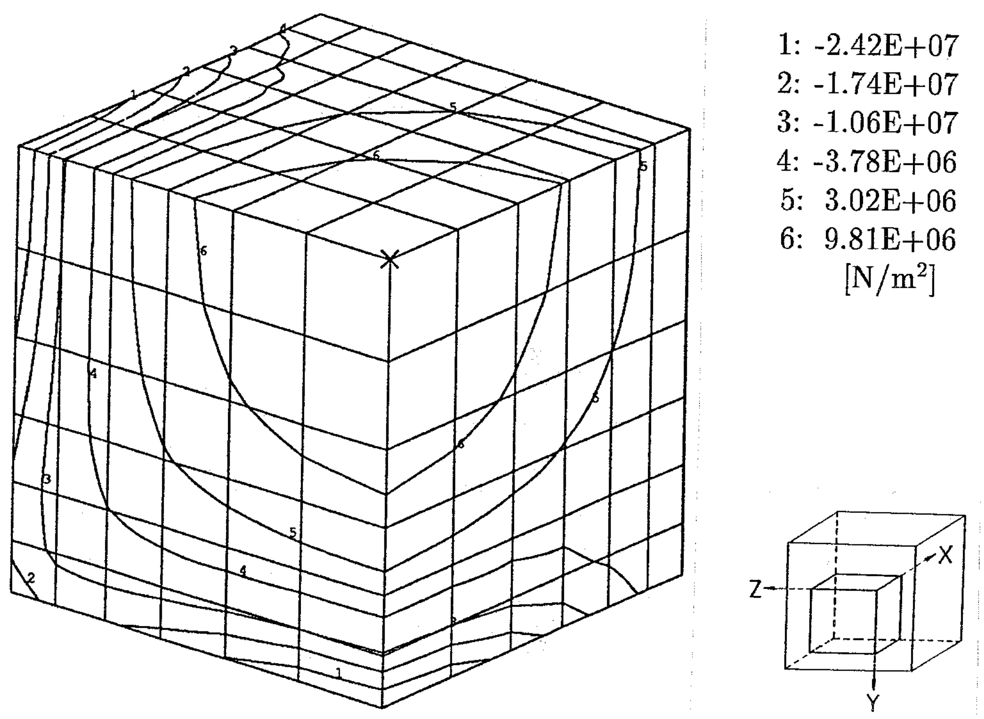

Figure J.2: Case 1, stress component σ_{xx}, symmetry surfaces.

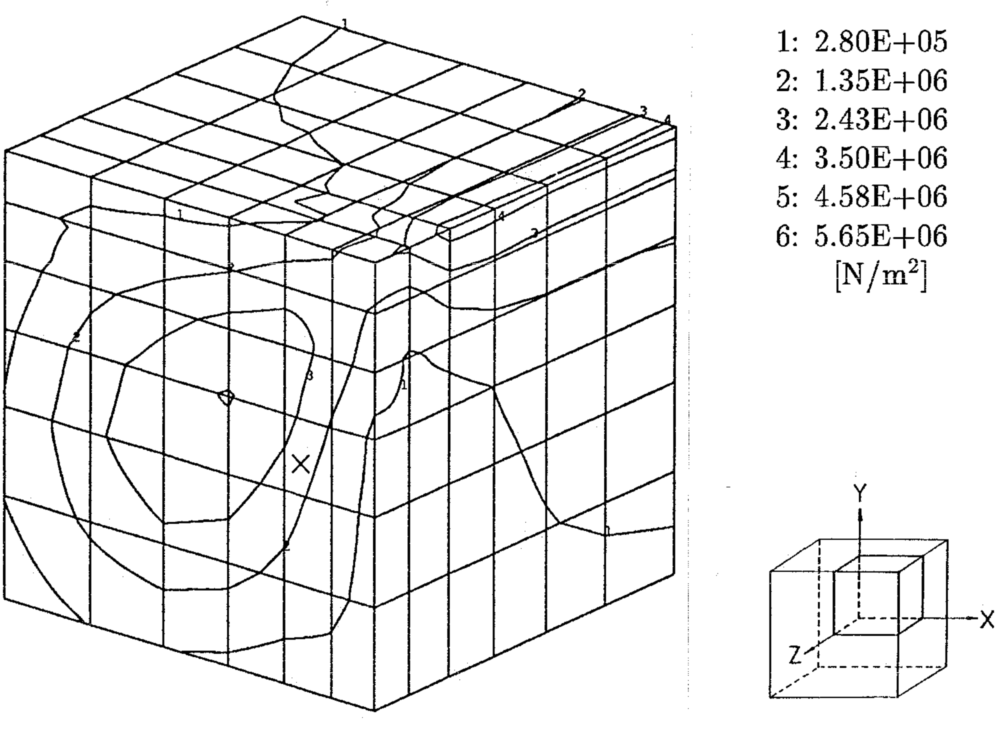

Figure J.3: Case 1, stress component σ_{xy}, outside surfaces.

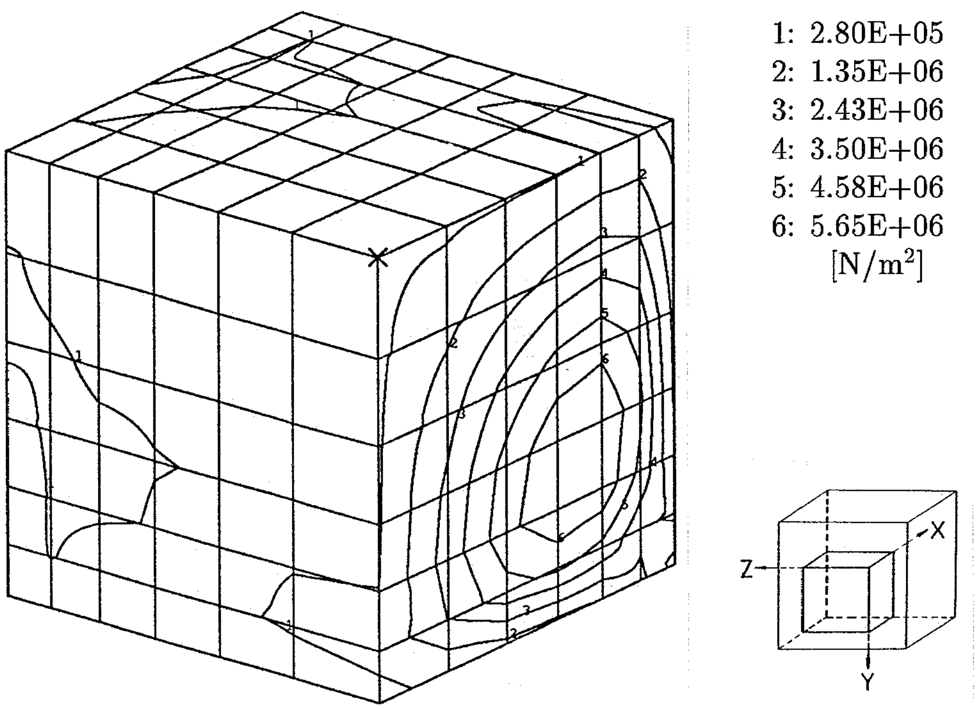

Figure J.4: Case 1, stress component σ_{xy}, symmetry surfaces.

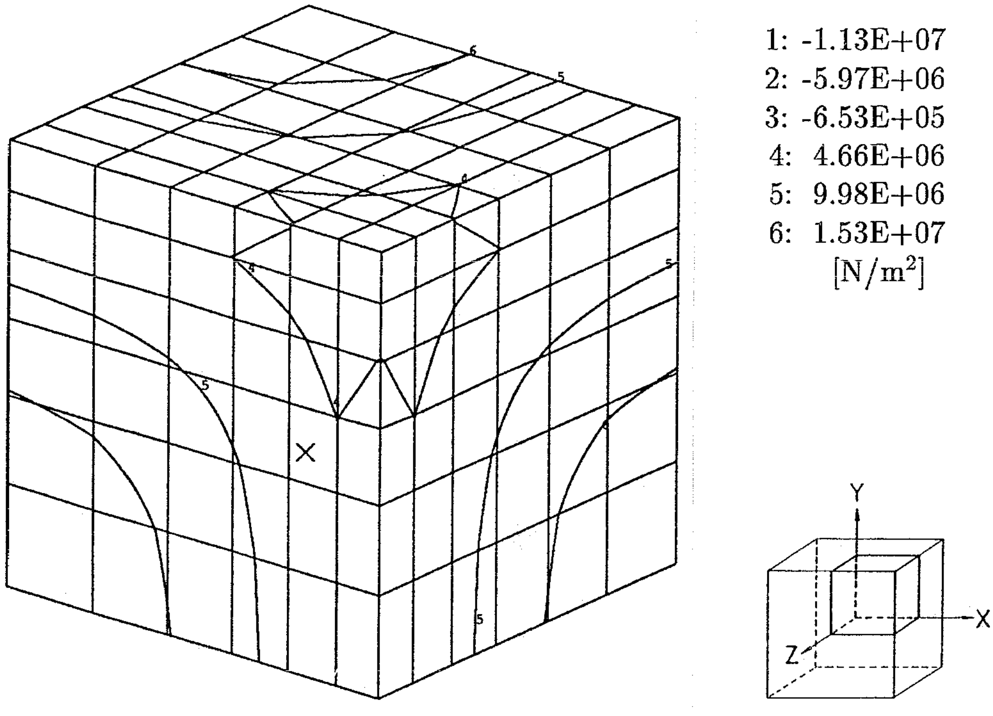

Figure J.5: Case 1, hydrostatic pressure, outside surfaces.

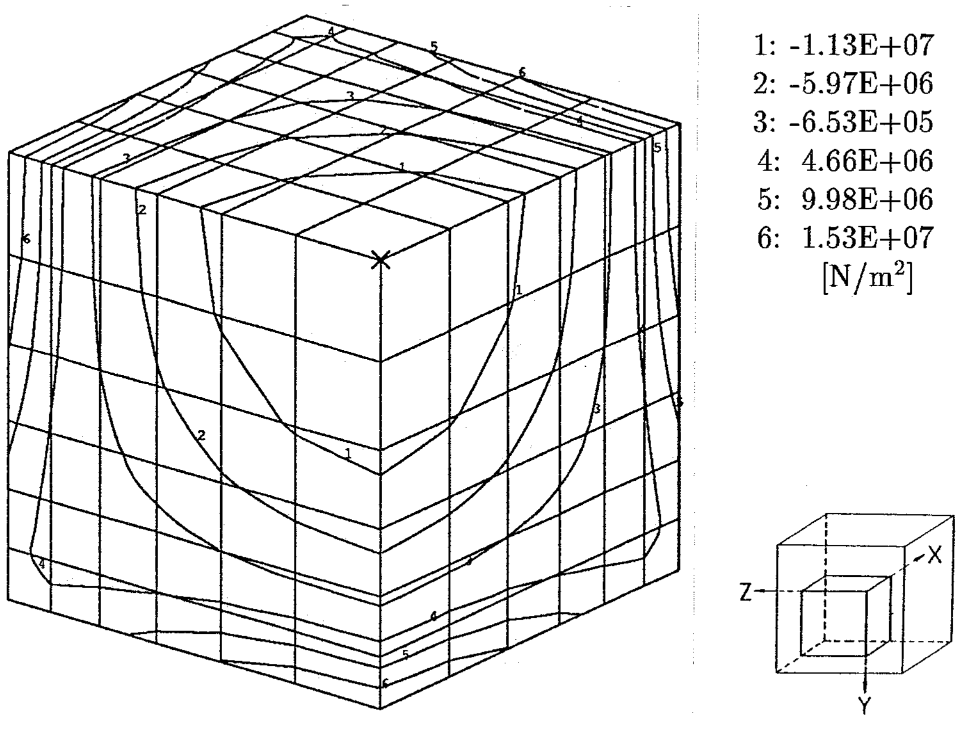

Figure J.6: Case 1, hydrostatic pressure, symmetry surfaces.

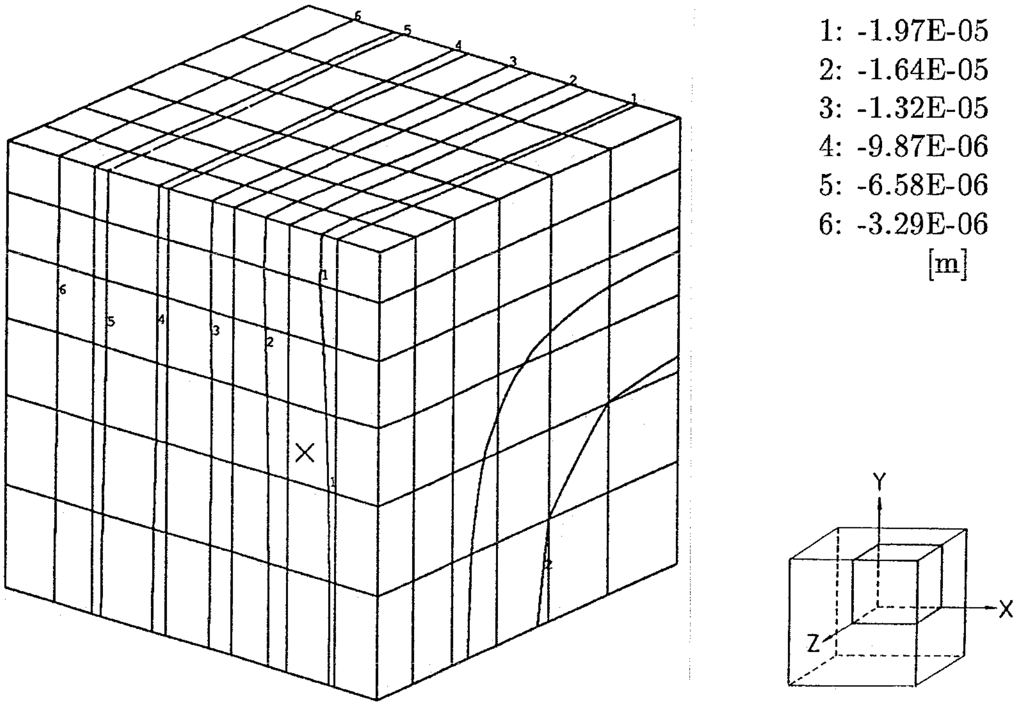

Figure J.7: Case 1, displacement component x, outside surfaces.

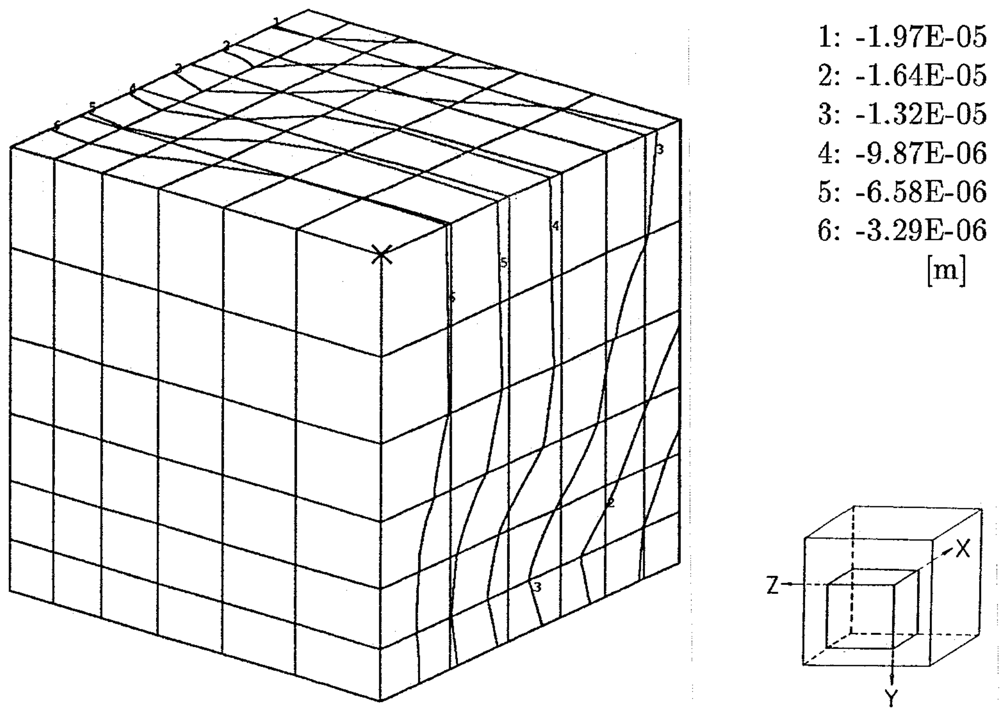

Figure J.8: Case 1, displacement component x, symmetry surfaces.

J.2 Case 2

Material		:	polycarbonate Makrolon CD 2000
Size of cube		:	2x2x2mm
$T(t=0)$	[K]	=	465.0
T_∞	[K]	=	290.0
t_{end}	[sec]	=	6.0
Δt	[sec]	=	0.01
h	[W/Km^2]	=	1000.0
Mesh size		:	10x10x10 elements

At $t = t_{end}$:

T, min.	[K]	=	290.11
T, max.	[K]	=	293.16
σ_{xx}, min.	[N/m^2]	=	-3.16E+07
σ_{xx}, max.	[N/m^2]	=	1.63E+07
σ_{xy}, min.	[N/m^2]	=	-6.04E+05
σ_{xy}, max.	[N/m^2]	=	6.95E+06
Hydrostatic pressure, min.	[N/m^2]	=	-1.63E+07
Hydrostatic pressure, max.	[N/m^2]	=	2.12E+07

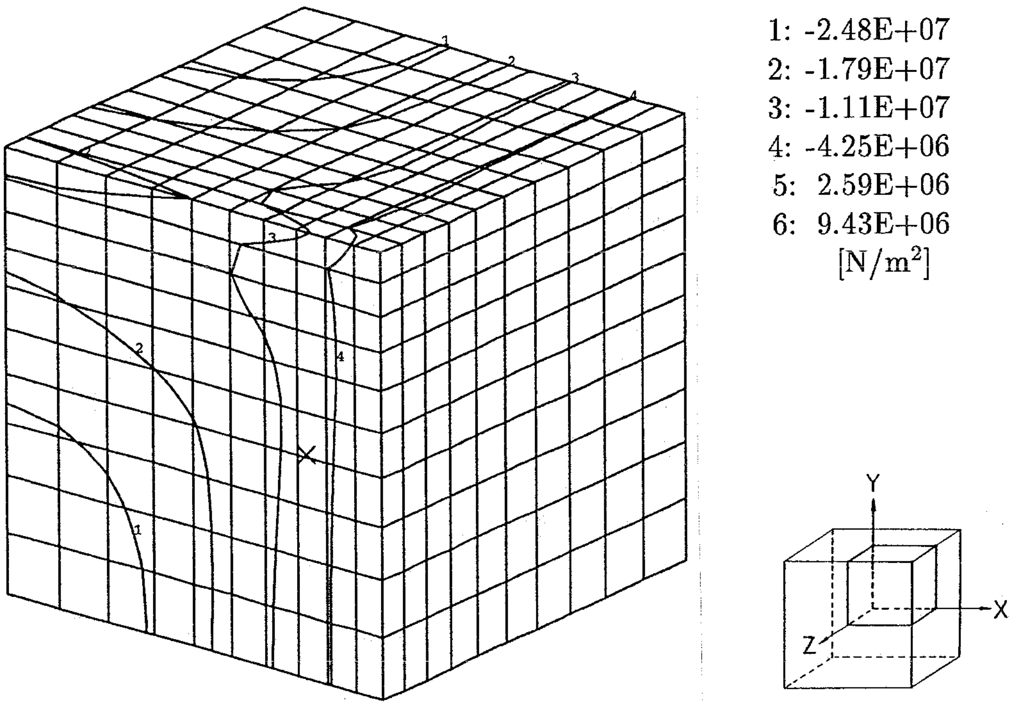

Figure J.9: Case 2, stress component σ_{xx}, outside surfaces.

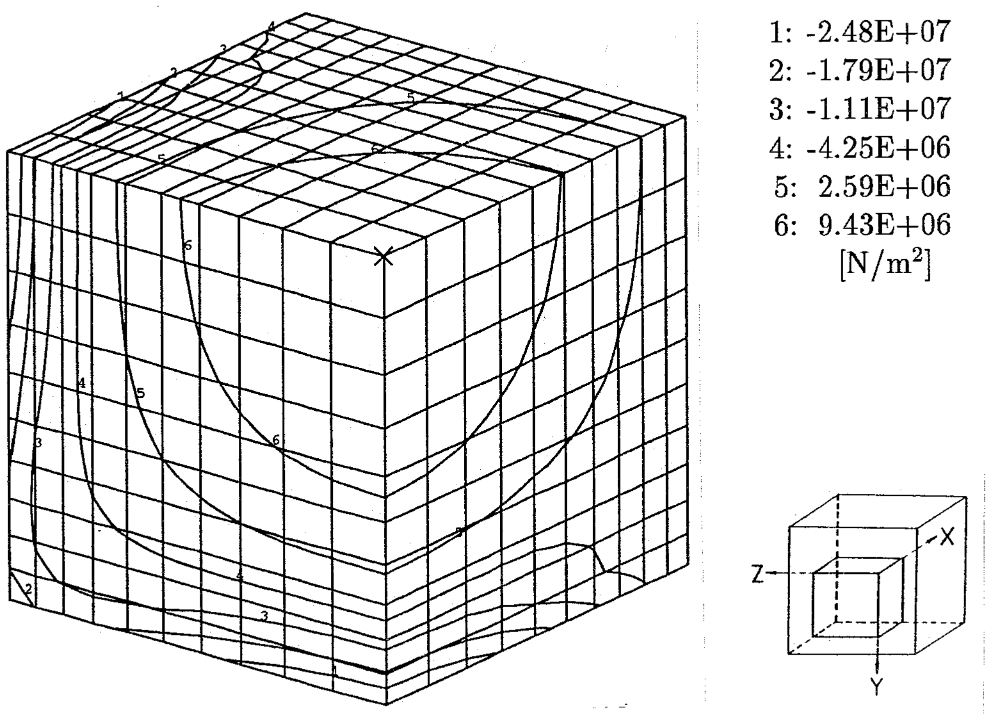

Figure J.10: Case 2, stress component σ_{xx}, symmetry surfaces.

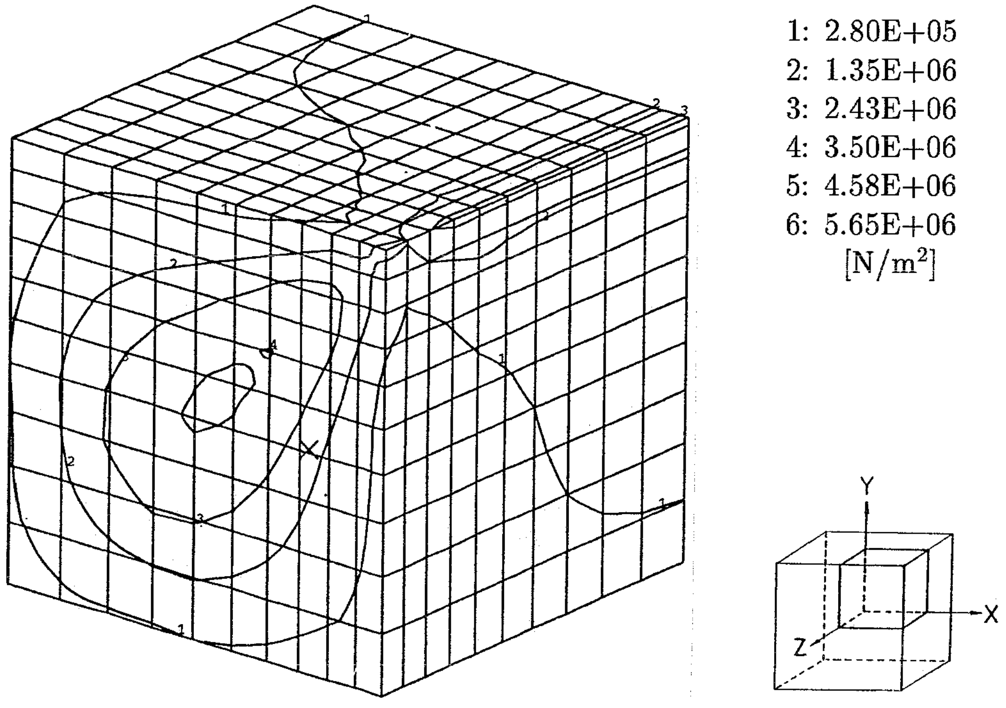

1: 2.80E+05
2: 1.35E+06
3: 2.43E+06
4: 3.50E+06
5: 4.58E+06
6: 5.65E+06
[N/m^2]

Figure J.11: Case 2, stress component σ_{xy}, outside surfaces.

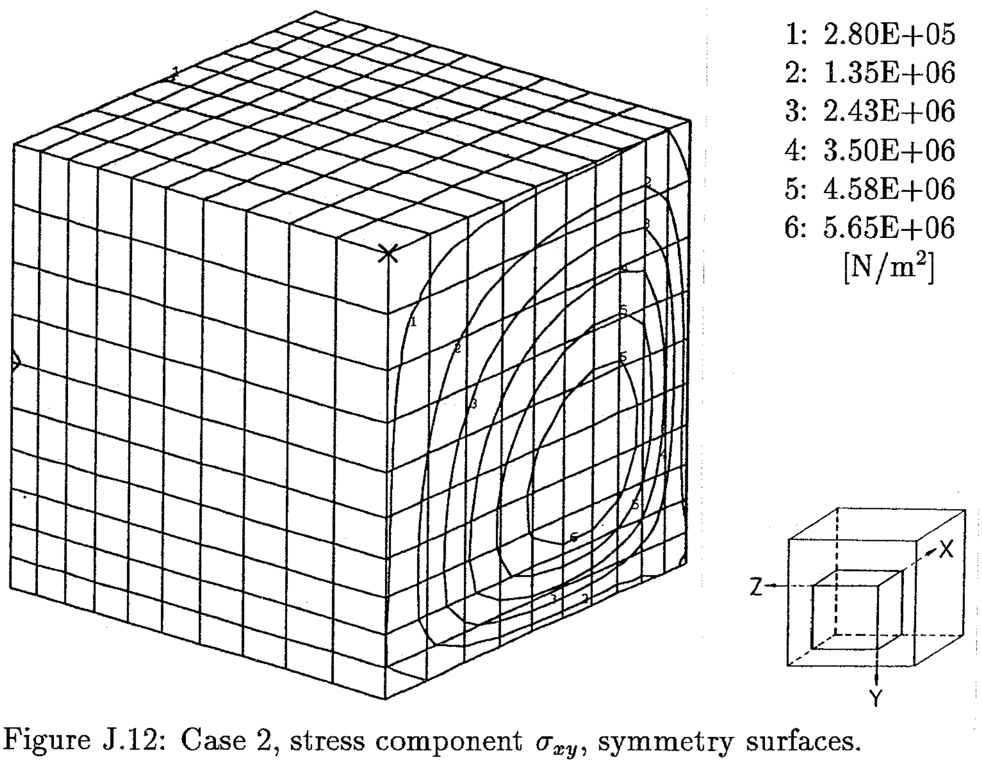

1: 2.80E+05
2: 1.35E+06
3: 2.43E+06
4: 3.50E+06
5: 4.58E+06
6: 5.65E+06
[N/m^2]

Figure J.12: Case 2, stress component σ_{xy}, symmetry surfaces.

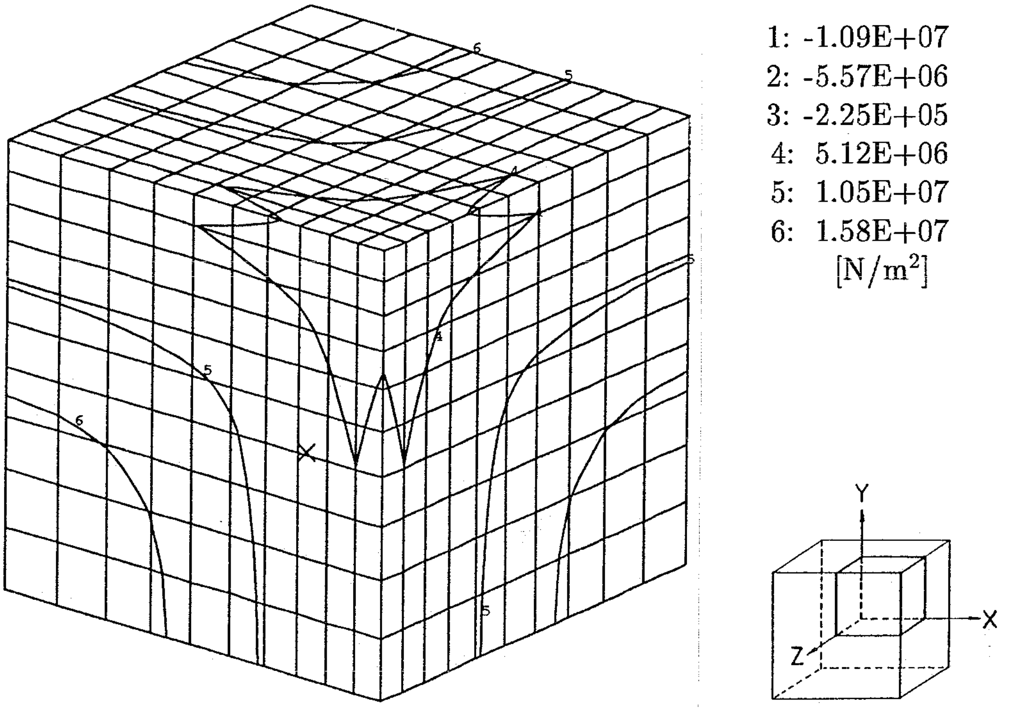

Figure J.13: Case 2, hydrostatic pressure, outside surfaces.

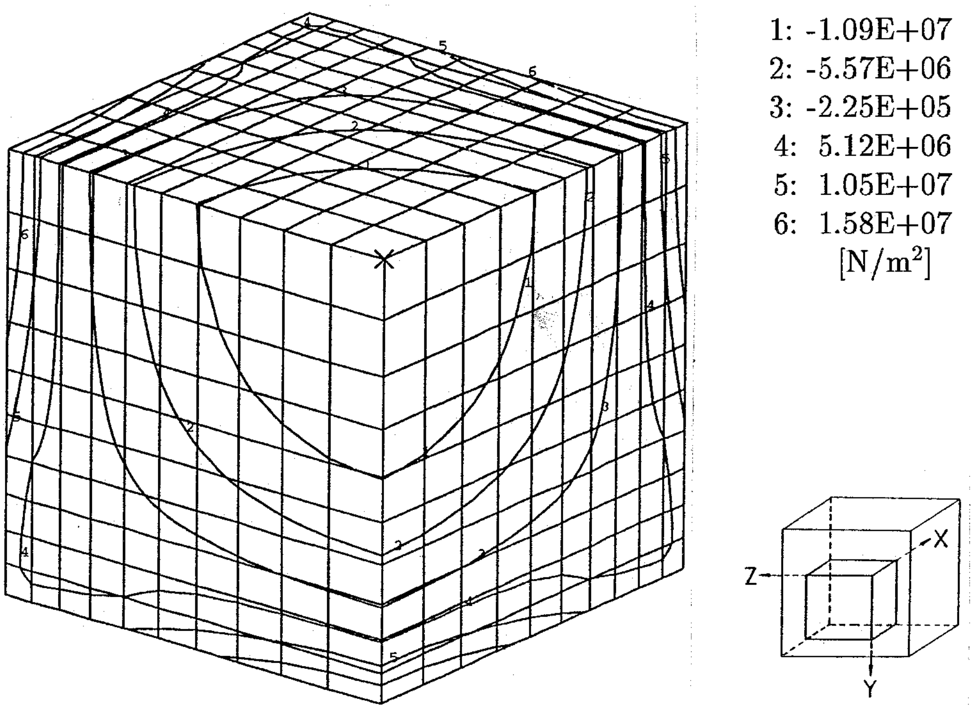

Figure J.14: Case 2, hydrostatic pressure, symmetry surfaces.

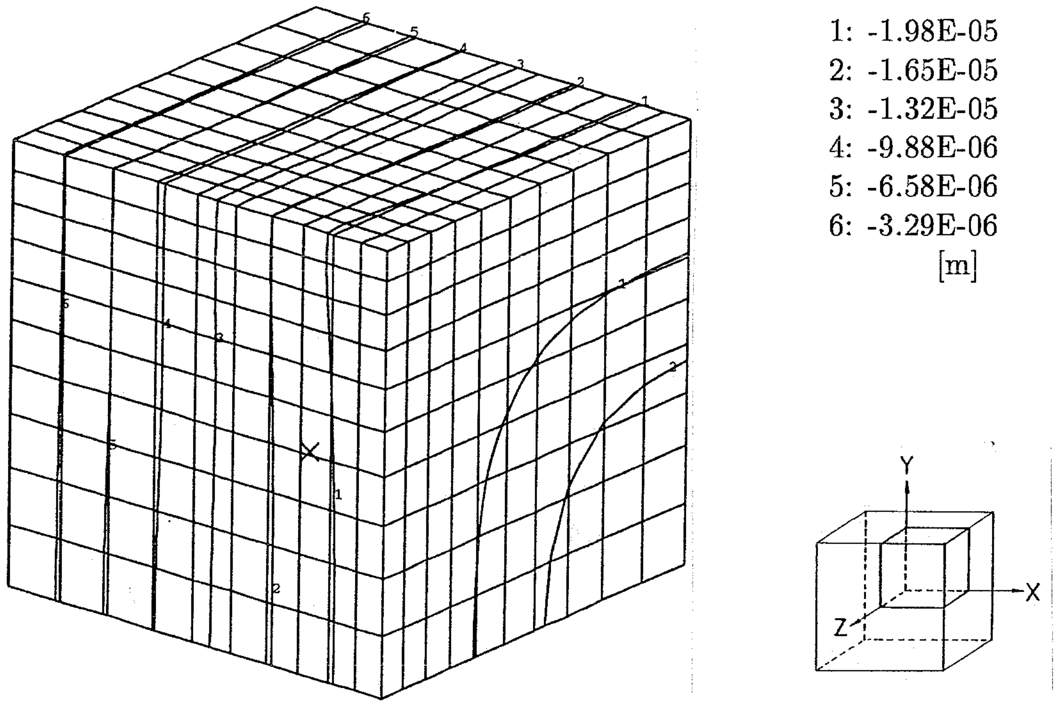

Figure J.15: Case 2, displacement component x, outside surfaces.

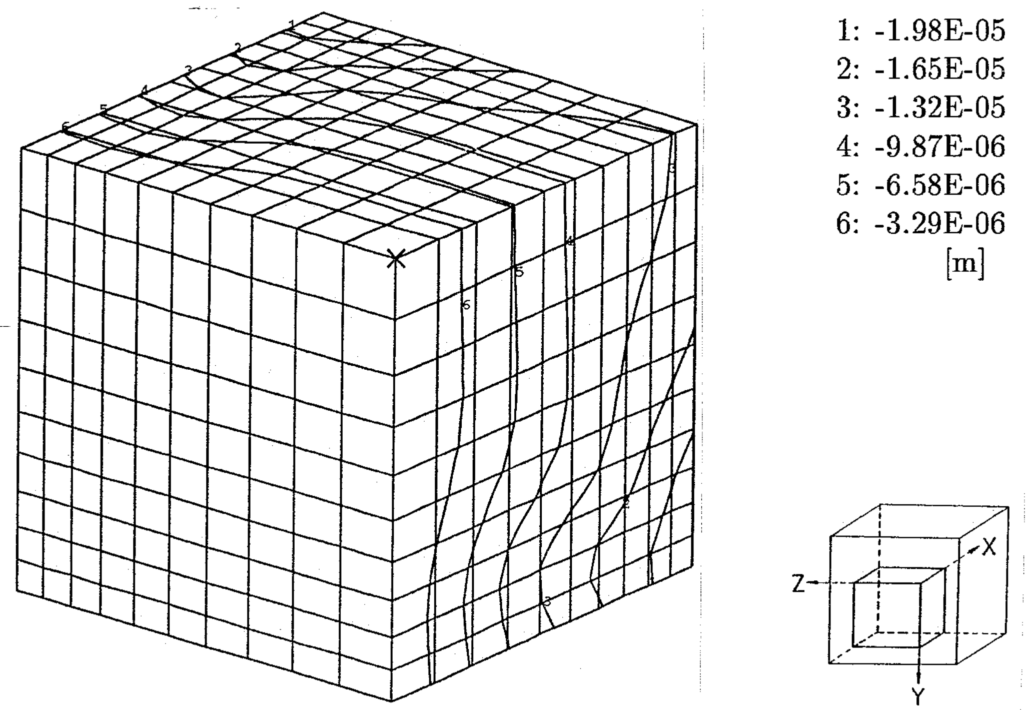

Figure J.16: Case 2, displacement component x, symmetry surfaces.

J.3 Case 3

Material		:	polycarbonate Makrolon CD 2000
Size of cube		:	2x2x2mm
$T(t=0)$	[K]	=	465.0
T_∞	[K]	=	290.0
t_{end}	[sec]	=	6.11
Δt	[sec]	=	$0.011 ln(1.094 + t)$
h	[W/Km^2]	=	1000.0
Mesh size		:	6x6x6 elements

At $t = t_{end}$:

T, min.	[K]	=	290.10
T, max.	[K]	=	292.92
σ_{xx}, min.	[N/m^2]	=	-3.13E+07
σ_{xx}, max.	[N/m^2]	=	1.67E+07
σ_{xy}, min.	[N/m^2]	=	-8.72E+05
σ_{xy}, max.	[N/m^2]	=	6.79E+06
Hydrostatic pressure, min.	[N/m^2]	=	-1.67E+07
Hydrostatic pressure, max.	[N/m^2]	=	2.09E+07

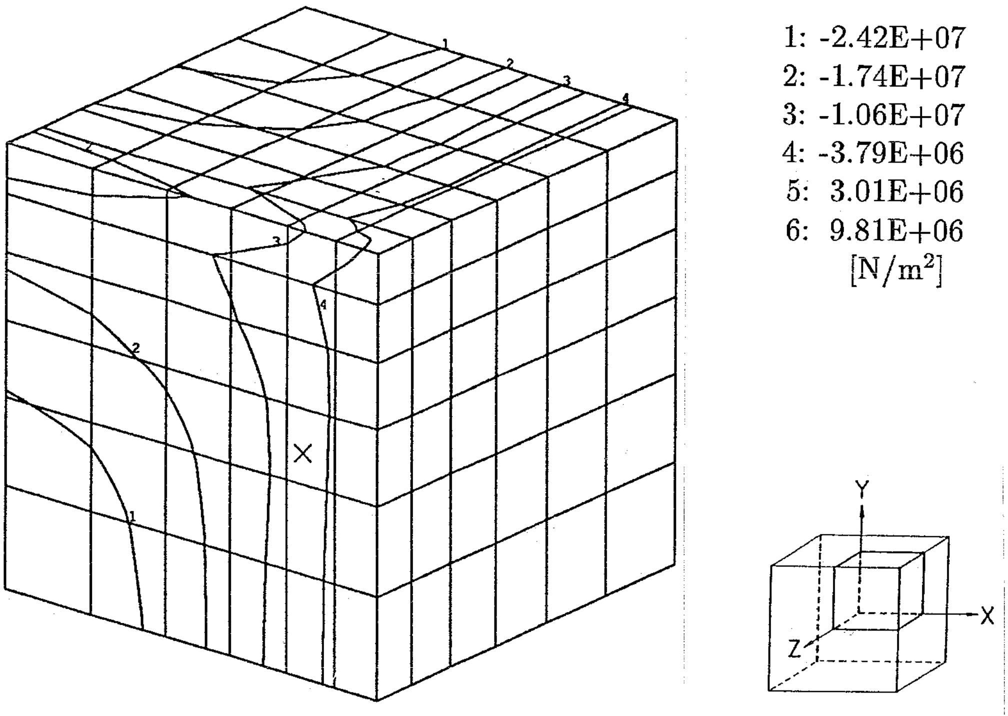

Figure J.17: Case 3, stress component σ_{xx}, outside surfaces.

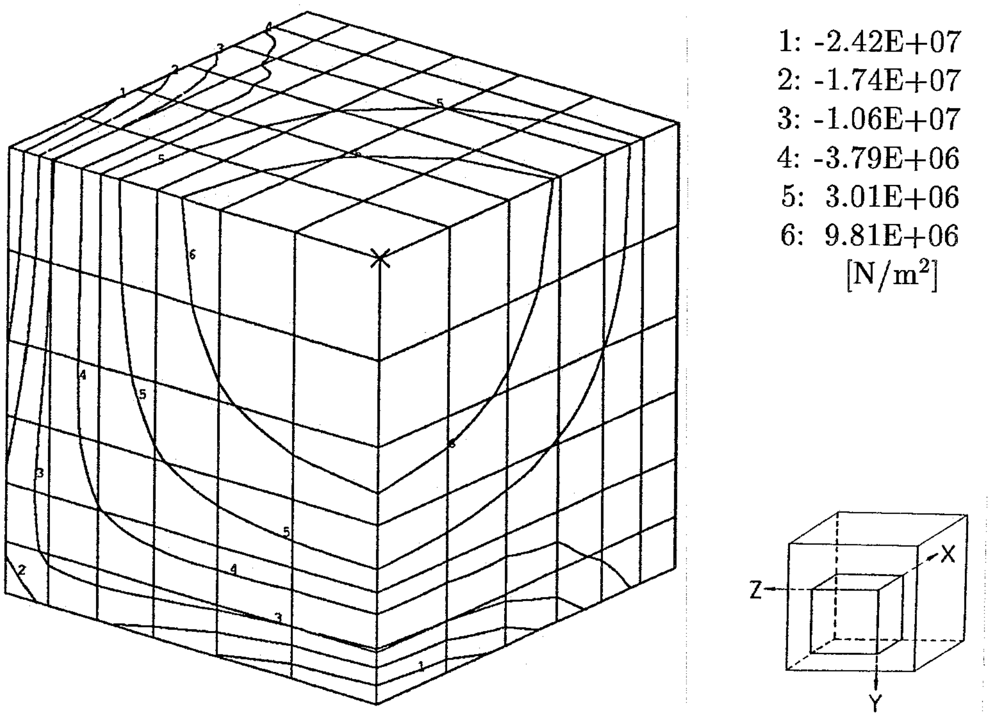

Figure J.18: Case 3, stress component σ_{xx}, symmetry surfaces.

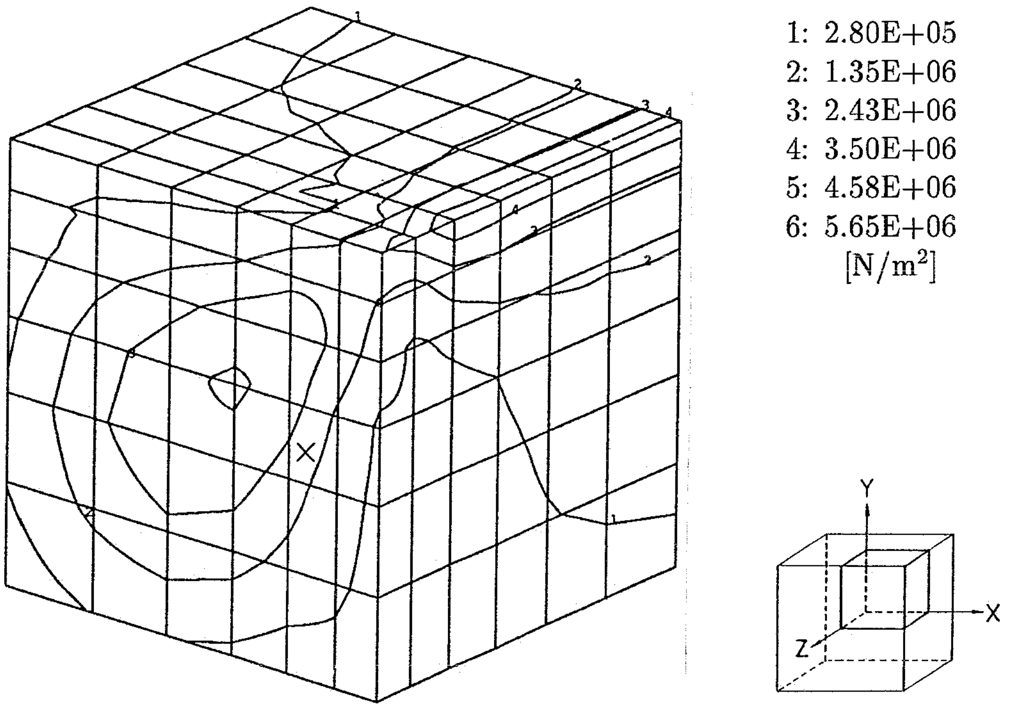

Figure J.19: Case 3, stress component σ_{xy}, outside surfaces.

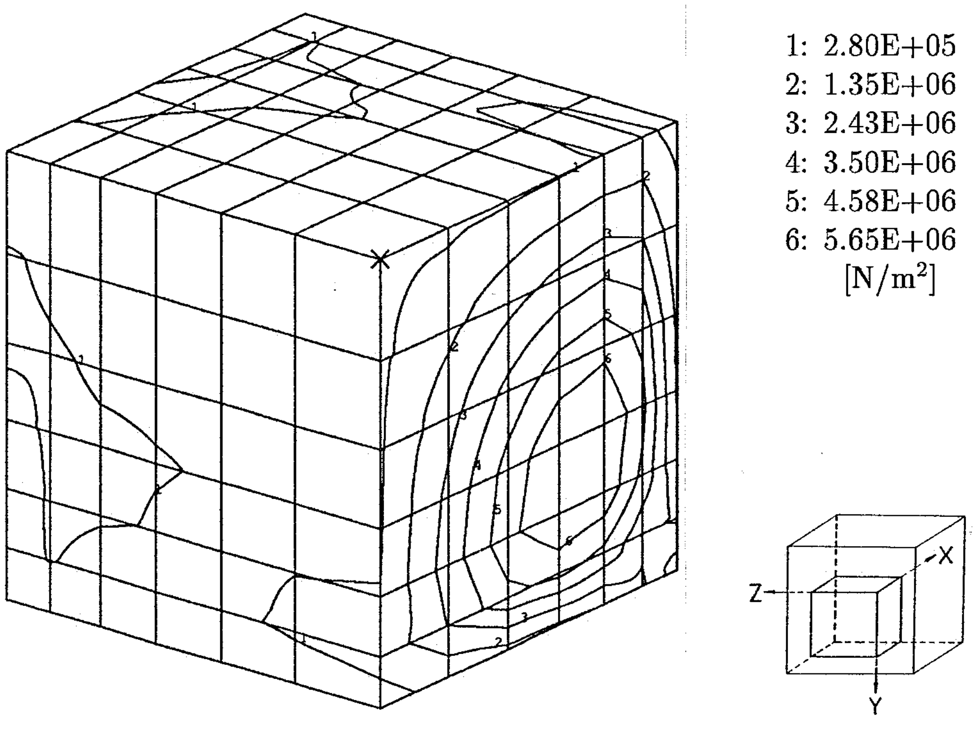

Figure J.20: Case 3, stress component σ_{xy}, symmetry surfaces.

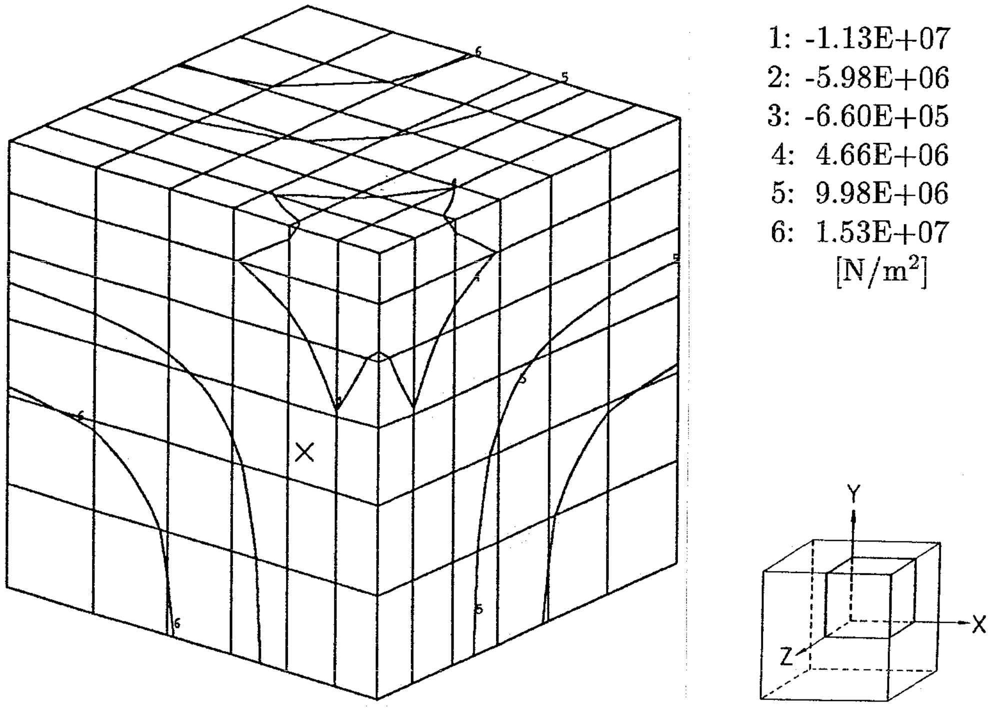

Figure J.21: Case 3, hydrostatic pressure, outside surfaces.

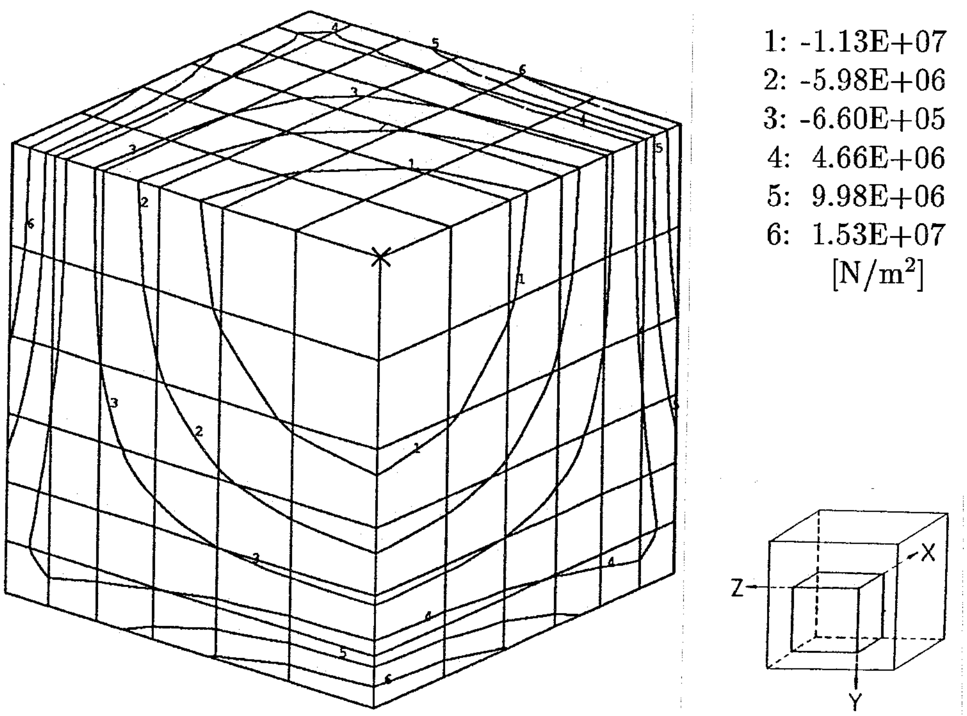

Figure J.22: Case 3, hydrostatic pressure, symmetry surfaces.

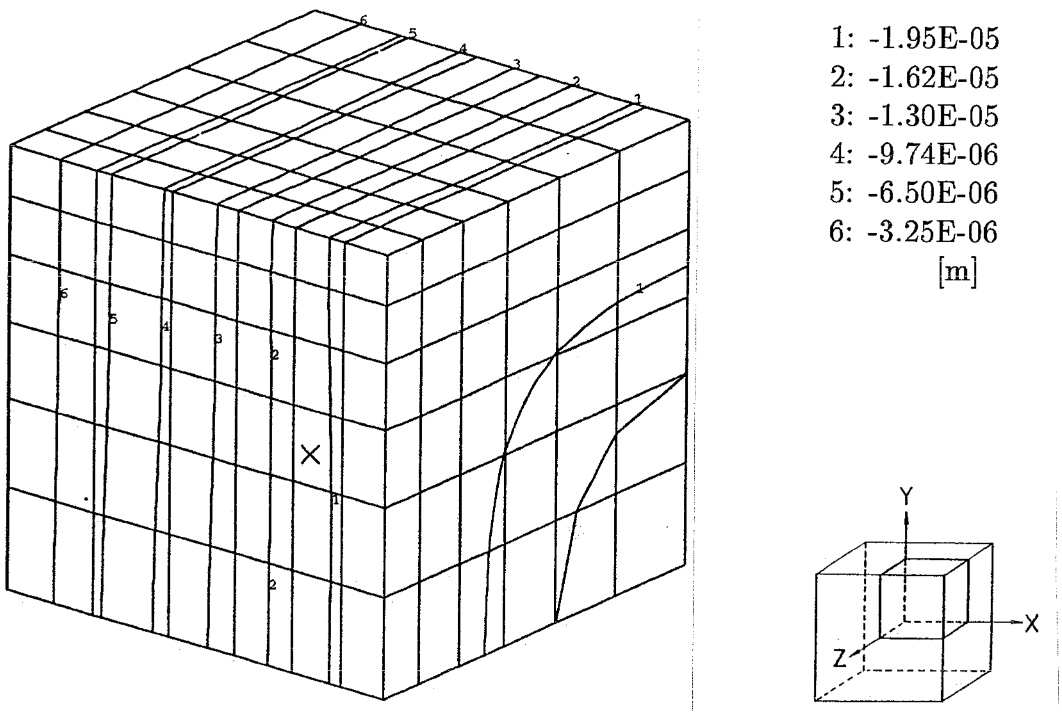

Figure J.23: Case 3, displacement component x, outside surfaces.

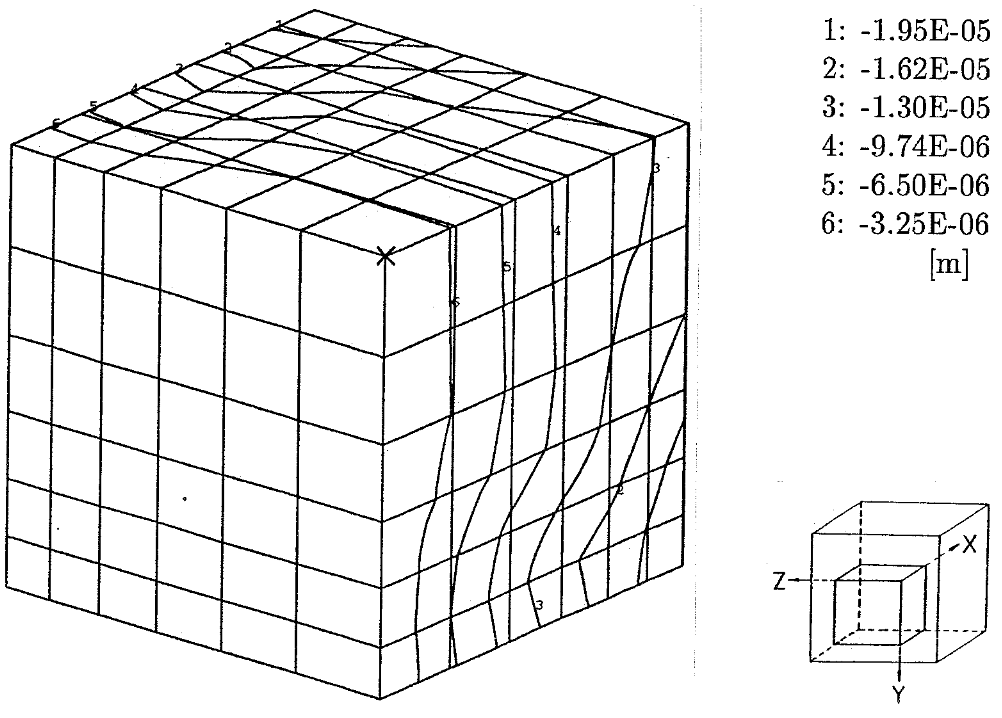

Figure J.24: Case 3, displacement component x, symmetry surfaces.

J.4 Case 4

Material		:	polycarbonate Makrolon CD 2000
Size of cube		:	2x2x2mm
$T(t=0)$	[K]	=	465.0
T_∞	[K]	=	290.0
t_{end}	[sec]	=	6.0
Δt	[sec]	=	0.01
h	[W/Km^2]	=	500.0
Mesh size		:	10x10x10 elements

At $t = t_{end}$:

T, min.	[K]	=	291.42
T, max.	[K]	=	301.32
σ_{xx}, min.	[N/m^2]	=	-2.57E+07
σ_{xx}, max.	[N/m^2]	=	1.21E+07
σ_{xy}, min.	[N/m^2]	=	-2.25E+05
σ_{xy}, max.	[N/m^2]	=	5.21E+06
Hydrostatic pressure, min.	[N/m^2]	=	-1.21E+07
Hydrostatic pressure, max.	[N/m^2]	=	1.70E+07

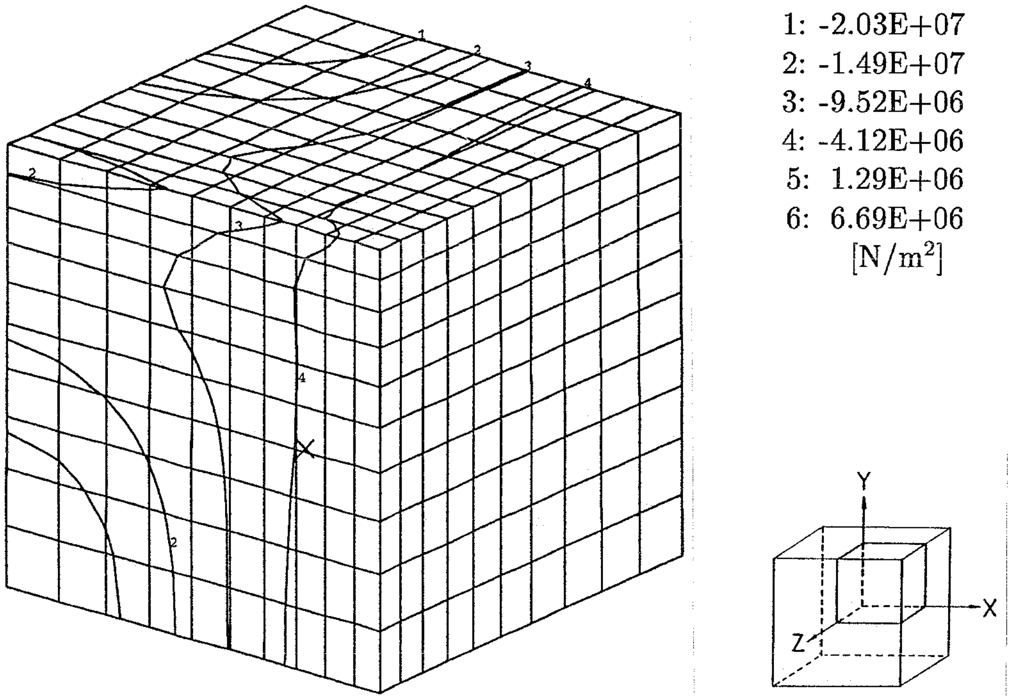

Figure J.25: Case 4, stress component σ_{xx}, outside surfaces.

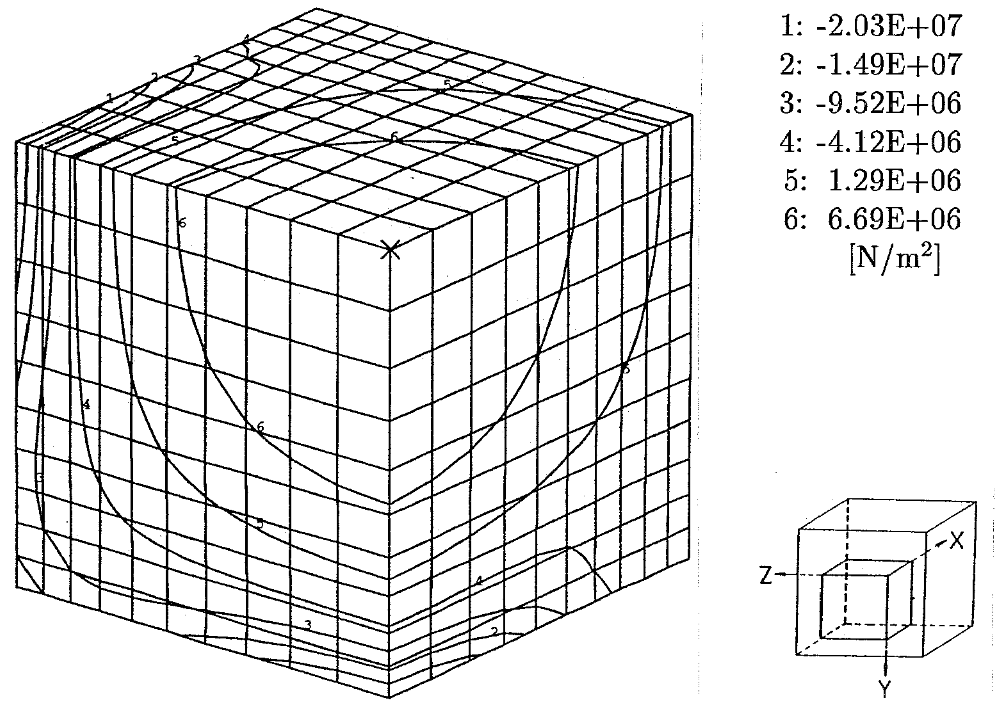

Figure J.26: Case 4, stress component σ_{xx}, symmetry surfaces.

J.5 Case 5

Material		:	polycarbonate Makrolon CD 2000
Size of cube		:	2x2x2mm
$T(t=0)$	[K]	=	465.0
T_∞	[K]	=	290.0
t_{end}	[sec]	=	10.0
Δt	[sec]	=	0.01
h	[W/Km^2]	=	250.0
Mesh size		:	10x10x10 elements

At $t = t_{end}$:

T, min.	[K]	=	291.74
T, max.	[K]	=	295.64
σ_{xx}, min.	[N/m^2]	=	-1.75E+07
σ_{xx}, max.	[N/m^2]	=	8.24E+06
σ_{xy}, min.	[N/m^2]	=	-2.96E+05
σ_{xy}, max.	[N/m^2]	=	3.56E+06
Hydrostatic pressure, min.	[N/m^2]	=	-8.24E+06
Hydrostatic pressure, max.	[N/m^2]	=	1.15E+07

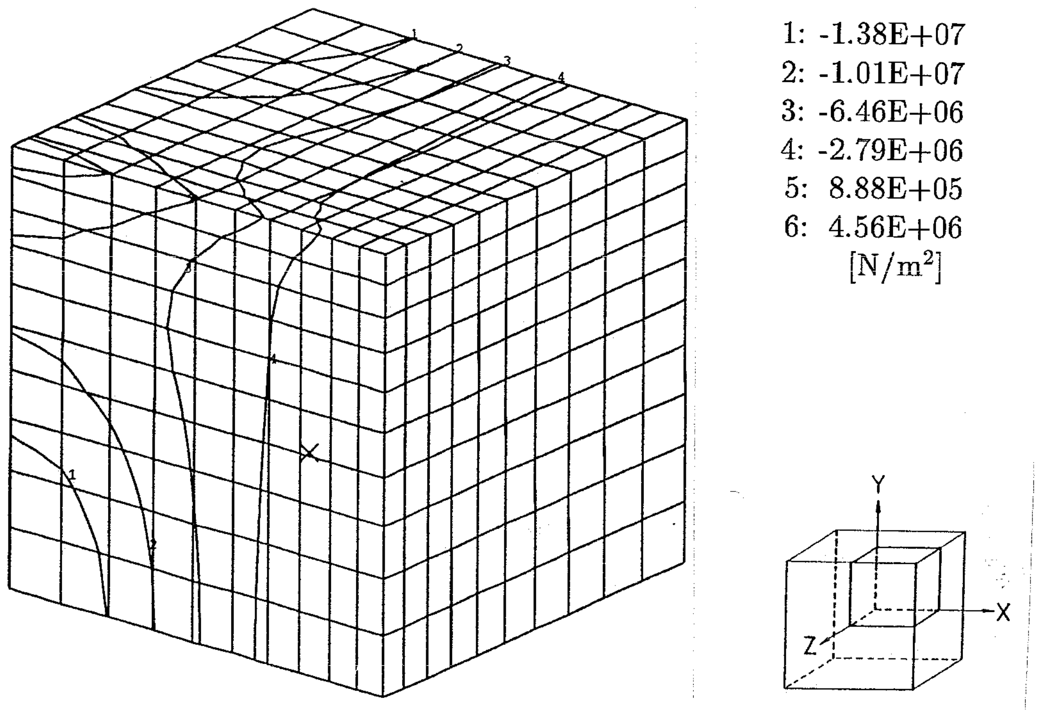

Figure J.27: Case 5, stress component σ_{xx}, outside surfaces.

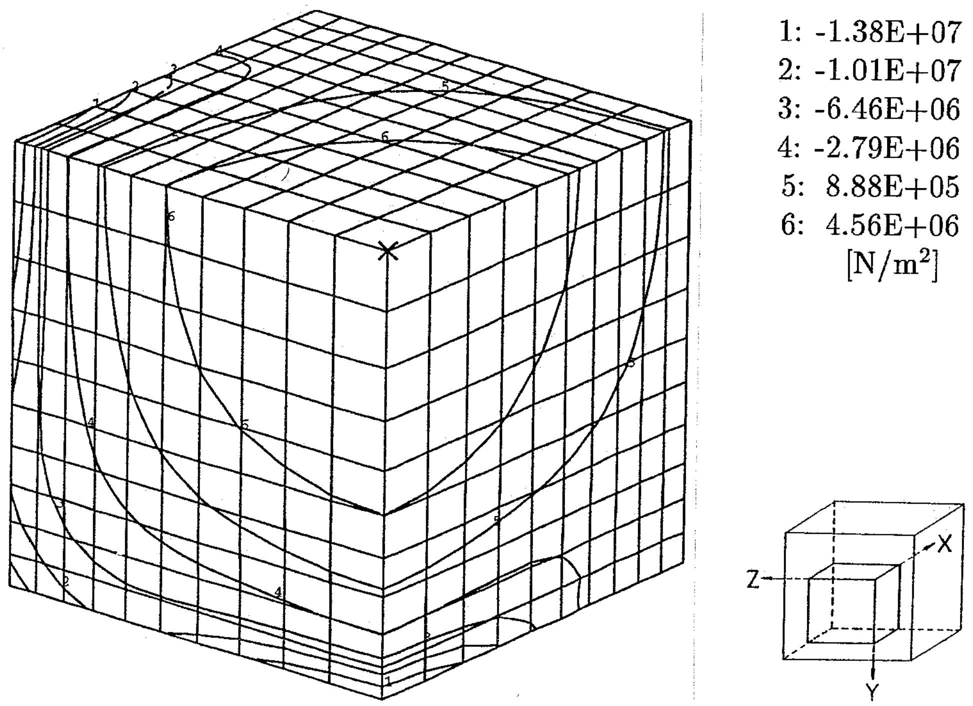

Figure J.28: Case 5, stress component σ_{xx}, symmetry surfaces.

J.6 Case 6

Material		:	polycarbonate Makrolon CD 2000
Size of cube		:	2x4x2mm
$T(t=0)$	[K]	=	465.0
T_∞	[K]	=	290.0
t_{end}	[sec]	=	6.0
Δt	[sec]	=	0.01
h	[W/Km^2]	=	1000.0
Mesh size		:	6x12x6 elements

At $t = t_{end}$:

T, min.	[K]	=	290.20
T, max.	[K]	=	300.14
σ_{xx}, min.	[N/m^2]	=	-3.34E+07
σ_{xx}, max.	[N/m^2]	=	1.22E+07
σ_{xy}, min.	[N/m^2]	=	-1.20E+06
σ_{xy}, max.	[N/m^2]	=	5.47E+06
Hydrostatic pressure, min.	[N/m^2]	=	-1.35E+07
Hydrostatic pressure, max.	[N/m^2]	=	1.94E+07

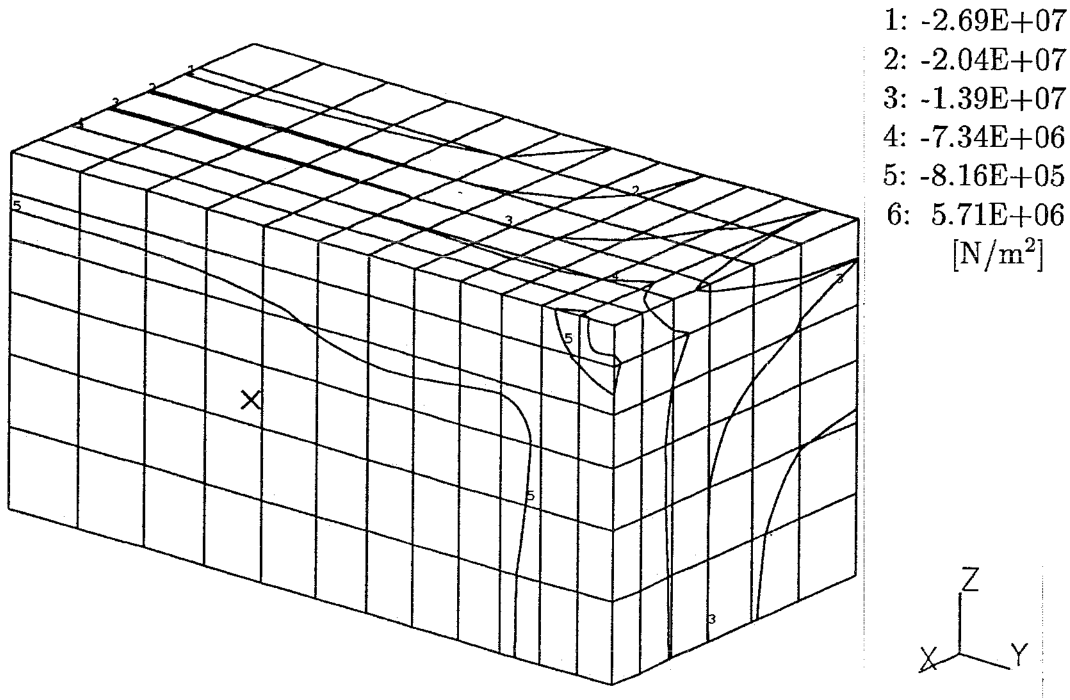

Figure J.29: Case 6, stress component σ_{xx}, outside surfaces.

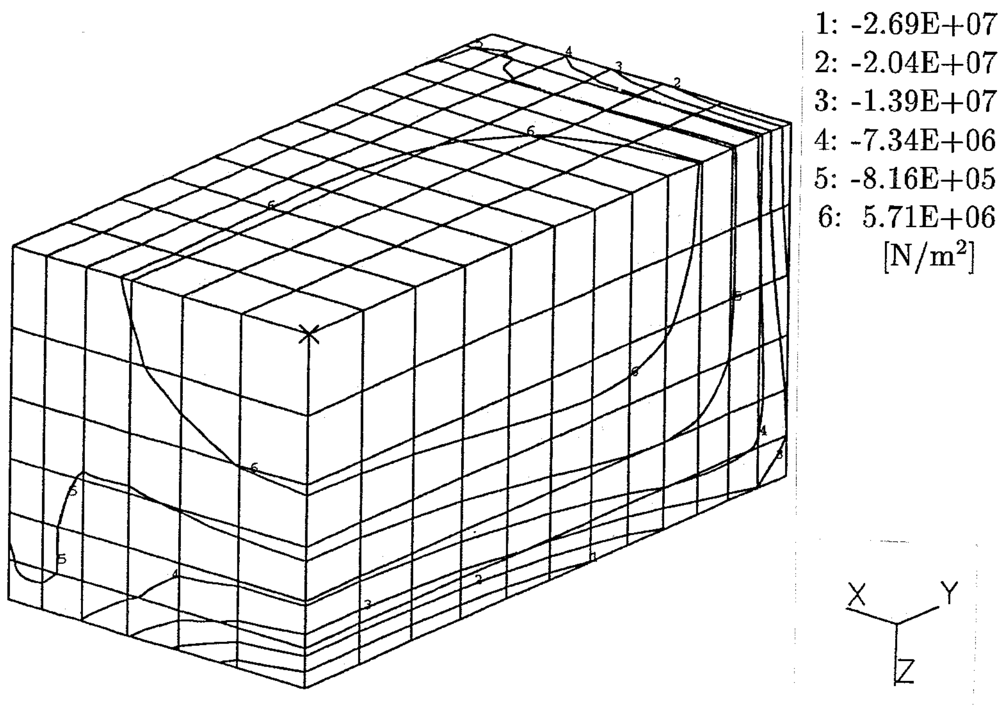

Figure J.30: Case 6, stress component σ_{xx}, symmetry surfaces.

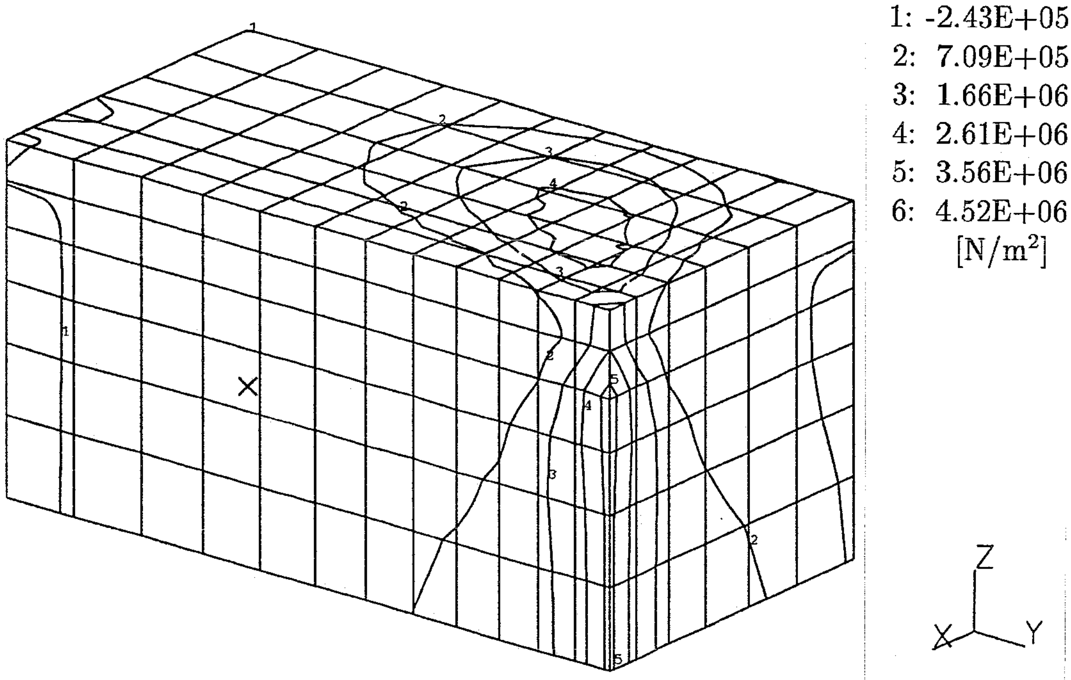

Figure J.31: Case 6, stress component σ_{xy}, outside surfaces.

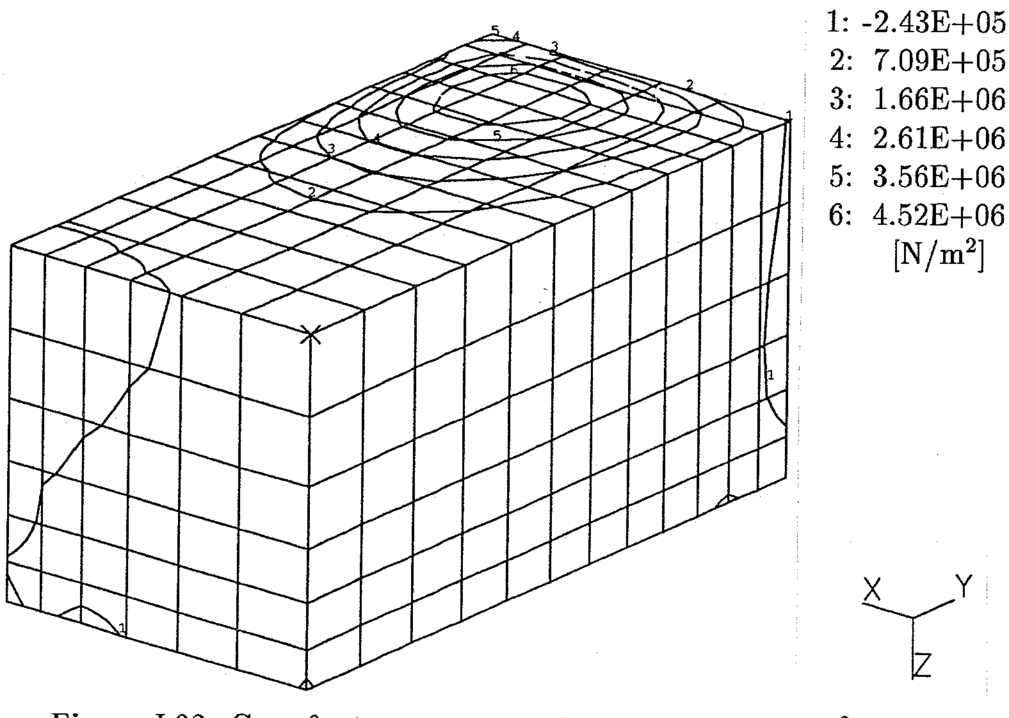

Figure J.32: Case 6, stress component σ_{xy}, symmetry surfaces.

J.7 Case 7

Material		:	polycarbonate Makrolon CD 2000
Size of cube		:	2x2x2mm
$T(t=0)$	[K]	=	465.0
T_∞	[K]	=	290.0
t_{end}	[sec]	=	6.0
Δt	[sec]	=	0.01
h	[W/Km^2]	=	1000.0
Mesh size		:	6x6x6 elements

Nonlinear application.

At $t = t_{end}$:

T, min.	[K]	=	290.11
T, max.	[K]	=	293.18
σ_{xx}, min.	[N/m^2]	=	-3.07E+07
σ_{xx}, max.	[N/m^2]	=	1.65E+07
σ_{xy}, min.	[N/m^2]	=	-7.99E+05
σ_{xy}, max.	[N/m^2]	=	6.68E+06
Hydrostatic pressure, min.	[N/m^2]	=	-1.65E+07
Hydrostatic pressure, max.	[N/m^2]	=	2.04E+07

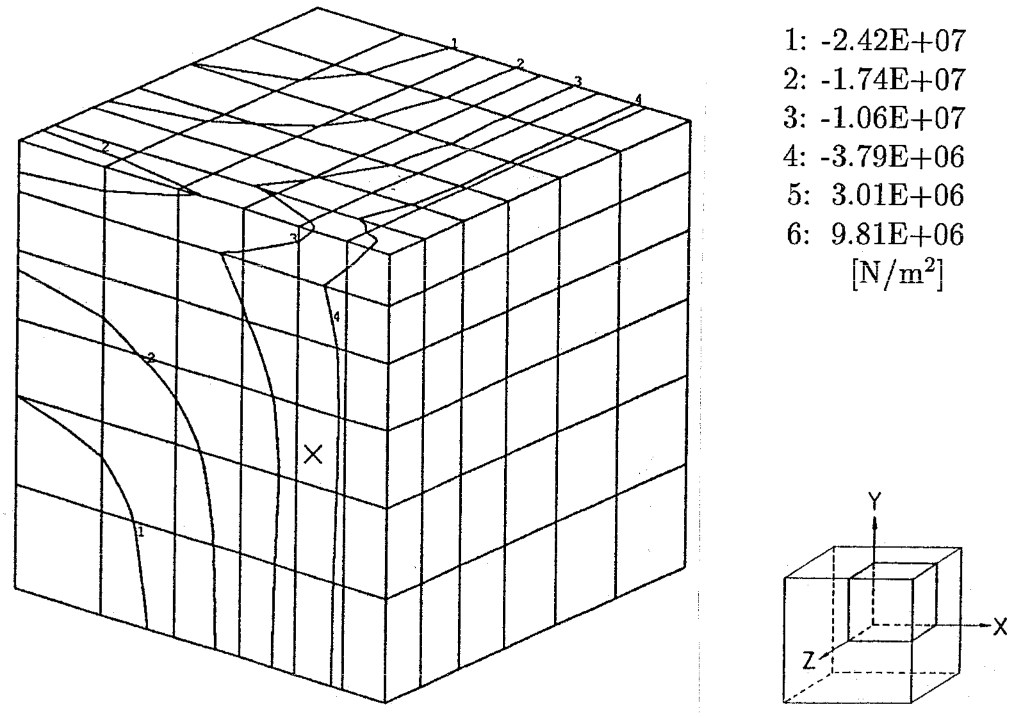

Figure J.33: Case 7, stress component σ_{xx}, outside surfaces.

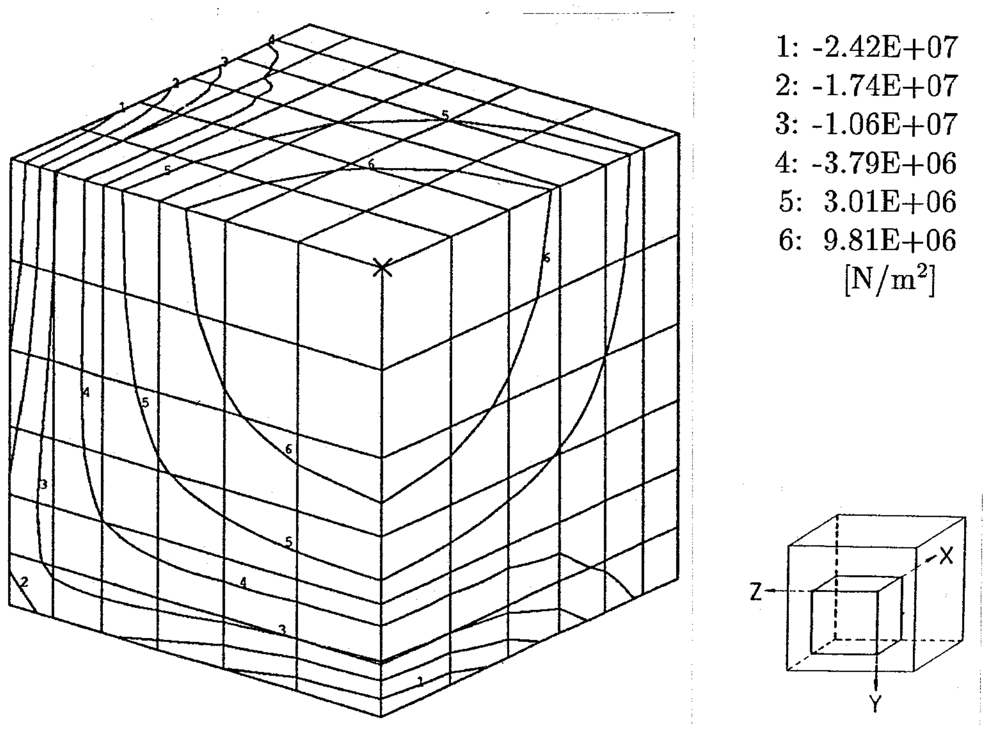

Figure J.34: Case 7, stress component σ_{xx}, symmetry surfaces.

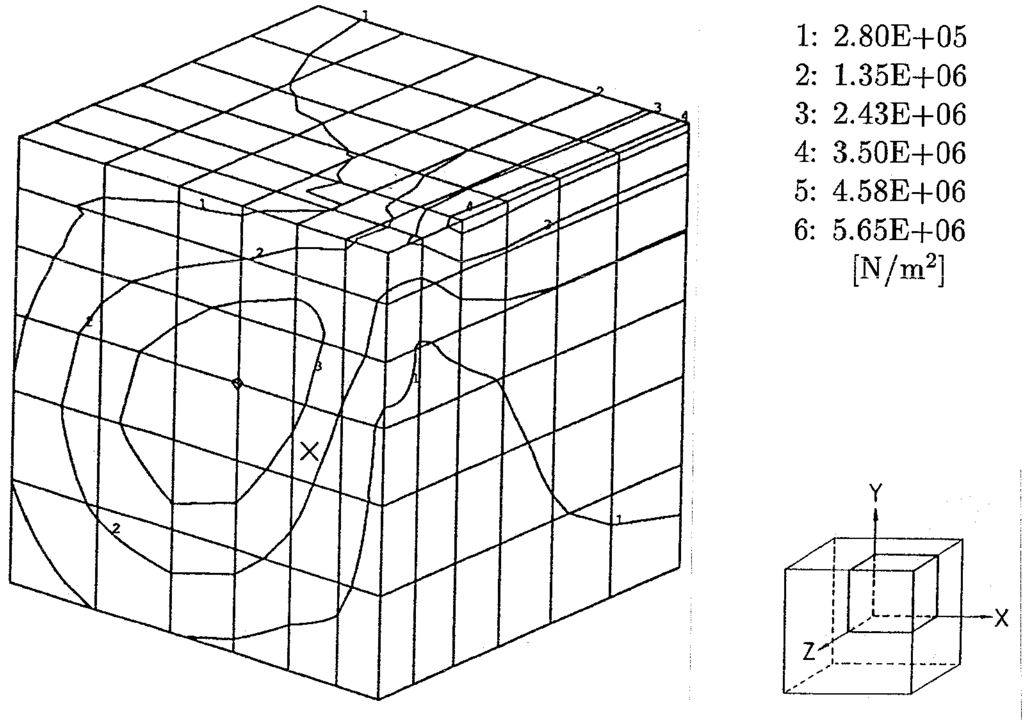

Figure J.35: Case 7, stress component σ_{xy}, outside surfaces.

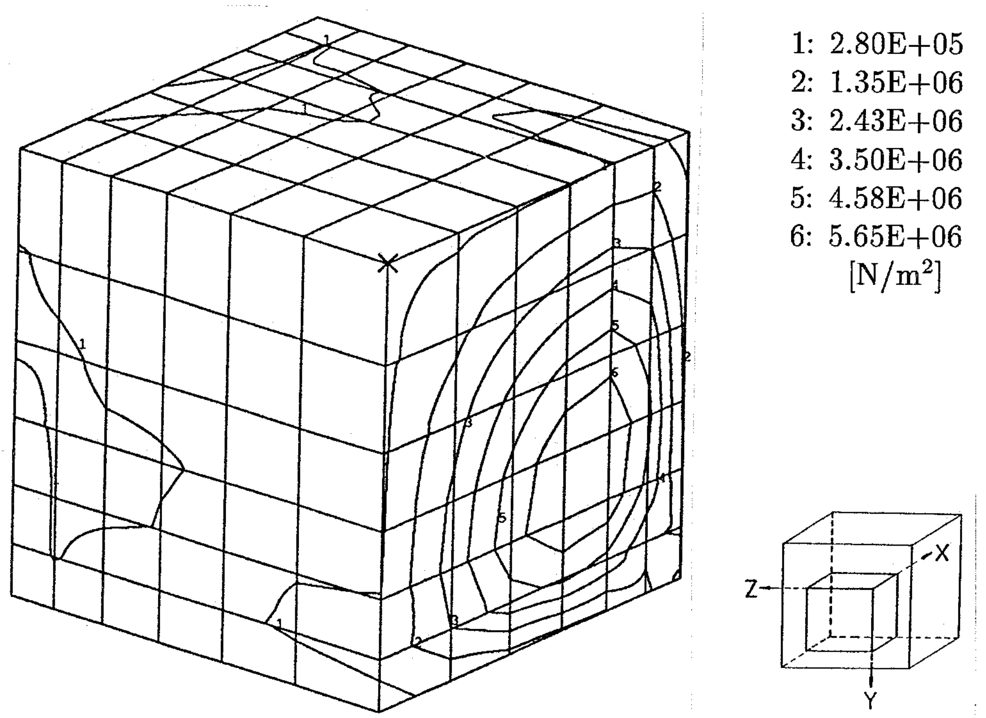

Figure J.36: Case 7, stress component σ_{xy}, symmetry surfaces.

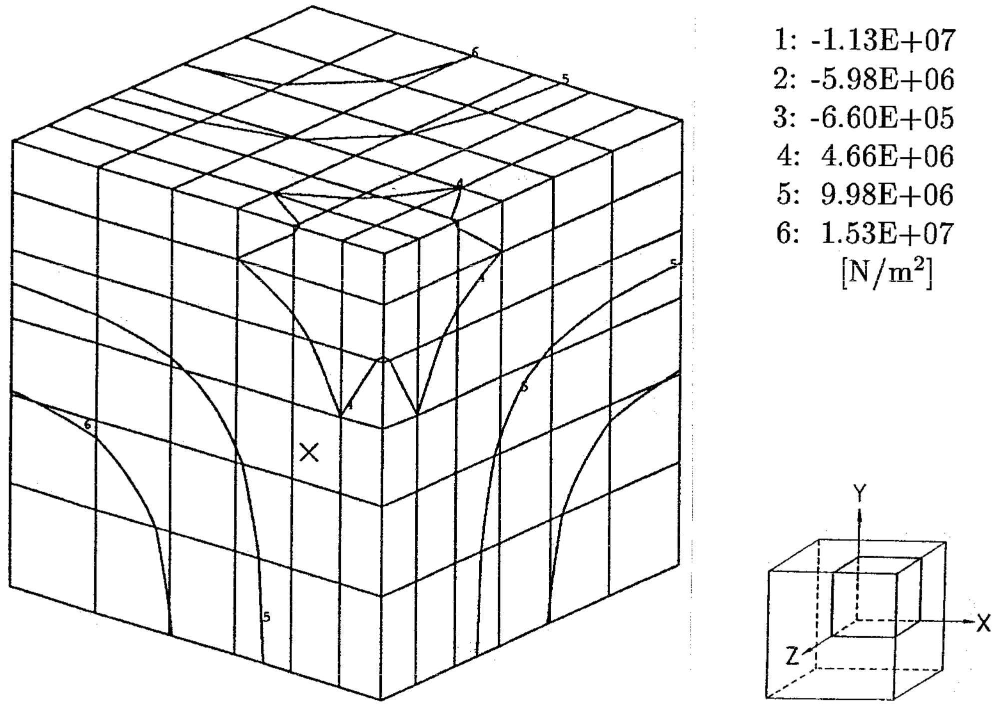

Figure J.37: Case 7, hydrostatic pressure, outside surfaces.

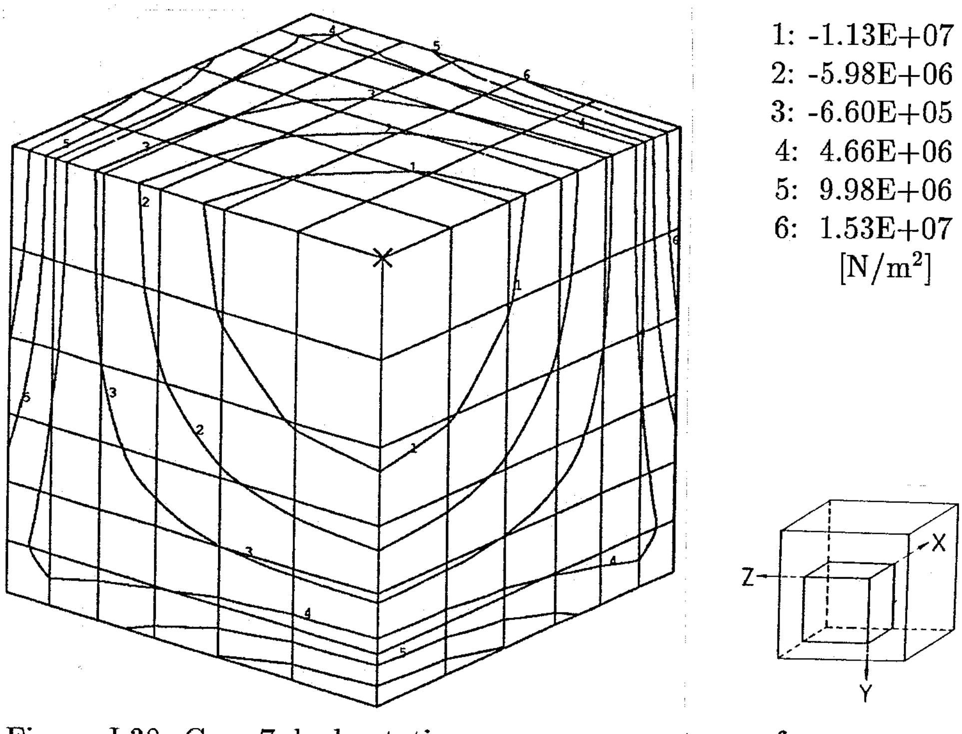

Figure J.38: Case 7, hydrostatic pressure, symmetry surfaces.

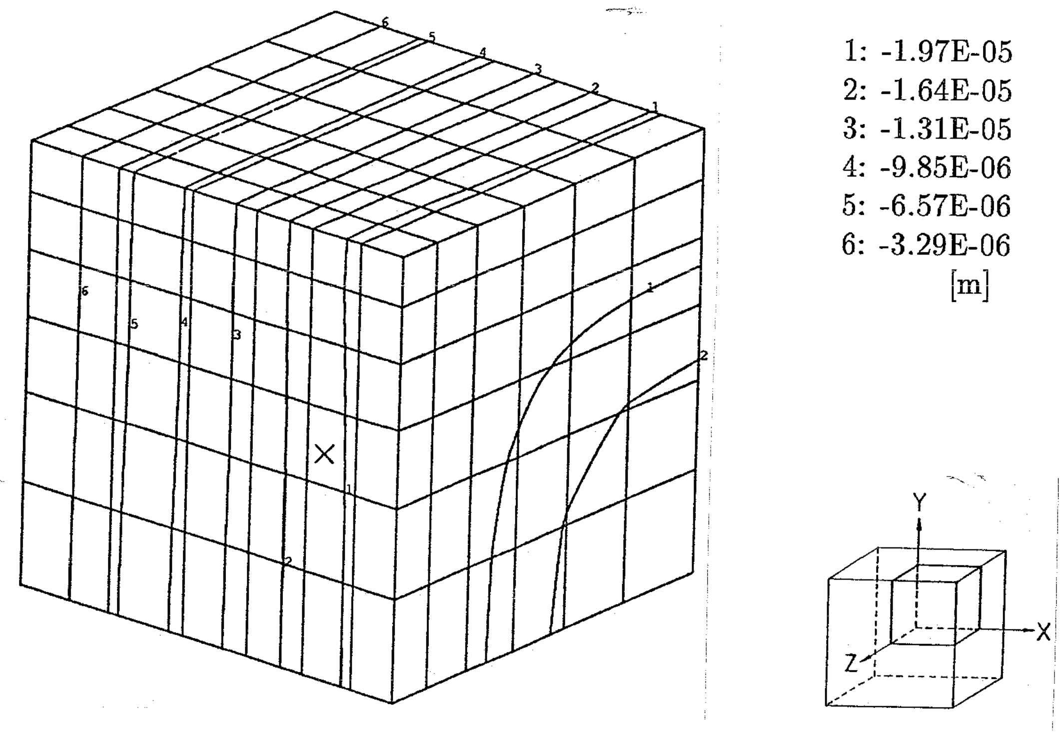

Figure J.39: Case 7, displacement component x, outside surfaces.

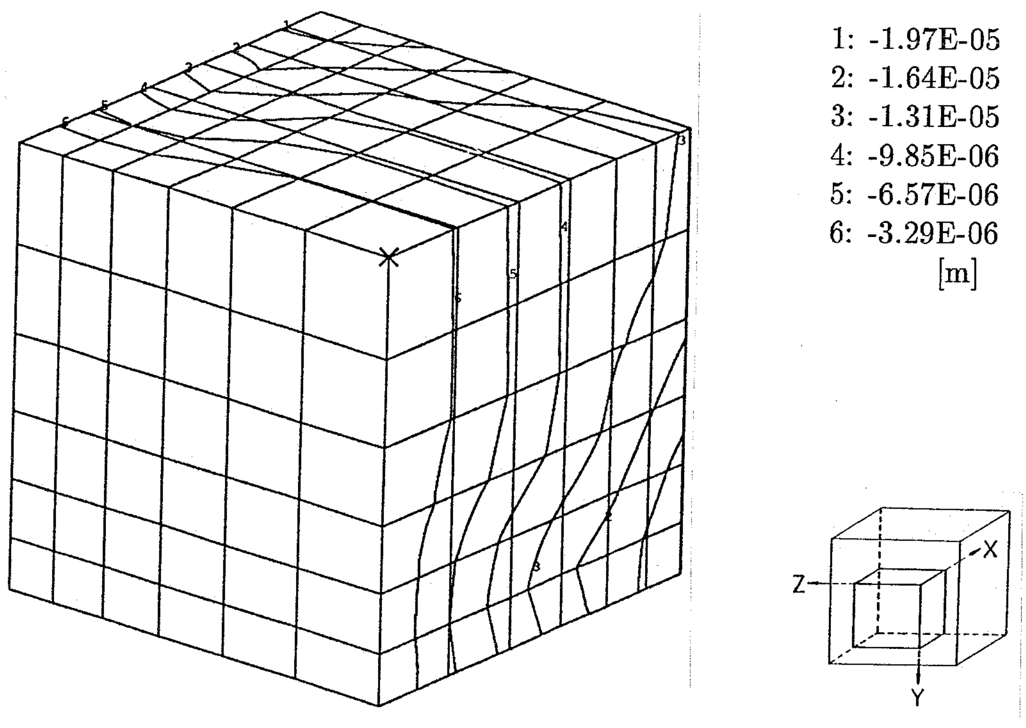

Figure J.40: Case 7, displacement component x, symmetry surfaces.